

ELECTROCHEMICALLY INITIATED

LIVING POLYMERIZATION OF 1,3-BUTADIENE

by

VLADIMIR HORNOF

M.Sc., University of Chemical  
Technology, Prague, Czechoslovakia, 1963

A DISSERTATION SUBMITTED IN PARTIAL FULFILLMENT  
OF THE REQUIREMENTS FOR THE DEGREE OF  
DOCTOR OF PHILOSOPHY  
in the Department  
of  
Chemistry

© VLADIMIR HORNOF 1971  
SIMON FRASER UNIVERSITY  
MAY 1971

APPROVAL

Name: Vladimir Hornof  
Degree: Doctor of Philosophy  
Title of Thesis: Electrochemically Initiated Living  
Polymerization of 1,3-Butadiene  
Examining Committee:

Chairman: D. Sutton

B. L. Funt  
Senior Supervisor

T. N. Bell

D<sup>v</sup> G. Tuck

L. E. St. Pierre  
External Examiner  
Professor  
McGill University  
Montreal, Quebec

Date Approved:

### ABSTRACT

Living polymerization of butadiene was initiated in polar solvents by passage of electric current. Alkali metal salts of tetraphenylborate were used as supporting electrolytes. The living anionic character of the polymerization was proved by additions of monomer, by determining the microstructure of the resulting polybutadiene and by copolymerization studies.

The reaction was carried out in an electrolytic cell whose cathodic and anodic compartments were separated by a fritted disc. When current was passed through a solution containing tetrahydrofuran, sodium tetraphenylborate and butadiene, a yellow color was generated at the cathode, which was due to butadiene living anions. Their concentration depended stoichiometrically on the charge passed. Passage of current of reversed polarity caused a stoichiometric destruction of the living anions. The electrochemical regulation of the concentration of growing anions leads to a control of rates of reaction and of molecular weight distribution, but for this to be applied quantitatively rate constants must be determined for conditions prevailing in the reaction medium.

The propagation rates of butadiene polymerization were determined at temperatures from  $-72$  to  $-10^{\circ}\text{C}$ . Within this interval, the Arrhenius temperature dependence of the propagation rate was:

$$k_p = 1.45 \times 10^2 \exp ( -2600/RT ) .$$

As butadiene living anions undergo attrition reactions, a simple correction method was developed to facilitate the evaluation of rate constants based on the average effective concentration of living anions.

The relatively slow propagation rate of this monomer rendered it possible to prepare polymers with predetermined molecular weights and molecular weight distributions. Polymer was formed by a series of pulses which successively initiated polymerization, permitted growth in the absence of current and electrochemically terminated polymerization. The polymers thus produced showed good agreement with calculated composition and distribution in the molecular weight range from 10,000 to 50,000.

The influence of the cation in the supporting electrolyte on the microstructure of the resultant polybutadiene was also investigated. No significant effect was encountered for the Ia group metals and the polymers were found to consist mainly of 1,2-polybutadiene with a small amount of 1,4 linkages. Similarly, a change in solvent polarity did not bring about any appreciable change in polymer microstructure. These results are compared with data published by other authors and an explanation of the differences is suggested.

Butadiene was copolymerized with styrene using different feed ratios. The composition of the copolymers was found to be very similar to that reported previously for conventionally initiated systems. This is compared with the electrochemical behavior of the systems.

Gel permeation chromatography was used for determining molecular weights and molecular weight distributions of the polymers. A simple universal calibration method was developed based on the similarity of the thermodynamic behavior of 1,2-polybutadiene and polystyrene in tetrahydrofuran solution. The method is compared with other universal calibration techniques in terms of attainable accuracy. The present method gave a very similar

result to that based on the unperturbed dimensions of the polymers in solution, whilst the extended length method was found to be unreliable for this particular pair of polymers.

## ORIGINAL CONTRIBUTIONS TO KNOWLEDGE

1. A direct control of molecular weight distribution by cyclic variation of current was demonstrated.
2. The quantity and molecular weight of individual fractions were controlled by varying pulse duration and number of pulses employed.
3. Polybutadienes of low polydispersity ( $\overline{M}_w/\overline{M}_n < 1.2$ ) were prepared by this electrochemical technique.
4. Propagation rate constants and Arrhenius activation energy were determined.
5. Variation of solvent polarity and metal cation was found to have no significant effect on polybutadiene microstructure.
6. A simplified universal calibration method for gel permeation chromatography (GPC) was developed.

## ACKNOWLEDGMENTS

I should like to record my gratitude to Dr. B. L. Funt for his help and encouragement in all aspects of this work.

Thanks are also due to Dr. J. Tanner, Mr. J. Rybicky and Mr. I. McGregor for their helpful comments and stimulating discussions.

The assistance of the Simon Fraser Glassblowing shop is gratefully acknowledged.

Last, I wish to extend my thanks to Mrs. J. Tanner for proofreading this thesis.

## TABLE OF CONTENTS

| SECTION  | PAGE |
|--|------|
| 1. THEORETICAL PART  | 1    |
| 1.1. Introduction  | 1    |
| 1.2. Electrolytically Initiated Polymerizations  | 4    |
| 1.2.1. Historical Development and Types of Initiation  | 4    |
| 1.2.2. Electroanalytical Techniques and Controlled Potential Electrolysis                    | 7    |
| 1.3. Living Anionic Polymerization   | 9    |
| 1.3.1. Introduction  | 9    |
| 1.3.2. Propagation in Living Anionic Polymerization  | 12   |
| 1.3.3. Molecular Weights and Molecular Weight Distributions in Living Anionic Polymerization | 16   |
| 1.3.4. Living Anionic Polymerization Initiated by Electrolysis                               | 19   |
| 1.4. Butadiene Polymers  | 23   |
| 1.4.1. Introduction  | 23   |
| 1.4.2. Anionic Polymerization of Butadiene   | 25   |
| 1.4.3. Kinetics of the Anionic Polymerization of Butadiene                                   | 31   |
| 1.4.4. Stability of Butadiene Living Polymers in Polar Solvents                              | 34   |
| 1.4.5. Electrolytically Initiated Polymerization of Butadiene                                | 34   |



| SECTION  | PAGE |
|--|------|
| 2. EXPERIMENTAL METHODS  | 36   |
| 2.1. Chemicals and Their Purifications   | 36   |
| 2.2. Polymerization Procedure  | 38   |
| 2.3. Determination of Microstructure   | 41   |
| 2.3.1. Infrared Spectroscopy   | 41   |
| 2.3.2. NMR Spectroscopy  | 44   |
| 2.4. Determination of Molecular Weights and<br>Molecular Weight Distributions    | 44   |
| 2.5. Determination of the Limiting Viscosity Number                              | 49   |
| 2.6. Cyclic Voltammetry  | 49   |
| 3. RESULTS AND DISCUSSION  | 50   |
| 3.1. Introduction  | 50   |
| 3.2. Polymerization of Butadiene   | 50   |
| 3.2.1. Kinetics of Polymerization  | 50   |
| 3.2.2. Molecular Weights   | 61   |
| 3.2.3. Preparation of Polymers with Multimodal<br>Molecular Weight Distributions | 67   |
| 3.2.4. Effect of Solvent and Counterion on Microstructure                        | 80   |
| 3.2.5. Butadiene - Styrene Copolymerization                                      | 89   |
| 3.2.6. Controlled Potential Electrolysis<br>of 1,3-Butadiene                     | 93   |

| SECTION | PAGE  |     |
|---------|---|-----|
| 3.3.    | Criteria for a Simplified Universal<br>Calibration in Gel Permeation Chromatography | 95  |
| 3.3.1.  | General Considerations  | 95  |
| 3.3.2.  | Results and Discussion  | 98  |
| 4.      | CONCLUSIONS   | 103 |
|         | Appendix I - Analysis of Errors   | 106 |
| 5.      | LIST OF REFERENCES  | 111 |

## LIST OF TABLES

|             |   | page |
|-------------|---|------|
| Table I:    | Propagation of Anionic Polymerization of Living Polystyrene in Tetrahydrofuran (Ref. 32)                    | 15   |
| Table II:   | Polymerization of Butadiene in n-Heptane in Absence and Presence of Ethers (Ref. 68)                        | 25   |
| Table III:  | Microstructure of Alkali Metal Initiated Polybutadienes in Hydrocarbon Media (Ref. 79)                      | 30   |
| Table IV:   | Effect of Counterion on Polybutadiene Microstructure in Tetrahydrofuran (Ref. 80)                           | 30   |
| Table V:    | Dependence of Polybutadiene Microstructure on Temperature (Ref. 82)   | 31   |
| Table VI:   | Propagation Constants of the Anionic Polymerization of Butadiene (Ref. 82)                                  | 33   |
| Table VII:  | Absorption Coefficients for the Infrared Analysis of Polybutadienes (Ref. 102)                              | 42   |
| Table VIII: | Evaluation of Polystyrene Standards by the MWD I Program  | 47   |
| Table IX:   | Determination of Rate Constants at $-10^{\circ}\text{C}$  | 56   |
| Table X:    | Temperature Dependence of Reaction Rate at High Concentration of Supporting Electrolyte                     | 56   |
| Table XI:   | Temperature Dependence of Reaction Rate at Low Concentration of Supporting Electrolyte                      | 57   |
| Table XII:  | Molecular Weights and Polydisperties of Butadiene Polymers at High Concentration of Supporting Electrolyte  | 62   |
| Table XIII: | Molecular Weights and Polydispersities of Butadiene Polymers at Low Concentration of Supporting Electrolyte | 64   |
| Table XIV:  | Effect of Salt Concentration on Molecular Weight of Butadiene Polymers                                      | 65   |

|  | page |
|--|------|
| Table XV: Effect of Initiation Time - Propagation Time Ratio on Polydispersity of Butadiene Polymers | 66   |
| Table XVI: Compensation for Monomer Depletion at -10°C   | 71   |
| Table XVII: Compensation for Monomer Depletion at -50°C  | 72   |
| Table XVIII: Comparison of Experimental and Calculated Distributions for Bimodal Polymers            | 73   |
| Table XIX: Comparison of Experimental and Calculated Distribution for Trimodal Polymer               | 79   |
| Table XX: Effect of Charge Passed on Polybutadiene Microstructure                                    | 82   |
| Table XXI: Polymerization of Butadiene in THF-Cyclohexane Mixture                                    | 83   |
| Table XXII: Polymerization of Butadiene in HMPA with Different Cations                               | 84   |
| Table XXIII: Polymerization of Butadiene in THF - HMPA Mixture with Different Cations                | 85   |
| Table XXIV: Effect of Counterion on Microstructure   | 86   |
| Table XXV: Comparison of IR and NMR Analysis of Anionic Polybutadienes                               | 89   |
| Table XXVI: Butadiene - Styrene Copolymerization   | 90   |
| Table XXVII: Composition of Butadiene - Styrene Copolymers   | 91   |
| Table XXVIII: Simplified Universal Calibration in GPC  | 101  |
| Table XXIX: Replacement of Equation 76 by a Linear Relationship                                      | 101  |

## LIST OF FIGURES

|             |   | page |
|-------------|---|------|
| Figure 1.   | Representative Electrode Potentials (Ref. 1)  | 2    |
| Figure 2.   | Polarograms of Acrylonitrile, $\alpha$ -Methylstyrene, Isoprene and Tetrabutylammonium Perchlorate (Ref. 12); SCE $\equiv$ standard calomel electrode | 10   |
| Figure 3a,b | Distillation Assembly for the Purification of Hexamethylphosphoramide   | 37   |
| Figure 4.   | Polymerization Cell and Filling Assembly<br>A..... filling bulb; a,b..... breakseals  | 39   |
| Figure 5.   | Infrared Spectrum of a Predominantly 1,2-Polybutadiene  | 43   |
| Figure 6.   | 60 MHz NMR Spectrum of Atactic 1,2-Polybutadiene Containing 10% by Weight 1,4 Addition Units (Ref. 104)   | 45   |
| Figure 7.   | 60 MHz Aromatic Proton NMR Spectrum of Atactic Polystyrene (Ref. 104)   | 45   |
| Figure 8.   | Block Diagram of the GPC Instrument   | 46   |
| Figure 9.   | Primary Polystyrene Calibration Graph for GPC<br>$M_p$ ..... GPC peak molecular weight  | 48   |

|   | page |
|---|------|
| Figure 10. Model Profile Living Anion Concentration During One Electrochemical Cycle; Broken Curve Ideal without Attrition; Solid Curve Corrected for Attrition   | 54   |
| Figure 11. Dependence of Propagation Rate Constant on Temperature at High Concentration of Sodium Tetrphenylboride. Solid Line Least Squares Fit to Data.<br>Error bars denote limit of error derived from propagation-of-error analysis (Appendix I) | 58   |
| Figure 12. Comparison of Present Kinetic Data with Those of Morton (86) and Medvedev (82)   | 59   |
| Figure 13. Dependence of Propagation Rate Constant on Temperature at Low Concentration of Sodium Tetrphenylboride.<br>Error bars denote limit of error derived from propagation-of-error analysis (Appendix I)  | 60   |
| Figure 14. Schematic Representation of Time-Current Profile   | 69   |
| Figure 15. Molecular Weight Distribution for Bimodal Polymer B116<br>solid line..... integral distribution<br>broken line..... differential distribution  | 74   |
| Figure 16. Molecular Weight Distribution for Bimodal Polymer B117<br>solid line..... integral distribution<br>broken line..... differential distribution  | 75   |

|  | page |
|--|------|
| Figure 17. Molecular Weight Distribution for Bimodal<br>Polymer B118<br>solid line..... integral distribution<br>broken line..... differential distribution  | 76   |
| Figure 18. Superimposed Integral Distribution Curves<br>for Bimodal Polymers B116, B117, B118  | 77   |
| Figure 19. Molecular Weight distribution for Trimodal<br>Polymer B119<br>solid line..... integral distribution<br>broken line..... differential distribution | 78   |
| Figure 20. Dependence of Hydrodynamic Volume on Molecular<br>Weight for Polystyrene Standards  | 99   |

## 1. THEORETICAL PART

### 1.1. Introduction.

In common with other chain reactions, addition polymerizations are initiated by reactive species or intermediates, such as free radicals, carbanions, carbonium ions and charge transfer complexes. To "trigger" the reaction, the reactive centers are generated in the system via a suitable chemical process. Such processes include the formation of radicals by thermal decomposition of peroxides, generation of radical-anions by a transfer of an electron onto a double bond, and many other reactions.

All initiation reactions are characterized by the relatively labile electronic structure of their products. Many of these processes are basically of a redox nature and one may immediately conceive of electrolysis as being an ideal method to supply or withdraw electrons. In their recent review, Fleischmann and Pletcher(1) give a good illustration of the reductive or oxidative capability of electrolytic reactions. Referring to a scale of standard electrode potentials shown in Figure 1, they note that, for example, spontaneous reactions using oxygen or air as the oxidant, or hydrogen as a reducing agent, are only possible (in electrochemical terms) within the potential range limited by the reduction of oxygen and the oxidation of hydrogen. This driving force amounts to roughly .5 eV or 42 kJ/mole. By contrast, it is possible to carry out electrochemical reactions within a much larger potential range. If suitable electrolytes are chosen (e.g. perchlorates for oxidations and quaternary ammonium salts for reductions), electrochemical reactions can be carried out between +3.5V and -2.5V. The large driving force for such processes is therefore of the order of 3 eV or 250 kJ/mole.

Most electrode processes are irreversible and it is not strictly valid to compare the available driving force with the standard potential and the standard free energy. Such factors as electrode



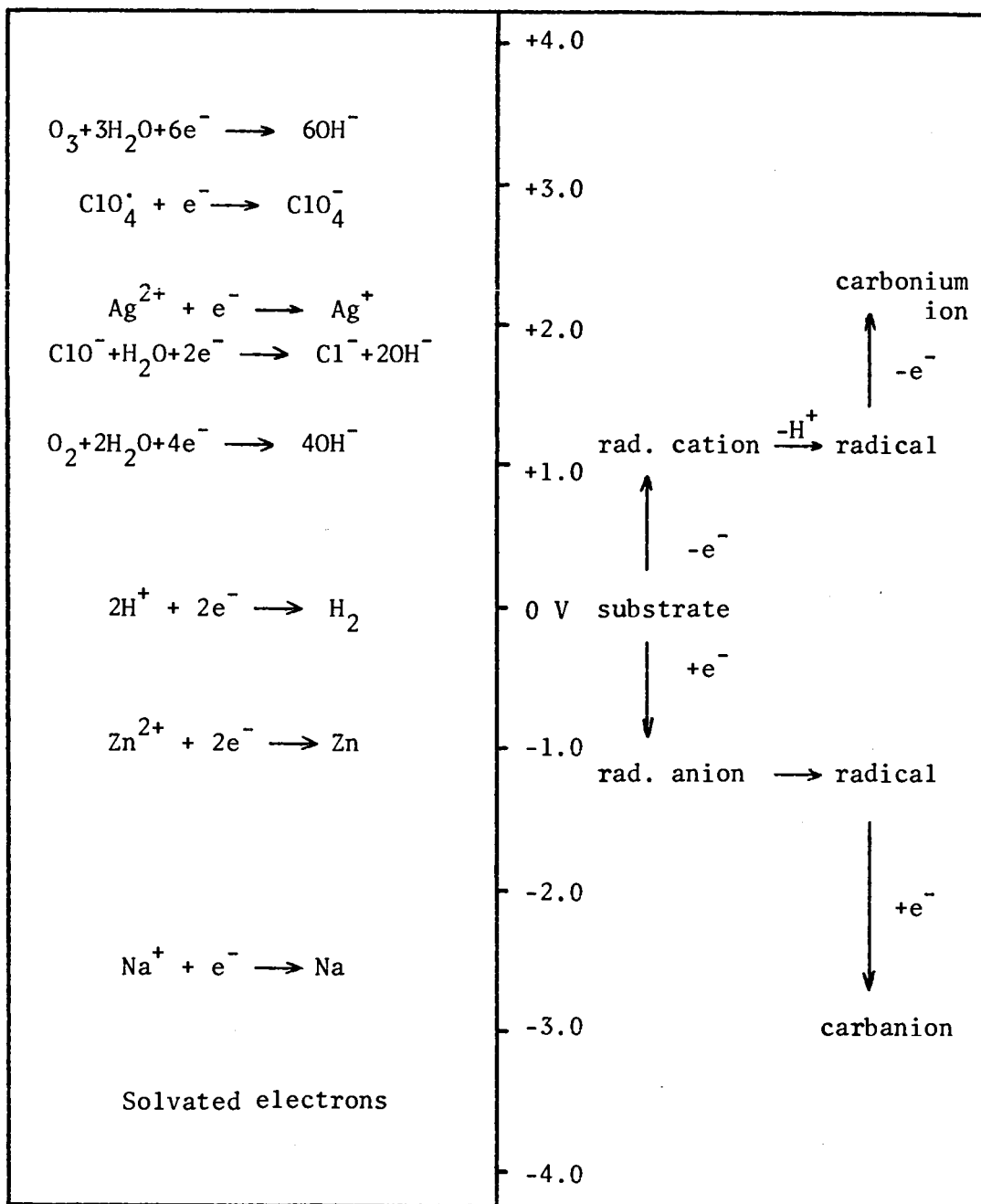


FIGURE 1. Representative electrode potentials (Ref. 1)

overpotential, adsorption, migration and diffusion phenomena have a profound influence on the course of an electrolytic reaction and must be considered. Much of modern electrochemistry is concerned with a description and evaluation of these features.

A considerable spectrum of possibilities exists in the electrochemical formation of polymers. The present work is concerned with electrochemically initiated living anionic polymerization. Such systems have been shown to be of great interest by earlier research carried out in this laboratory. Whilst living polymerization itself can produce polymers with predetermined molecular weights and molecular weight distributions, its combination with electrolysis gives a system in which exact control over both initiation and termination reactions can be effected by the passage of current. The molecular weight distribution in living polymerization is, other parameters being fixed, a function of the concentration profile of living ends. Accordingly, by varying the current, one should be able to produce polymers with any molecular weight and distribution of molecular weights.

In practice, the situation is much more complicated, because the rate of propagation of many monomers is too fast in comparison to the rate of electrolytic initiation. For this reason in this work the monomer 1, 3 - butadiene was chosen since pilot experiments had shown it to have a relatively slow rate of propagation.

The microstructure of the resulting polybutadienes was studied in relation to solvent polarity and alkali metal counterion and compared with the microstructure of polymers prepared in conventional living anionic studies. Similarly, copolymerization studies were of interest in view of possible electrode effects.

## 1.2. Electrolytically Initiated Polymerizations

### 1.2.1. Historical Development and Types of Initiation.

-----

Perhaps the earliest mention of electroinitiated polymerization appeared in an article published at the turn of this century by Szarvasy (2). No further results appeared until 1947 when a Ph.D. thesis by Rembold (3) mentioned the polymerization of methyl methacrylate initiated by electrolysis. In 1949, Wilson et al. (4) made reference to the polymerization of acrylic acid whilst studying the electroreduction of various compounds.

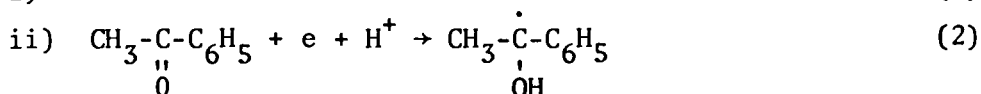
It was later shown by Parravano (5) in 1951 that the polymerization of methylmethacrylate was due to hydrogen atoms produced at the cathode.

It was not until the late fifties and the early sixties, however, that the possibilities of this new type of initiation had begun to be recognized and utilized by polymer chemists. Since then the field has been growing rapidly as is reflected in the number of published papers. A number of excellent reviews (6, 7, 8, 9, 10) have been presented by various workers active in the field and it is hence unnecessary to provide a comprehensive review of the subject within the scope of this text. The various features and potential uses of electrochemical initiation will rather be classified and demonstrated by a number of examples.

The great diversity of possible electrode reactions makes

it expedient to introduce a classification scheme. Yamazaki's classification (9) recognizes two major types of reactions: cathodic and anodic. The cathodic reactions are classified as follows:

A: Generation of free radicals

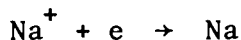


iii) Reduction of oxidizing agents  
(peroxides)



B: Generation of radical-anions

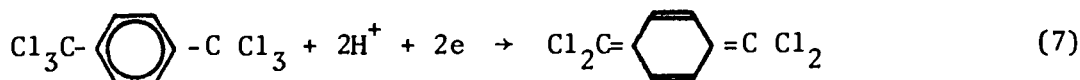
i) Indirect electron transfer to monomer



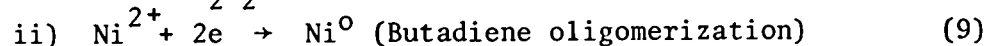
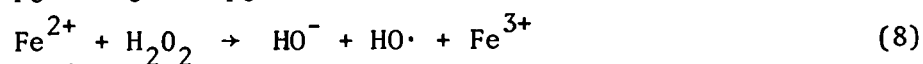
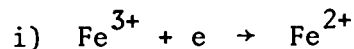
ii) Direct electron transfer to monomer



C: Formation of unstable monomer

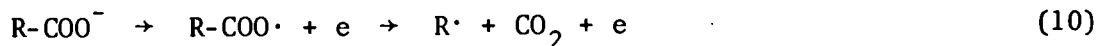


D: Formation of an active catalyst (or redox)

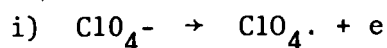


The anodic reactions, on the other hand, give rise to oxidation products which are classified as follows:

E: Formation of free radicals by the Kolbe reaction

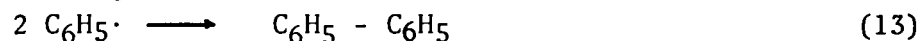


F: Formation of radical-cations



G: Ring opening polymerization according to Equation 11

H: Oxidative condensation polymerization



Electrolytic initiation often implies a significant degree of control over the rate of the initiation reaction. This can be demonstrated on the example of a reduction-oxidation initiator system, such as described by Equation 8. The hydroxyl radicals produced by the reaction of hydrogen peroxide with ferrous ion initiate the polymerization of a vinyl monomer. Taking advantage of electrolysis, one may start with an inactive system composed of  $Fe^{3+}$  ions and  $H_2O_2$  and produce the required amount of active  $Fe^{2+}$  ions by the electrolytic reduction. Variations of the current are reflected in the variations in the concentration of  $Fe^{2+}$  and thereby in the rate of initiation. From this point of view, the electrolytic method possesses a great degree of flexibility as to the instantaneous control of initiator concentration.

It is important to note, that in most electrochemical polymerizations it is only the initiating step that can be affected by the variation of electrochemical parameters. Under a given set of conditions, a radical polymerization of styrene will proceed by the same mechanism regardless of whether it was initiated by electrolysis or by a chemical initiator, provided that diffusion from the surface of the electrode is fast enough and adsorption effects are negligible. However, if the two electrodes are not separated and the solution can move freely from one electrode to the other, products formed at the counterelectrode may react with the initiating species or with the growing chains. Such reactions may cause termination or chain transfer. A more detailed account of this particular aspect will be given in the part dealing with

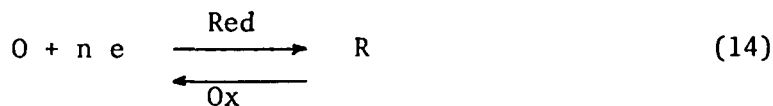
electrolytically initiated living polymerizations.

The choice of experimental conditions for electro-initiated polymerizations is frequently difficult owing to contravening demands of the electrolytic process on one hand and the polymerization reaction on the other. Conductivity must be sufficiently high ( $L > 10^{-5}$  mho) to permit electrolysis at reasonable voltages ( $U < 1000$  V); hence aqueous or at least a highly polar environment is needed, in which a suitable supporting electrolyte can be dissolved. Monomers and polymers, however, are mostly non-polar substances, but they too must be soluble in the same solvent if the reaction is to be carried out homogeneously and with some control. This requires a careful selection of all the components of the reaction system, so that the polymerization can occur without interference under easily attainable conditions. Consequently, many "ideal" systems cannot be employed in practice.

#### 1.2.2. Electroanalytical Techniques and Controlled Potential Electrolysis.

In a given system, the reaction that takes place at an electrode depends on electrode potential. Electrode kinetics are also important, though this may be regarded as secondary to the transfer of the electron. The feasibility of governing the yields and products of an electrochemical reaction was realized by Haber as early as 1898. The cornerstone of electroanalysis was laid by Heyrovsky in 1922 with his discovery of polarography. Further development in this field has provided an invaluable tool for both inorganic and organic chemists.

The kinetics and thermodynamics of processes accompanying electrolysis under equilibrium conditions are relatively well understood. The reactions taking place are basically ordinary redox processes, where one of the reactants is replaced by the electron-donating or electron-accepting electrode:



In this equation, O and R respectively denote the components which accept and give up electrons. The number of electrons exchanged in the process is denoted by n. The equilibrium state under given conditions is characterized by an equilibrium constant.

$$K = \frac{a_R}{a_O \cdot a_e^n}, \quad (15)$$

Where  $a_{R,O,e}$  denotes the activities of the individual components. The equilibrium constant is related to the standard free energy of the reaction and by the same token to the standard half-cell potential:

$$G^0 = -RT \ln K = -nFE^0 \quad (16)$$

Combination of Equations 15 and 16 yields

$$E^0 = \frac{RT}{nF} \ln \frac{a_R}{a_O \cdot a_e^n} = \frac{RT}{nF} \ln \frac{a_R}{a_O} - \frac{RT}{F} \ln a_e \quad (17)$$

This equation states, that for a given activity ratio of the redox pair under a given set of conditions, the activity of electrons is also fixed. The last term in Equation 17 is called the "electrode potential" E and is expressed by the Nernst equation:

$$E = E^0 - \frac{RT}{nF} \ln \frac{a_R}{a_O} \quad (18)$$

The physical meaning of this relationship is that a change in the  $a_R/a_O$  ratio results in a change of potential. The converse is also true. As the absolute value of E cannot be determined, the potential of the normal hydrogen electrode was chosen as the standard zero potential. The hydrogen electrode is not very suitable for practical measurements, and a number of reference electrode systems have been developed (11).

If two electrodes are immersed into a solution containing electroactive substances and external voltage is applied across the cell, current will flow through the circuit. The total impressed voltage V may be divided in the following manner:

$$V = E_a + E_c + iR \quad (19)$$

$E_a$  and  $E_c$  are the potentials of the anode and the cathode referred to a reference electrode,  $R$  is the resistance of the cell and  $i$  is the current. For a given  $V$ , the magnitude of current depends on the resistance, which again is a function of a number of parameters. It follows from Equation 18, that, for an electrode reaction to take place, the potential of the electrode must not be lower than a certain minimum value. This principle is well demonstrated in Figure 2, which shows polarograms of acrylonitrile,  $\alpha$ -methylstyrene and isoprene recorded by Yamazaki, Tanaka and Nakahama (12). If there is a solution containing all three monomers, selective reduction of acrylonitrile can be effected by keeping the cathodic potential less negative than the discharge potentials of the two other monomers. Similarly, if a given substrate can undergo two or more electron transfers at different potentials, the reaction can be induced to give the required product by a suitable choice of the electrode potential. In order to carry out such "controlled potential" electrolyses, one must determine the electrochemical behavior of the given system by electroanalytical techniques such as polarography or cyclic voltammetry. In organic systems of high impedance, the interpretation of such results is often difficult and data related to electrolytic polymerizations are rare. Reactions of 4-vinylpyridine in pyridine were successfully studied by Bhadani and Parravano (13) using the technique of cyclic voltammetry. The general feasibility of using cyclic voltammetry for the investigation of some electro-polymerization systems was shown by Funt and Gray (14, 15).

### 1.3. Living Anionic Polymerization

#### 1.3.1. Introduction.

Addition polymerizations generally involve three principal steps: initiation, propagation and termination. If a reaction can be carried out in such a way that the termination step is excluded,



Figure 2. POLAROGRAMS OF ACRYLONITRILE,  $\alpha$ -METHYLSTYRENE, ISOPRENE  
AND TETRABUTYLAMMONIUM PERCHLORATE (Ref. 12)  
SCE  $\equiv$  standard calomel electrode

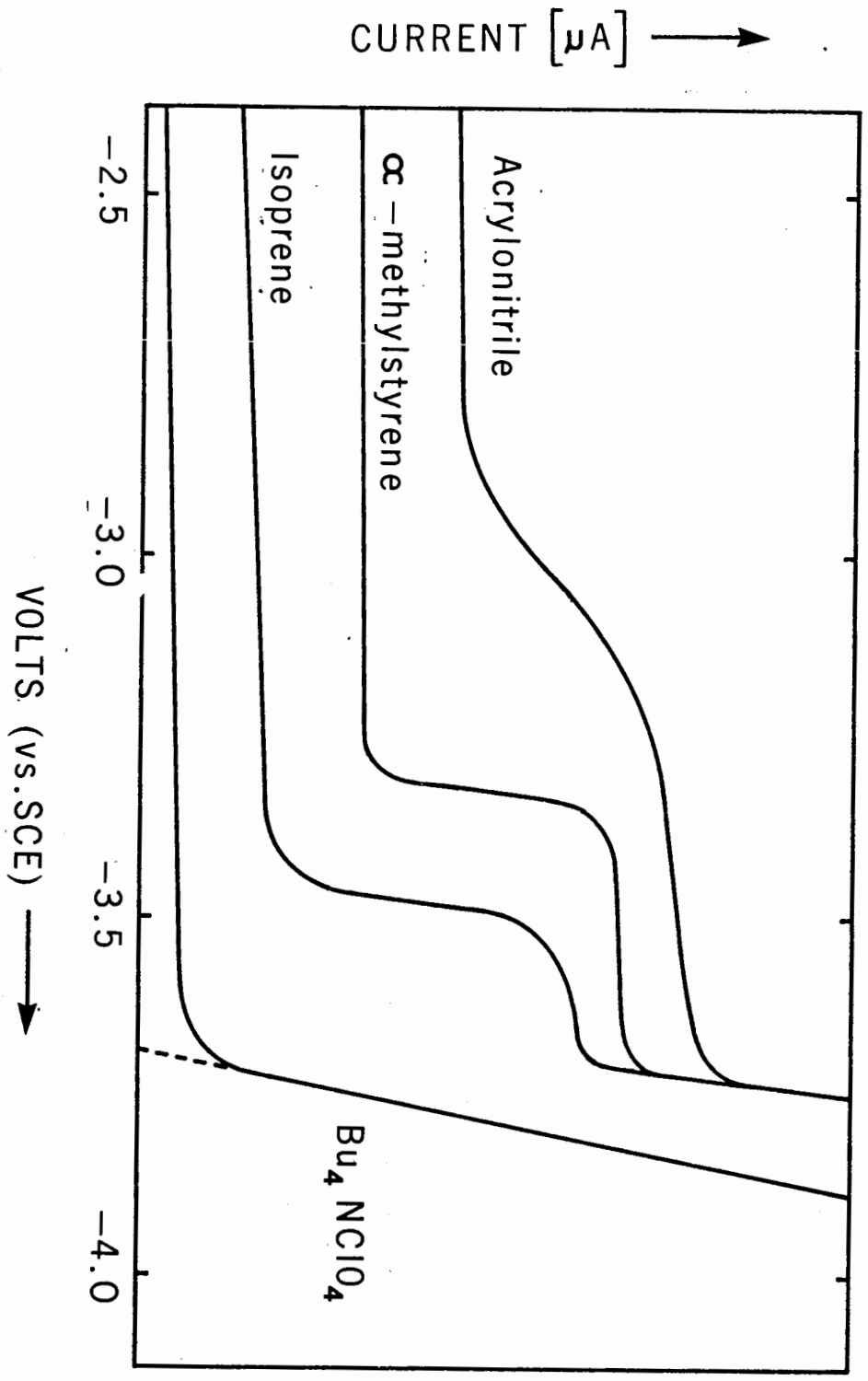
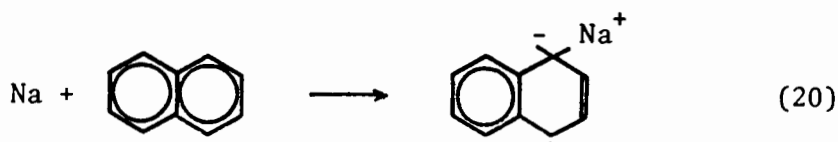


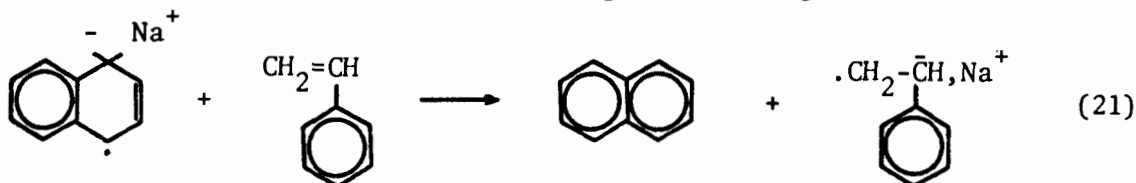
FIGURE 2

the growing species will continue to propagate until the monomer is depleted. Furthermore, the chain ends will retain their activity and will resume their growth on subsequent addition of monomer.

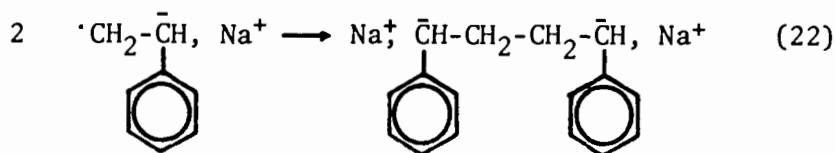
Szwarc and coworkers (16, 17, 18, 19, 20, 21) demonstrated that the polymerization of styrene can be initiated by a complex of sodium with an aromatic hydrocarbon such as naphthalene or anthracene. The reaction was found to involve no termination and was given the name "living" polymerization. The initiation step is generally believed to proceed in the following manner:



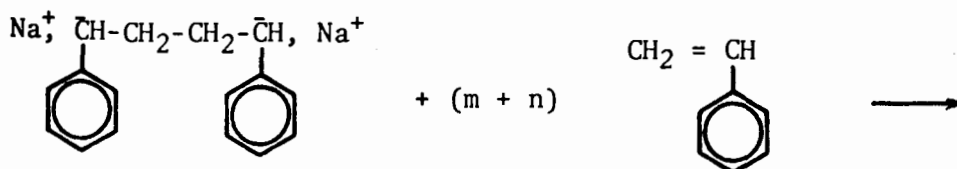
The radical-anion of naphthalene reacts with the monomer, whereby styrene anion-radical is formed and naphthalene regenerated:

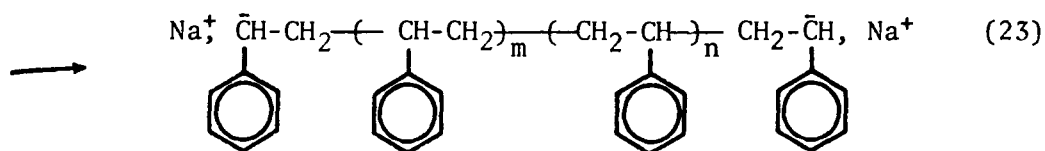


The initiation step is apparently not complete until dimerization of radicals takes place:



Propagation therefore proceeds at both ends of the chain by an anionic mechanism:





The discovery of living polymers had a great impact upon the synthetic techniques of polymer chemistry. In the absence of a statistical termination, the number average degree of polymerization,  $\bar{P}_n$ , is given simply by the molar ratio of the consumed monomer to the concentration of growing ends. Polymerizations which combine this absence of termination with instantaneous initiation result in products having a very narrow molecular weight distribution. The technique also allows the introduction of desired functional groups into the polymers and the synthesis of block copolymers. The next three sections will deal with various aspects of living polymerization systems in more detail.

### 1.3.2. Propagation in Living Anionic Polymerization.

The absence of a termination step and the possibility of eliminating the initiation step under suitable conditions greatly simplifies kinetic investigations of anionic polymerizations.

As the concentration of the growing macromolecules is predetermined by the experimenter and remains, ideally, constant during the course of the reaction, the propagation is kinetically first order in respect to monomer:

$$-\frac{d[M]}{dt} = \text{const.} \times [M] \quad (24)$$

In this expression,  $[M]$  represents the instantaneous concentration of monomer and the proportionality constant is equal to the product  $k_p[LE]$ , where  $[LE]$  is the concentration of active ends and  $k_p$  is the absolute second order rate constant of propagation. This can be calculated directly from the kinetic data (22, 23).

The propagation step is considerably more complex in polar solvents such as tetrahydrofuran or dimethoxyethane than in non-polar hydrocarbon solvents. Data reported by Geacintov, Smid and Szwarc (24) indicated that in a polar environment the rate of polymerization of styrene depended on the concentration of living ends. Bhattacharyya and coworkers (25, 26) studied the reaction in more detail and demonstrated that the dissociation of ion-pairs into free ions was responsible for the variations in  $k_p$ . Corroborating evidence was obtained by Hostalka, Figini and Schulz (27) and Hostalka and Schulz (28).

The concept of free ions, ion-pairs and their equilibria was reviewed and discussed by Szwarc (21, 29, 30). If the equilibrium between ion-pairs and free ions is given by



the equilibrium constant can be written as follows:

$$K_{diss} = \frac{f^2}{(1-f)} [LE] \quad (26)$$

In the last equation,  $f$  is the fraction of living ends which are dissociated into free ions. The apparent propagation rate observed in the system is given by the sum  $(1-f)k_{\pm} + fk_{-}$ , where  $k_{\pm}$  is the ion-pair propagation constant and  $k_{-}$  is the free anion propagation constant.

In most living polymerization systems the value of  $f$  is very small and approaches zero; hence the observed propagation rate constant can be calculated according to the following equation:

$$k_p = k_{\pm} + (k_{-} - k_{\pm}) (K_{diss})^{1/2} [LE]^{-1/2} \quad (27)$$

For most systems,  $k_{-} \gg k_{\pm}$ , hence

$$k_p = k_{\pm} + k_{-} (K_{diss})^{1/2} [LE]^{-1/2} \quad (28)$$

The graphical interpretation of Bhattacharyya's data (25, 26) agreed well with this scheme.

The validity of the free ion - ion-pair hypothesis is also confirmed by experiments on common ion effect. This involves adding to the reaction mixture a salt with the same cation as the "living end" ion-pair. Such an addition suppresses the ionic dissociation of living ends and should thus lower the apparent propagation rate. Alkali metal salts of tetraphenylboride\* are suitable for this purpose because of their high degree of ionization (31).

In the presence of such a salt, virtually all the free cations are derived from its dissociation and the following expression for the apparent rate constant applies:

$$k_p = k_{\pm} + (k_- - k_{\pm}) K_{\text{diss}}/[M^+] \quad (29)$$

where  $[M^+]$  is the concentration of the metal cation. Studies of Bhattacharyya et al. (26), Shimomura et al. (32) and Schulz and Hostalka (28) proved the validity of this assumption. Results of Dainton and coworkers (33) show that if the concentration of the tetraphenylboride salt is in the region  $10^{-2}$  -  $10^{-5}$  mole/litre, the propagation of living polystyrene in tetrahydropyran proceeds exclusively via ion-pairs. Bywater and coworkers report the same effect for the polymerization of isoprene in tetrahydrofuran (34) and styrene in tetrahydropyran (35).

The reactivities of free ions and ion-pairs differ immensely. For example, the propagation rate of a free polystyryl ion in tetrahydrofuran at 25°C is almost 1000 x higher than that of a corresponding ion-pair. Whilst the free ion rate is not significantly affected by the solvent, the ion-pair rates are extremely dependent on the solvent and the character of the counterion. Table I presents data reported by Shimomura et al. (32) on living polymerization of styrene in tetrahydrofuran.

An important feature of these results is the occurrence of negative Arrhenius activation energy  $E_a$ . It is noted that,

\*The correct name is "tetraphenylborate"; however, "tetraphenylboride" is more common (Ref. 21) and will be used throughout this work.

whilst the free ion propagation rate decreases when temperature is lowered, the propagation rate of the polystyryl sodium ion-pair increases.

TABLE I

Propagation of Anionic Polymerization of Living Polystyrene in Tetrahydrofuran (Ref.32)

| Counterion      | Temperature<br>[°C] | $k_p$<br>[litre/mole sec] | $k_t$ [litre/mole sec] |                 |
|-----------------|---------------------|---------------------------|------------------------|-----------------|
|                 |                     |                           | Na <sup>+</sup>        | Cs <sup>+</sup> |
| Na <sup>+</sup> | 25                  | 65,000                    | 80                     |                 |
| Cs <sup>+</sup> | 25                  | 63,000                    |                        | 21              |
| Na <sup>+</sup> | 0                   | 16,000                    | 90                     |                 |
| Cs <sup>+</sup> | 0                   | 22,000                    |                        | 9               |
| Na <sup>+</sup> | -33                 | 13,900                    | 130                    |                 |
| Cs <sup>+</sup> | -30                 | 6,200                     |                        | 2.4             |
| Na <sup>+</sup> | -60                 | 1,460                     | 250                    |                 |
| Cs <sup>+</sup> | -60                 | 1,100                     |                        | 1.0             |
| Na <sup>+</sup> | -80                 | 1,030                     | 280                    |                 |

S<sup>-</sup> free ion . . . . .  $E_a = 5.9$  kcal/mole  
 S<sup>-</sup>, Na<sup>+</sup> ion-pair . . . . .  $E_a = -1.5$  kcal/mole  
 S<sup>-</sup>, Cs<sup>+</sup> ion-pair . . . . .  $E_a = 5.7$  kcal/mole

This phenomenon is explained by Szwarc (21) in terms of different degrees of solvation. The physical properties of a solvent such as tetrahydrofuran change significantly with the change of temperature. In fact, tetrahydrofuran at 25°C is a vastly different solvent from tetrahydrofuran at -70°C, having a different dielectric constant, viscosity etc. The enhanced reactivity of ion-pairs at lower temperatures is attributed to the presence of a highly reactive, thermodynamically distinct species, viz., solvent-separated ion-pairs,

the proportion of which increases on lowering the temperature of polymerization. Böhm, Barnikol and Schulz (36) furnished an unequivocal proof of the presence of two types of polystyryl sodium ion-pairs in tetrahydropyran at different temperatures. Sodium tetraphenylboride was reported to behave in a similar manner (37).

Korotkov and Podolsky (38, 39) raised some objections against the mechanisms described above. However, the majority of experimental data seems to amply support the free ion - ion-pair scheme.

### 1.3.3. Molecular Weights and Molecular Weight Distributions in Living Anionic Polymerization.

One of the most important characteristics of polymeric substances is their polydispersity. The shape and breadth of the molecular weight distribution reflects the statistical nature of the various steps in the reaction mechanism.

Consider a simple polymerization process, where the growing chain has only two alternatives: to grow or to terminate. The probability of formation of a  $j$ -mer is given by:

$$P_j = p^{j-1} (1-p), \quad (30)$$

where  $p$  is the probability of attaching a monomer unit to the growing macromolecule. Hence, the weight fraction of a  $j$ -mer is defined as follows:

$$w_j = jp^{j-1} (1-p) / \sum_{i=1}^{\infty} \{ ip^{i-1} (1-p) \} = jp^{j-1} (1-p)^2 \quad (30a)$$

Consequently, the number and weight averages can be calculated:

$$\langle j_n \rangle = \frac{1}{1-p} \quad (31)$$

$$\langle j_w \rangle = \frac{1+p}{1-p} \quad (32)$$

The ratio of  $\langle j_w \rangle / \langle j_n \rangle$  is a measure of the molecular weight distribution. Combination of Equations 31 and 32 gives:

$$\langle j_w \rangle / \langle j_n \rangle = 1 + p \quad (33)$$

For high polymers,  $p$  always has a value close to 1; hence the



polydispersity factor is equal to two and the polymer has a so-called most probable distribution. In most actual processes numerous factors such as chain transfer, the existence of more than one mechanism of termination etc., tend to broaden the distribution and the polydispersity factor has a value  $\langle j_w \rangle / \langle j_n \rangle \geq 2$ .

On the other hand, in systems where the termination reactions as well as transfer reactions are excluded, much narrower molecular weight distributions are to be expected. According to Flory (40, 41), such a distribution is mathematically described by the Poisson function:

$$P_j = e^{-\nu} \nu^{j-1} / (j-1)! \quad (34)$$

$$w_j = [ \nu / (\nu + 1) ] j e^{-\nu} ( \nu^{j-2} ) / (j-1)! \quad (35)$$

This distribution function is valid for an ideal case of living polymerization, where  $\nu$  denotes the ratio of consumed monomer to the number of living ends and thereby represents the average number of monomer units added to one active chain end. The  $\langle j_w \rangle / \langle j_n \rangle$  ratio for a Poisson distribution is given by:

$$\langle j_w \rangle / \langle j_n \rangle = 1 + \nu / (\nu + 1)^2 \quad (36)$$

It follows from Equation 36, that polymers with long chains will be more nearly monodisperse than low molecular weight polymers.

In real systems, the molecular weight distribution of living polymers will again be broadened by a number of factors and the ideal Poisson distribution can only be approached under the most rigorous conditions. Henderson and Szwarc (42) summarize the necessary conditions required for attaining Poisson molecular weight distribution in a synthetic polymer:

- a) Termination and transfer must be rigorously prevented.
- b) All the initiating species must be present and active at the onset of the reaction.
- c) Fluctuations of monomer concentration must be excluded. i.e. monomer concentration must be the same in all parts of the

reaction vessel at all times.

d) The rate constant of each consecutive addition of a monomer molecule to a growing chain should be independent of its size.

e) Only one type of propagating species must be present, in order that the propagation rate of all chains be equal. This condition is not fulfilled in numerous living systems; e.g. the simultaneous growth by free ions and ion-pairs will result in a broader distribution.

f) Propagation must be thermodynamically irreversible, i.e. for the reaction:



the inequality  $k_p \gg k_d$  must be valid.

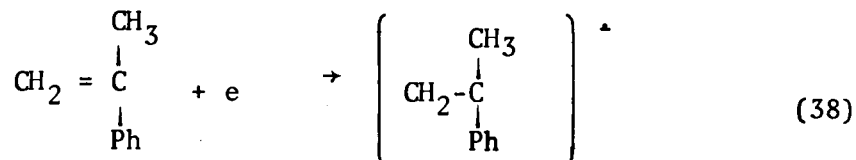
g) The last effect concerns the growth of chains possessing two active ends. Under ideal conditions, such distributions should be narrower than those produced by a monofunctional growth (41). However, if termination by impurities takes place to some extent, bifunctional growth may lead to bimodal distribution reflecting the destruction of only one active end on a part of the chains. The resulting distribution depends on the relative rates of growth and termination (43, 44).

A number of mathematical approaches have been devised to compute the expected molecular weight distributions for non-ideal systems. Szwarc and Litt (45) worked out a scheme for a particular system where part of the living ends is destroyed by impurities in continuously added monomer. Peebles (46) treats the case of molecular weight distributions affected by chain transfer to monomer. Nanda and Jain (47) proposed an elegant approach to the solution of problems involving the simultaneous effect of impurities, slow initiation and chain transfer by monomer on the distribution.

No attempt will be made here to give the details of the mathematical analysis underlying such calculations. Most valuable information can be found in treatises by Henderson and Szwarc (42) and Szwarc (21).

1.3.4. Living Polymerization Initiated by Electrolysis.

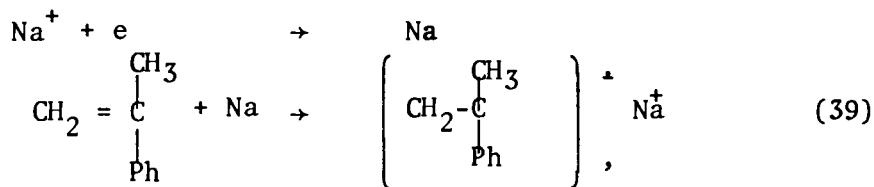
The first mention of electrolytically initiated living polymerization appeared in 1965, when Yamazaki, Nakahama and Kambara (48) produced living poly- $\alpha$ -methylstyrene in tetrahydrofuran solutions of sodium tetraethylaluminium salts and lithium aluminium hydride. They suggested that the initiation of the monomer was due to direct electron transfer to the double bond at the cathode:



Anion-radical

The anion-radical dimerizes forming a dimer dianion and the reaction proceeds according to Equations 22 and 23.

This mechanism was revoked in a later paper by Yamazaki and coworkers (12) on the basis of polarographic measurements. It was concluded that indirect electron transfer through the alkali metal reduced at the cathode gave rise to the polymerization reaction. The cation to be reduced comes from the supporting electrolyte:



The electrolysis was accompanied by the formation of a red color in the cathodic compartment, attributed to the  $\alpha$ -methylstyrene dianions. The low ceiling temperature of this monomer enabled Yamazaki et al.(12) to prepare polymers with reproducible molecular weights by performing



of II. However, with isoprene II was not formed and I was presumed.

The question of the suitability of various solvent-supporting electrolyte systems for living polymerizations was brought up by Anderson (53). He found that the sodium tetraphenylboride salt was not suitable for a direct electron transfer initiation of styrene because of the low discharge potential of the Na cation. The electrochemically more suitable tetrabutylammonium salt, on the other hand, acted as a terminating agent and could not be used if the living character of the polymerization was to be retained.

Anderson also tested the possibility of using hexamethylphosphoramide as solvent and found it suitable for living polymerizations. He reported that  $\text{Me}_4\text{NBPh}_4$  in this solvent provided a system in which styrene could be initiated directly below the discharge potential of the salt. The inertness of the  $\text{Me}_4\text{N}^+$  ion was explained by the absence of  $\beta$ -hydrogens on the alkyl groups.

Laurin and Parravano (54, 55) studied the polymerization of 4-vinylpyridine in liquid ammonia initiated by electrolysis. As poly-4-vinylpyridine was insoluble in the solvent, the polymer remained at the cathode as a porous deposit. The orange-red color of a 4-vinylpyridine solution in  $\text{NH}_3$  containing sodium indicated that the polymerization proceeded via an anionic mechanism. Laurin and Parravano suggested that the reaction was initiated by a solvated electron, generated in the proximity of the cathode. In a later paper Bhadani and Parravano (13) reported a homogeneous polymerization of the same monomer, this time in pyridine solutions of sodium tetraphenylboride. Once again, polymer was formed only in the cathodic compartment, where the solution became orange-red after about 15 minutes of electrolysis. The polymerization was of a living type as shown by an increase in molecular weight on subsequent addition of monomer. Comparisons were made between the homogeneous polymerizations performed in pyridine solutions and heterogeneous polymerization carried out in  $\text{NH}_3$  solutions.

An interesting technique was devised by Funt and Bhadani (56) which enabled them to maintain a constant concentration of living ends in systems where these are slowly destroyed by some kinds of attrition reactions. In the particular case of isoprene in tetrahydrofuran, the current was automatically regulated by an electronic feedback device to maintain constant optical absorbance, viz., a constant concentration of living ends. The technique presents some practical difficulties however, in that one must be assured of having exactly the same concentration of living ends in all parts of the cell at a given time. Secondly, the report by Worsfold and Bywater (57) indicates, that isoprene living anions in tetrahydrofuran are subject to isomerization reactions leading to very complex UV spectra. As the relative initiating ability of the individual isomers is not known, the selection of a wavelength at which to monitor the concentration of living ends is rather arbitrary. Nevertheless, kinetic studies under these conditions showed a first-order rate dependence on the concentration of monomer, which was in agreement with the general theory of living polymerization.

The possibility of employing the electroinitiation technique to produce polymers with predetermined molecular weights and molecular weight distributions was investigated by Funt and Richardson (58). They found that the styrene monomer was not suitable for studies by direct initiation due to its extremely high rate of propagation in polar media necessary for electrolysis. However, this difficulty could be circumvented by using an indirect method, i.e., by initiating the polymerization of styrene by living  $\alpha$ -methylstyrene oligomers, prepared by electrolysis prior to addition of styrene.

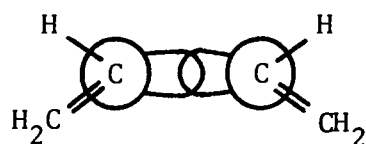
A mathematical interpretation of parameters, which have influence on the molecular weight and molecular weight distribution for polymerizations initiated by electrolysis was presented by Laurin and Parravano (59). Their objective was to maintain a constant kinetic chain length by controlling the current during the

polymerization. Two typical cases were considered, viz., a direct current control of a system propagating by a free radical mechanism, and an alternating current control of ionically polymerizing systems.

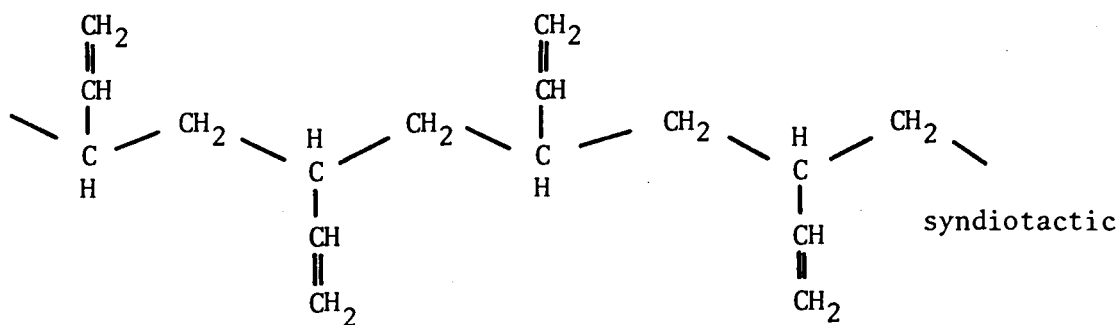
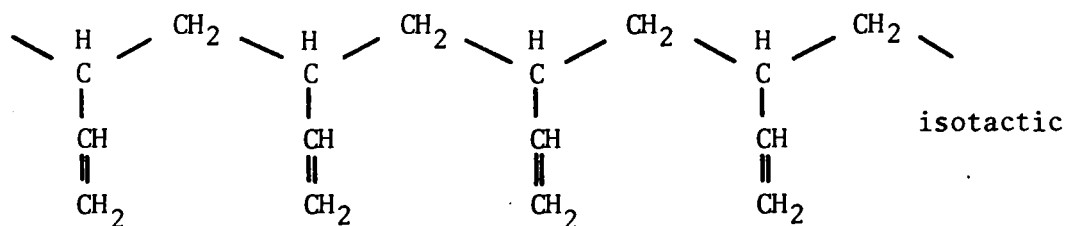
#### 1.4. Butadiene Polymers

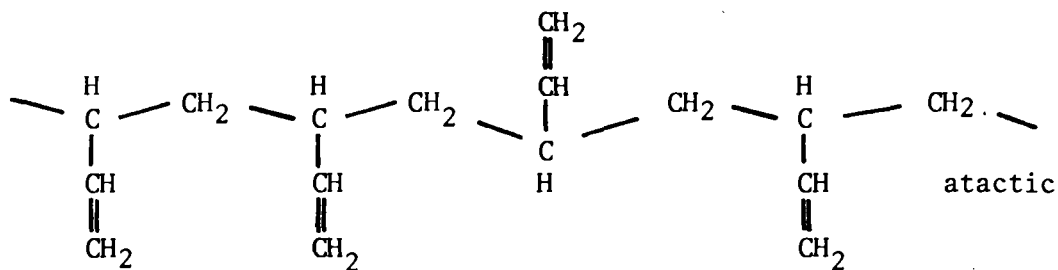
##### 1.4.1. Introduction.

The presence of two double bonds in a molecule of butadiene gives rise to a variety of possible polymer structures unparalleled in simple vinyl monomers. The  $C_2-C_3$  bond in the monomer is shorter than a single C-C bond, but has more  $\sigma$ -character than  $C_1-C_2$  and  $C_3-C_4$  bonds.

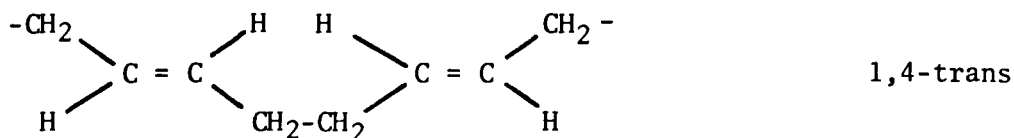
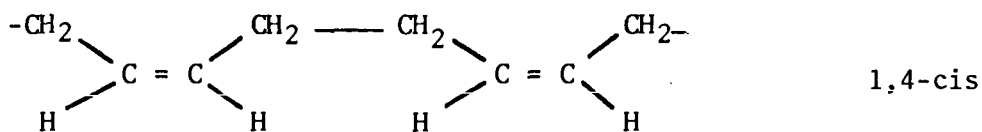


Because of this character, molecules of butadiene can be concatenated via a 1,4- or 1,2-addition. A 1,2-addition is essentially identical with the polymerization of vinyl monomers such as styrene, and can produce three types of polymers, viz., isotactic, syndiotactic and atactic.





A 1,4-addition, on the other hand, gives rise to two types of polymer, viz., 1,4-cis and 1,4-trans polybutadiene:



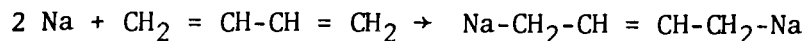
This gives us a total of five possible steric arrangements. Most polymerization processes yield macromolecules which are composed of all the isomers in various proportions. Such polymers can be regarded as true copolymers, since the individual stereo isomers in pure state differ markedly from each other as to their physical and chemical properties. For example, 1,4-cis polybutadiene is a rubber, whilst 1,4-trans polybutadiene is a crystalline powder.

An investigation of butadiene polymerization is complicated by another problem. Whereas in the polymerization of simple vinyl compounds the double bond of the monomer disappears in the polymer, in diene polymerization the polymer retains one double bond per monomer unit either in the main chain (1,4-addition) or as a pendant vinyl group (1,2-addition). This unsaturation may be disadvantageous. Under some conditions the polymer units can act as a further vinyl unit and undergo inter- or intramolecular cross-linking and branching reactions with a corresponding change in the properties of the resultant polymer. Similarly, unwanted oxidation reactions may occur with the same result.



1.4.2. Anionic Polymerization of Butadiene.

The first anionic polymerization of butadiene by the action of alkali metal (Na) was reported as early as 1910 by Lebedev (60). The studies were continued by the same author and Ziegler in the twenties. According to Ziegler (61, 62, 63), the process was heterogeneous and initiated by disodium compounds, e.g.



The "sodium" polymers of butadiene were utilized in Russia and Germany before and during the World War II as substitutes for natural rubber (BUNA). Their production was later abandoned, because rubbers of better quality could be produced by the copolymerization of butadiene with styrene in emulsion (BUNA-S).

The possibility of polymerizing butadiene by organolithium compounds was discovered by Ziegler and Jakob (64) in 1934. The process was patented in 1956 (65). Russian researchers (66, 67) and Kuntz and Gerber (68) studied the effects of various factors on the microstructure of the resultant polymer. TABLE II shows the results of experiments carried out by Kuntz and Gerber in pure n-heptane and in the presence of small amounts of ethylether, tetrahydrofuran and methyl tetrahydrofuran:

TABLE II

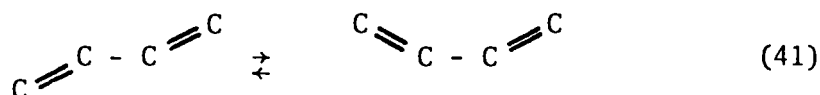
Polymerization of Butadiene in n-Heptane in Absence and Presence of Ethers (Ref. 68)

| Structure     | Ether |            |     |        |
|---------------|-------|------------|-----|--------|
|               | None  | Ethylether | THF | Me-THF |
| 1,2 [%]       | 10    | 29         | 51  | 46     |
| 1,4-trans [%] | 44    | 38         | 24  | 30     |
| 1,4-cis [%]   | 46    | 33         | 25  | 24     |

An experiment in which butadiene was polymerized in the presence of a very large concentration of tetrahydrofuran yielded a polymer with 87% of the 1,2-addition. It is therefore evident that the polar reagents alter the course of polymerization to yield enhanced 1,2 polymer microstructure. In a non-polar solvent such as heptane, the polymerization results in approximately equal amounts of 1,4-trans and 1,4-cis addition and a comparatively small amount of 1,2-addition.

It is interesting to compare these results with those reported for the analogous polymerization of isoprene. Morita and Tobolsky (69) reported that isoprene gives a polymer with 91% cis-1,4 and 9% 3,4-structure in heptane or benzene, whereas in tetrahydrofuran polyisoprene with 69% 3,4- and 31% 1,2-addition is obtained.

These phenomena have been studied by a number of authors. It is generally recognized that a molecule of butadiene can exist in the s-cis or s-trans configuration with rotation about the central carbon-carbon bond:



The trans form is more stable than the cis form by about 2000 cal/mole. The situation is reversed in the case of isoprene, where the cis conformation is more stable than the trans form by 900 cal/mole. As a result, butadiene at room temperature contains less than 4% of the cis form, whilst isoprene contains close to 90% of the cis conformer. These equilibria presumably have a dominant effect on the polymerization of diene monomers in non-polar solvents (70).

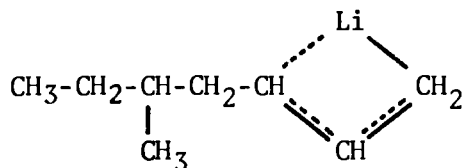
Makowski, Lynn and Bogard (71) studied the microstructure of polybutadiene as a function of the degree of polymerization.

Butyllithium was used as initiator in various aliphatic solvents. Interestingly, they found that the first few monomer units are incorporated largely in a 1,2 manner. With growing degree of polymerization the 1,2 percentage decreases, until it reaches about 10% at  $\bar{P}_n = 50$ . A later paper by Makowski and Lynn (72) studied the effects of polar lithium compounds such as alkoxides which are reported to enhance the amount of the 1,2-moiety.

The dramatic effect of polar compounds on the ratio of 1,2 and 1,4 structures has not yet been fully explained. It should be noted that the presence of a polar solvent such as tetrahydrofuran in the reaction mixture may result in a quite different reaction mechanism. Szwarc (73) has shown that addition of dienes to a chain end in tetrahydrofuran probably occurs only with the monomer being in a trans configuration. O'Driscoll (74) considered the effect of monomer configuration on the rate of propagation of butadiene, isoprene and 2,3-dimethylbutadiene. This configurational effect can be evaluated separately from the electronic effect of substitution of C<sub>2</sub>, C<sub>3</sub> hydrogens by methyl. Naylor, Hsieh and Randall (75, 76) carried out the reactions of 1,3-butadiene with sec-butyllithium in the ratios 1:2, 1:1, 2:1, 3:1 and 10:1, both in polar and non-polar media. The products were analyzed by a combination of chemical and physical methods. They suggested, that the polybutadiene configurations are the result of a two-step process:

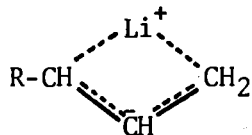
- a) addition of butadiene to an alkyllithium or living polymer end unit to form an alkenyllithium complex, and
- b) removal of the lithium through further addition or termination reactions which then result in a particular configuration.

For sec-butyllithium - butadiene adducts, a 5-methylheptyl complex of an allylic type (A) is considered reasonable, in which lithium is  $\sigma$ -bonded to the 1 position and back-bonded to the number 3 carbon.



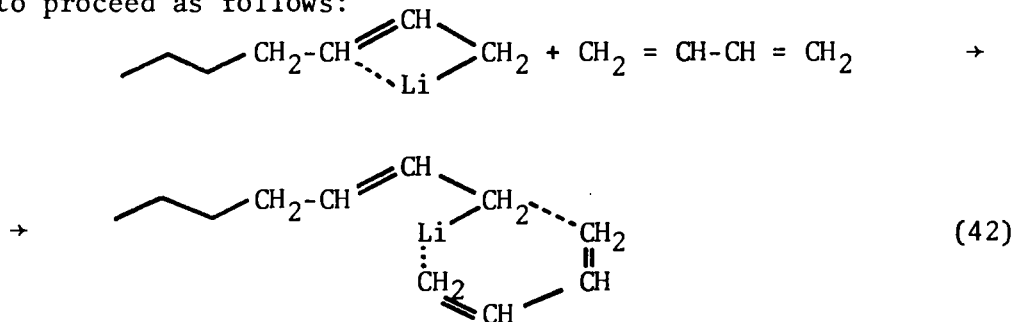
(A)

Hence, 1,4- or 1,2-addition in the polymer would occur by butadiene addition to the 1 or 3 position respectively. The presence of tetrahydrofuran in the reaction mixture can effect polarization in the complex to the extent that a substantial lithium-carbon bond is formed at the 3 position that may approach the delocalized  $\pi$ -complex B:

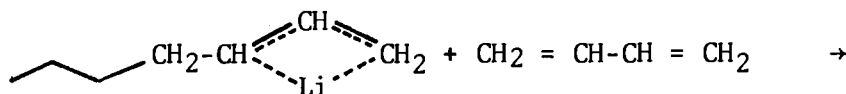


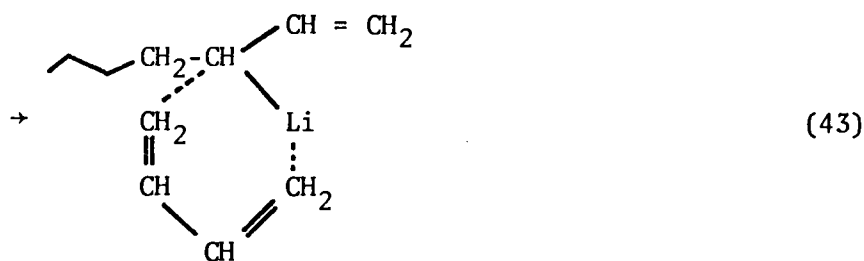
(B)

Consequently, polymerization in a nonpolar environment is envisioned to proceed as follows:



Polymerization under conditions which favor delocalization such as depicted by (B) will lead to a higher 1,2 content:





Randall and Silas (77) investigated hydrogenated butadiene oligomers by gas chromatography and determined the applicability of Markov chain statistics to the system. The hydrogenated butadiene oligomers could be defined in terms of Markov chain theory (78). For a first order Markov chain, transition probabilities for a two-unit sequence are considered as follows:

$P_{11}$  ... probability for a monomer unit to add 1,2 to a preceding 1,2 unit

$P_{10}$  ... probability for a monomer unit to add 1,4 to a preceding 1,2 unit

$P_{01}$  ... probability for a monomer unit to add 1,2 to a preceding 1,4 unit

$P_{00}$  ... probability for a monomer unit to add 1,4 to a preceding 1,4 unit.

A second order Markov chain takes into account the penultimate unit configuration, hence eight different additions as characterized by their transition probabilities ensue.

Moving from lithium to other alkali metals a more ionic character of the metal-hydrocarbon interaction is expected. This should affect the character of the transition state and consequently the microstructure of the resultant polymer. Very little investigation has been done in this direction. Meyer, Hampton and Davison (79) compared the microstructures of polybutadienes catalyzed by various alkali metals in a hydrocarbon solvent. The results compiled in Table III give ample evidence of the profound effect of the

alkali metal in this non-polar medium.

TABLE III

Microstructure of Alkali Metal Initiated Polybutadienes in Hydrocarbon Media (Ref. 79)

| Metal | Structure   |               |         |
|-------|-------------|---------------|---------|
|       | 1,4-cis [%] | 1,4-trans [%] | 1,2 [%] |
| Li    | 35          | 52            | 13      |
| Na    | 10          | 25            | 65      |
| K     | 15          | 40            | 45      |
| Rb    | 7           | 31            | 62      |
| Cs    | 6           | 35            | 59      |

On the other hand, a much smaller effect of the cation was reported in polar solvents. Tobolsky and coworkers (80) studied the effects of the counterion on microstructure for all alkali metals. The polymerizations were initiated by alkali metal naphthenates in tetrahydrofuran. The results are shown in Table IV.

TABLE IV

Effect of Counterion on Polybutadiene Microstructure in Tetrahydrofuran (Ref. 80)

| Metal | Li | Na | K    | Rb   | Cs   |
|-------|----|----|------|------|------|
| 1,2   | 96 | 91 | 82.5 | 75.3 | 74.7 |
| 1,4   | 4  | 9  | 17.5 | 24.7 | 25.3 |

It is evident, that the amount of 1,2 structure decreases with the growing atomic weight of the counterion.

The results of Basova et al. (81) and Arest-Yakubovich and Medvedev (82, 83) indicate that although some differences occur at temperatures over 0°C, the microstructure is practically independent of the counterion at temperatures below -50°C. The results of Arest-Yakubovich and Medvedev are shown in Table V.

TABLE V.

Dependence of Polybutadiene Microstructure on Temperature (Ref. 82)

| Temperature<br>[°C] | Structure* | % of structure in presence of cation |      |      |
|---------------------|------------|--------------------------------------|------|------|
|                     |            | Li                                   | Na   | K    |
| 40                  | 1          | 79.6                                 | 78.0 | 66.9 |
|                     | 2          | 10.4                                 | 17.2 | 26.3 |
|                     | 3          | 10.0                                 | 4.8  | 6.8  |
| 10                  | 1          |                                      | 79.9 | 68.8 |
|                     | 2          |                                      | 16.7 | 25.8 |
|                     | 3          |                                      | 3.4  | 5.4  |
| -30                 | 1          | 87.2                                 | 86.7 | 78.8 |
|                     | 2          | 12.8                                 | 13.3 | 19.2 |
|                     | 3          | 0                                    | 0    | 2.0  |
| -56                 | 1          | 90.3                                 | 89.1 | 87.0 |
|                     | 2          | 9.7                                  | 10.9 | 13.0 |
|                     | 3          | 0                                    | 0    | 0    |

\* 1: 1,2; 2: 1,4-trans; 3: 1,4-cis.

Solvent = Dimethoxyethane

#### 1.4.3. Kinetics of the Anionic Polymerization of Butadiene.

The kinetic aspects of the anionic polymerization of butadiene have been studied very little in comparison with monomers

such as styrene or  $\alpha$ -methylstyrene. In hydrocarbon solvents the study of polymerization rates in systems initiated by organolithium compounds is generally hampered by the association behavior of these initiators in such media (84). Various degrees of association are the most likely explanation for apparent discrepancies between the data published by various authors (85, 86, 87, 88).

The rates of polymerization observed in polar solvents are much higher than those determined in hydrocarbons. For example, Morton et al. (86) found that the second order propagation rate constant of n-butyllithium initiated polybutadiene at 30°C was 1.53 litre/mole sec in tetrahydrofuran and only 0.10 litre/mole sec in n-hexane.

Very few papers report kinetic measurements in polar solvents. Morton et al. (86) determined the rate constants of anionic polymerization of butadiene and isoprene in tetrahydrofuran by n-butyllithium. Their assertion that the propagation proceeds exclusively through ion-pairs is criticized by Bywater and Worsfold (34). They point out that the deductions made by Morton et al. may have been erroneous as they did not take into account the isomerization and/or attrition of growing species. Such reactions could be sufficient to mask the small deviations in kinetics caused by the dissociation of ion-pairs. Smid (89) also notes that in Morton's work the monomer concentration was very high (up to 7.5 mole/litre) and consequently the dielectric constant of the reaction mixture was substantially lower than that of pure tetrahydrofuran. Some degree of association of the butyllithium initiator was possible under such conditions.

The rate of polymerization depends to a high degree on the nature of the alkali metal and the solvent. Most informative in this respect are the papers by Arest-Yakubovich and Medvedev (82,83). Their results are compiled in Table VI. Data denoted by asterisk were extrapolated from reference (86).



TABLE VI

Propagation Constants of the Anionic Polymerization of Butadiene (Ref. 82)

| Cation      | Temperature [°C] | $k_p$ [litre/mole sec] |
|-------------|------------------|------------------------|
| Solvent THF |                  |                        |
| Li          | +10              | 0.85*                  |
| Li          | -30              | 0.14*                  |
| Li          | -56              | 0.03*                  |
| Na          | +10              | 5.4                    |
| Na          | -30              | 1.8                    |
| Na          | -43              | 1.05                   |
| Na          | -56              | 0.60                   |
| Na          | -82              | 0.40                   |
| Na          | -96              | 0.29                   |
| K           | +10              | 70                     |
| K           | -30              | 17.0                   |
| K           | -56              | 3.1                    |
| K           | -96              | 0.16                   |
| Solvent DME |                  |                        |
| Li          | -30              | 2.2                    |
| Li          | -56              | 1.0                    |
| Na          | -30              | 23                     |
| Na          | -56              | 8                      |
| K           | -56              | 16                     |

It should be noted, that the rate constants listed in Table VI are not absolute and comprise the contributions of both free ion and ion-pair propagation.

#### 1.4.4. Stability of Butadiene Living Polymers in Polar Solvents.

Whereas the stability of living polybutadiene in hydrocarbon solvents is quite good, the situation in the case of polar solvents is much more complicated. This is due to the possibility of spontaneous isomerization and destruction reactions. The ultraviolet absorption spectra of relevant systems were studied by Bywater and coworkers (90) and Polyakov et al. (91). Although polybutadienyl lithium did not isomerize, carbanions from butadiene with both sodium and potassium showed a far more complex behavior. For example, the initial species in the case of polybutadienyl sodium could not be observed because of a rapid isomerization. A similar situation was found when butadiene was replaced by isoprene. Gourdenne and Sigwalt (92, 93) investigated these phenomena in more detail, especially in respect to the reaction temperature. Their results show the very low stability of living anions at room temperature, whilst at temperatures below  $-40^{\circ}\text{C}$  the stability was sufficient for the synthesis of block copolymers.

#### 1.4.5. Electrolytically Initiated Polymerization of Butadiene.

Yamazaki (94, 9) attempted to electropolymerize butadiene in a living system using tetraethylaluminium salts as electrolytes. He reported, however, that the electroinitiation and successive rapid propagation took place simultaneously and the polymers had improbably wide molecular weight distributions. For this reason he abandoned further investigation of such systems.

Controlled potential electroinitiation of butadiene was reported by Yamazaki, Tanaka and Nakahama (12). Because of the non-living character of the system employed, only low molecular weight polymers were prepared in a very low yield. In particular, the termination was caused by the reaction of the carbanions with the tetrabutylammonium cation necessary for the controlled potential electrolysis.

Several groups investigated the reactions of the products of Kolbe electrolysis in the presence of butadiene (95, 96, 97). The reactions led to dimers or low oligomers on most occasions. Yamazaki and Murai (98) prepared n-hexadecatetraene by the tetramerization of butadiene, which was produced by an electrolytic reduction at the cathode. Dimerization of butadiene at the anode was reported by Schafer and Steckhan (99).

The work of Levy and Myers (100) is also noteworthy. They employed continuous electrolysis in liquid ammonia, and observed the ESR spectrum of 1,3-butadiene radical-anions. The spectra were compared with those predicted by simple Hückel theory.

## 2. EXPERIMENTAL METHODS

### 2.1. Chemicals and Their Purifications.

Tetrahydrofuran (Fisher Certified) was purified according to the procedure described by Fetters (101). The pure solvent was stored over a fresh sodium mirror on the vacuum line.

Cyclohexane (Fisher Certified) was passed through a column containing active alumina. The product was dried by stirring with calcium hydride and subsequently flash-distilled onto a sodium mirror. The pure solvent was stored over sodium-potassium alloy in vacuum.

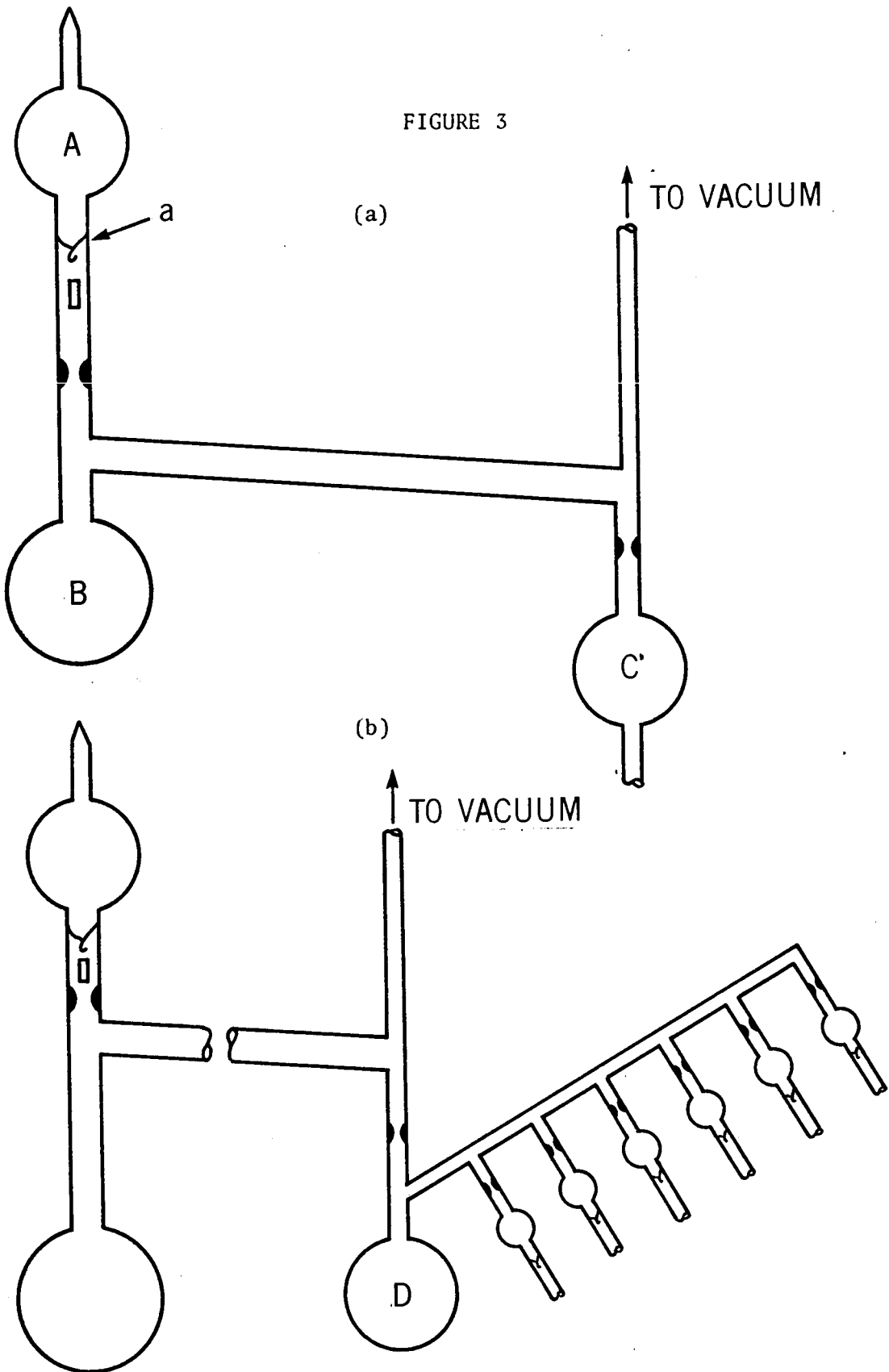
Sodium tetraphenylboride (Fisher Certified) was used as supplied by the manufacturer.

Lithium, potassium, rubidium, tetrabutylammonium and tetramethylammonium salts of tetraphenylboride were prepared by the methods reported by Bhattacharyya et al. (31). The re-crystallized salts were stored in a vacuum desiccator.

Hexamethylphosphoramide (HMPA) (Eastman Organic) was filtered through a column of active alumina and subsequently stirred over anhydrous  $\text{Na}_2\text{SO}_4$ . It was then distilled under 15 mm of argon into flask A provided with a break-seal and the flask sealed off. The flask was then attached to an all-glass distillation unit (Figure 3a). This was evacuated on the vacuum line and a sodium mirror produced in bulb B. Break-seal a was crushed and HMPA allowed to react with the mirror. The liquid was transferred into the bulb C by distillation. The entire procedure could be repeated as many times as required. In the final step, the solvent was distilled into a flask D furnished with a set of pre-calibrated break-sealed bulbs attached to a side arm (Figure 3b). By tilting the assembly, the liquid could be transferred into the bulbs, which were subsequently sealed off. The filled bulbs were stored in

Figure 3a,b DISTILLATION ASSEMBLY FOR THE PURIFICATION OF  
HEXAMETHYLPHOSPHORAMIDE

FIGURE 3



a refrigerator.

Butadiene (Matheson, instrumental grade) was dried by passing through columns of molecular sieve (A5) and silica gel, and stored over calcium hydride. Styrene (Eastman Organic) was dried by stirring over calcium hydride and then vacuum distilled. The central cut was then flash-distilled on the vacuum line and stored over calcium hydride at 0°C.

## 2.2. Polymerization Procedure.

A typical filling and polymerization assembly is shown in Figure 4. The apparatus consisted of an electrolytic cell, with anode and cathode compartments separated by a fine fritted disc. Square platinum electrodes, each  $6.451\text{cm}^2$  in area, were employed. The total capacity of the anode and cathode compartments was 110 ml.

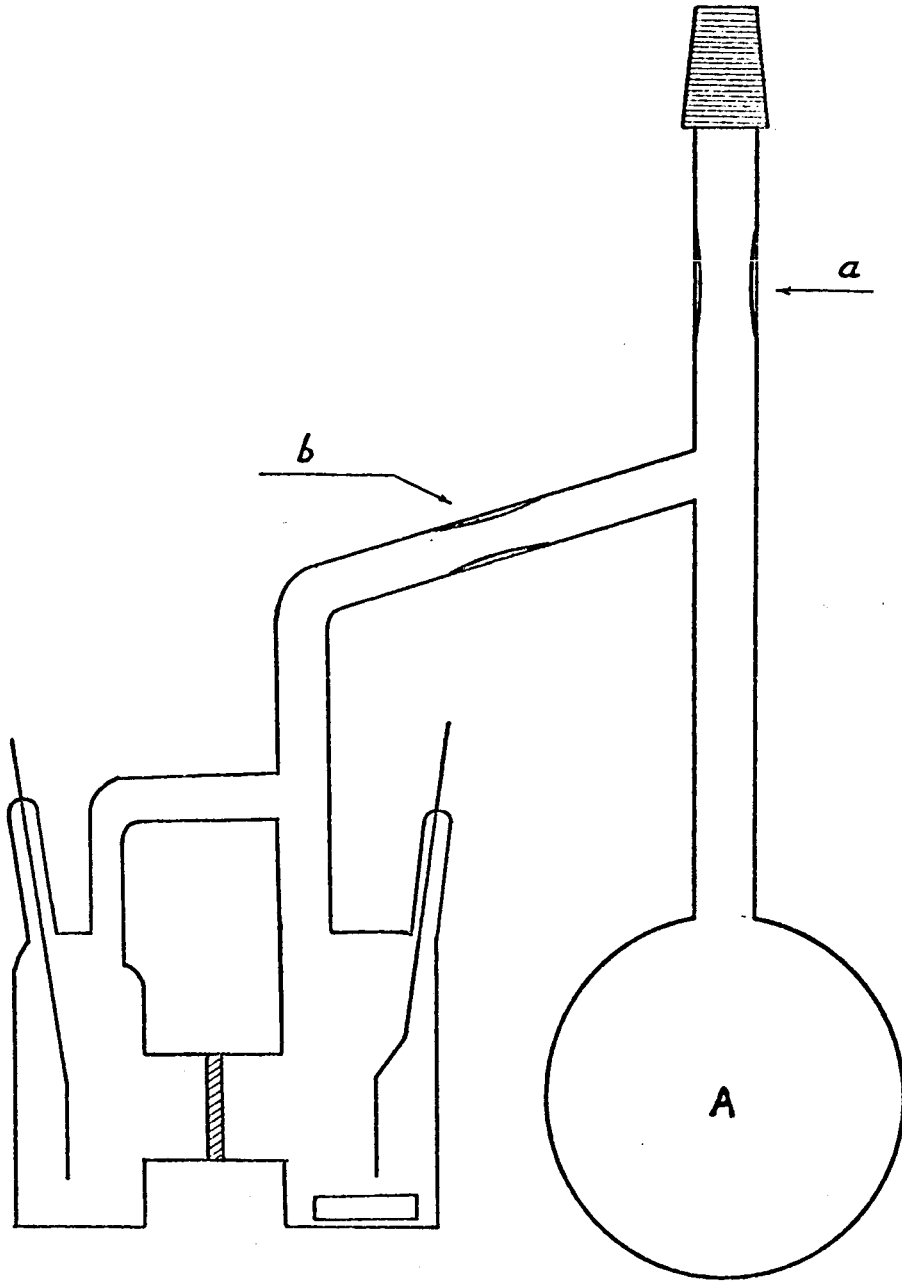
For an experiment, the required amount of the tetraphenylboride salt was placed into the filling bulb A and the assembly was attached to the vacuum line. The system was evacuated for 24 hours with intermittent heating to remove the volatile impurities. The solvent was then introduced into the filling bulb. Volatile solvents such as tetrahydrofuran or cyclohexane could be directly flash-distilled into the system from a graduated cylinder joined to the vacuum line. For the non-volatile HMPA, the assembly was equipped with a side-arm, to which a break-sealed storage bulb containing a known volume of the solvent could be attached. After the solvent had been transferred into the filling bulb by crushing the break-seal, the side-arm was sealed off.

The required amount of butadiene was then flash-distilled into the filling bulb submerged in liquid nitrogen, from a graduated cylinder held at -78°C. The frozen contents of the filling bulb were then allowed to thaw and were thoroughly degassed by alternate freeze and thaw cycles. The mixture was finally frozen with liquid nitrogen and the assembly was sealed off from the vacuum line at constriction a. The contents of the filling bulb were then

Figure 4. POLYMERIZATION CELL AND FILLING ASSEMBLY  
A..... filling bulb  
a,b..... breakseals



FIGURE 4



melted at  $-78^{\circ}\text{C}$  and transferred into the electrolytic cell. The low temperature ensured that the loss of the monomer due to vapor pressure was minimal. The charged cell was detached from the filling bulb by sealing off at constriction b.

The electrolytic cell was then placed in a constant temperature bath. A constant current was passed through the solution until a persistent yellow color was formed at the cathode. This indicated the complete removal of reactive impurities. Preliminary experiments indicated that current reversal destroyed the living anions stoichiometrically and thus zero concentration of the living anions could be achieved by this process of electrochemical titration. The intense yellow color of the polybutadienyl anions makes possible a visual or spectrophotometric determination of the end-point. Care was taken to produce only a very low concentration of living anions in the pre-electrolysis period in order to minimize the polymerization reaction.

The pre-electrolyzed solution was ready for an experiment. A known charge  $Q$  [coulombs] was passed through the solution. A KEPCO ABC 1000 (M) was used as a constant current supply. The required concentration of living ends was thus formed in the cathodic compartment. The sample was then allowed to polymerize for a selected period of time. Termination was effected either by opening the cell and injecting methanol into the sample, or by applying current of opposite direction. In the latter instance the termination was spread over a finite period of time and once again the zero-concentration point could be determined visually. The reaction could subsequently be re-initiated and the whole process repeated as many times as an experiment might demand. A more detailed description of current programming is included later.

Two methods of polymer isolation were used in this work. Polymers, whose molecular weight was sufficiently high ( $\bar{M}_n > 50000$ ), could be precipitated into an excess of methanol to which a small

amount of N-phenyl- $\beta$ -naphthylamine was added as an antioxidant. The precipitated polymer was re-dissolved in benzene, coagulated in methanol and dried to constant weight in vacuum. The dry polymer was weighed and stored at  $-30^{\circ}\text{C}$ .

Low-molecular weight polymers ( $\bar{M}_n < 50000$ ) were found to be partially soluble in methanol and were therefore not precipitated. After the polymerization, the cell was opened and the contents of the cathodic compartment stabilized by injecting a small amount of N-phenyl- $\beta$ -naphthylamine dissolved in methanol. The cathodic solution was subsequently withdrawn from the cell and transferred into a 125 ml Erlenmeyer flask. The residual butadiene was removed under vacuum. The concentration of the polymer was determined by pipetting an aliquot of the solution into a Petri dish and evaporating the solvent. The correct weight of the polymer was obtained by subtracting the weight of the supporting electrolyte in the aliquot from the total weight of the residue after evaporation.

The experimental technique used for the butadiene-styrene copolymerization experiments was very similar to the one just described. The styrene monomer was first flash-distilled into a graduated cylinder and the required amount was then transferred into the filling bulb in the same manner. The copolymer was isolated by precipitation from methanol.

### 2.3. Determination of Microstructure.

#### 2.3.1. Infrared Spectroscopy.

A polymer sample was dissolved in carbon disulphide to approximately 1% concentration by weight. The solution was filtered through a glass filter to remove foreign matter and the insoluble gel fraction of the polymer. The exact concentration of the solution was determined by pipetting an aliquot into a Petri dish and evaporating the solvent. The spectra were recorded using a Beckman IR-12 instrument. The calibration reported by Morero and coworkers (102) was employed

to calculate the percentages of the individual components from the spectra. The values of the absorption coefficients for the three principal configurations are listed in Table VII together with the particular wavelengths. Figure 5 shows an IR absorption spectra of a predominantly 1,2-polybutadiene.

The total absorption at each wavelength is given by the sum of absorption of the individual configurations; hence a set of three linear equations must be solved to find the concentrations of the 1,2, 1,4-trans and 1,4-cis components:

$$A_{10.34} = (K_{1,4\text{-trans}}^{10.34} \cdot P_{1,4\text{-trans}} + K_{1,2}^{10.34} \cdot P_{1,2} + K_{1,4\text{-cis}}^{10.34} \cdot P_{1,4\text{-cis}}) \cdot S \quad (44)$$

$$A_{10.95-10.98} = (K_{1,2}^{10.98} \cdot P_{1,2} + K_{1,4\text{-cis}}^{10.98}) \cdot S \quad (45)$$

$$A_{13.50-13.65} = (K_{1,2}^{13.50} \cdot P_{1,2} + K_{1,4\text{-cis}}^{13.50}) \cdot S \quad (46)$$

TABLE VII

Absorption Coefficients for the Infrared Analysis of Polybutadienes  
(in  $\text{mg}^{-1}\text{cm}^{-1} \cdot 10 \text{ ml}$ ) (Ref. 102)

| Wavelength<br>[ $\mu$ ] | 1,4-trans             | 1,2                    | 1,4-cis                |
|-------------------------|-----------------------|------------------------|------------------------|
| 10.34                   | $23.3 \times 10^{-3}$ | $0.828 \times 10^{-3}$ | $0.609 \times 10^{-3}$ |
| 10.95-10.98             | -                     | $26.7 \times 10^{-3}$  | $0.107 \times 10^{-3}$ |
| 13.50-13.65             | -                     | $0.231 \times 10^{-3}$ | $5.73 \times 10^{-3}$  |

In Equations 44 - 46,

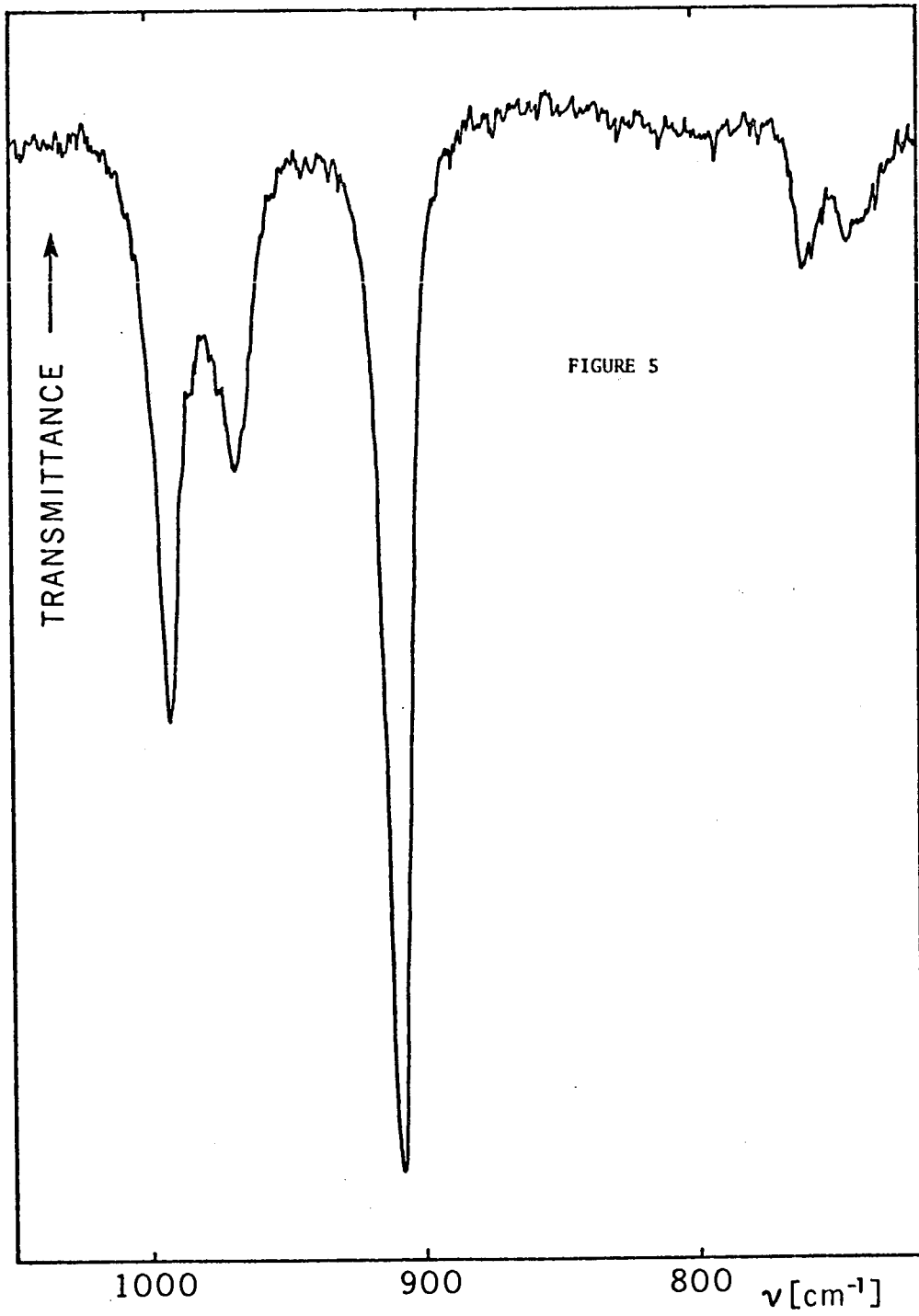
$A_{\lambda}$  is the absorbance at wavelength  $\lambda$

$K_n^{\lambda}$  is the absorption coefficient for wavelength  $\lambda$   
and configuration n, dimension [ $\text{mg}^{-1}\text{cm}^{-1} \cdot 10 \text{ ml}$ ]

$P_n$  is the weight of a component in 10 ml of solution

S is the optical path in [cm] .

Figure 5. INFRARED SPECTRUM OF A PREDOMINANTLY 1,2-POLYBUTADIENE



### 2.3.2. NMR Spectroscopy

A polymer sample was dissolved in carbon disulphide to form an approximately 10-15% solution. The solutions could not be filtered because of very high viscosity, and were transferred into an NMR tube by means of a hypodermic syringe. Spectra were recorded at room temperature using a Varian A-56/60A instrument. Tetramethylsilane was used as an internal standard.

Methods described by Senn (103) and Mochel (104) were employed to evaluate the spectra. No calibration is necessary, each spectrum is self-calibrating. The composition of a polymer can be calculated directly from the ratio of the areas under the corresponding peaks. Figure 6 shows a 60 MHz spectra of atactic 1,2-polybutadiene. An aromatic proton spectrum of atactic polystyrene is shown in Figure 7.

The same procedure was used for the analyses of butadiene-styrene copolymers. However, carbon disulphide was replaced by D-chloroform in this case.

### 2.4. Determination of Molecular Weights and Molecular Weight Distributions.

Molecular weights and molecular weight distributions were measured by the gel permeation chromatography. A model 301A chromatograph manufactured by Waters Associates was employed with a differential refractometer as the detecting device. Figure 8 shows a block diagram of the apparatus.

The chromatograph was equipped with five styragel columns of the following pore dimensions: 2000-5000 Å, 2000-7000 Å, 2 x 5000-15000 Å and 15000-50000 Å. All measurements were carried out in tetrahydrofuran. The instrument was in an air conditioned room maintained at 20°C. Constant flow rate of approximately 1 ml/minute was used throughout.

Samples containing approximately 0.25 g of polymer per 100 ml solution were used for the analysis. All solutions were filtered under pressure through a fine teflon filter to remove impurities

Figure 6. 60 MHz NMR SPECTRUM OF ATACTIC 1,2-POLYBUTADIENE  
CONTAINING 10% BY WEIGHT 1,4 ADDITION UNITS  
(Ref. 104)

Figure 7. 60 MHz AROMATIC PROTON NMR SPECTRUM OF ATACTIC  
POLYSTYRENE (Ref. 104)



FIGURE 6

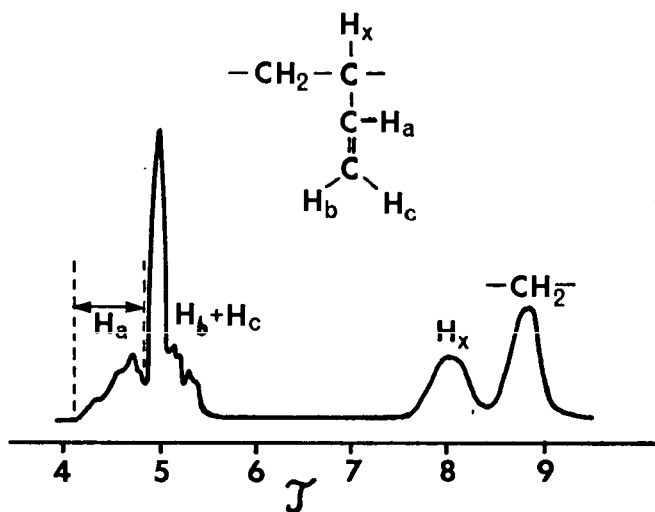


FIGURE 7

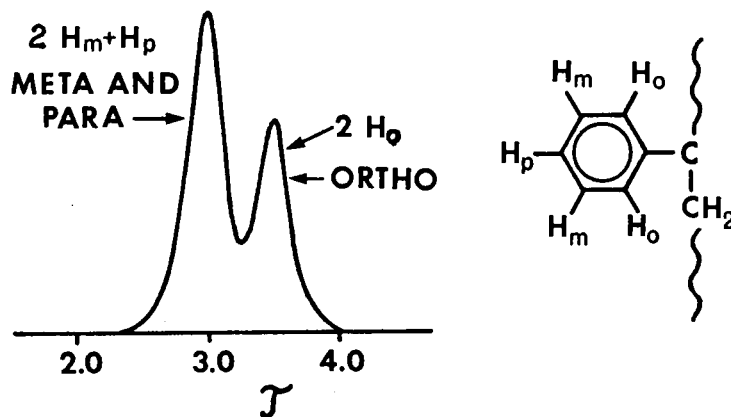


Figure 8. BLOCK DIAGRAM OF THE GPC INSTRUMENT

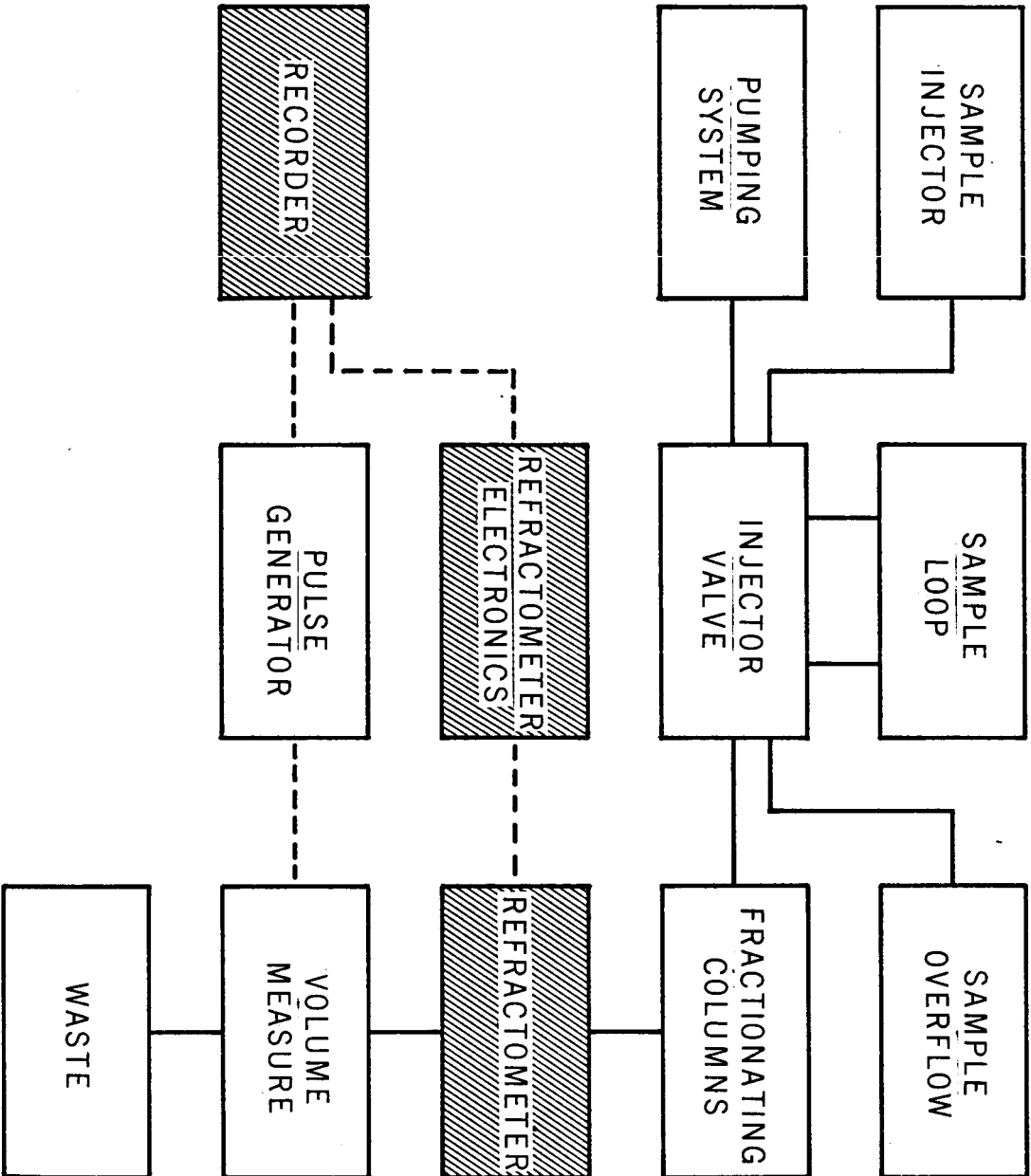


FIGURE 8

and undissolved polymer particles. Two millilitres of the sample solution were injected via the sample loop.

The separating efficiency of the instrument was checked regularly by recording the chromatogram of a 4  $\mu$ l sample of toluene. The number of plate counts calculated from such chromatograms was found to remain reasonably constant.

The columns were calibrated by a series of narrow molecular weight distribution polystyrene samples, supplied by Waters Associates. The calibration graph plots the peak molecular weights of standards against their GPC peak elution volume and is shown in Figure 9. Using this calibration curve, raw chromatograms of polystyrene samples could be evaluated in terms of molecular weights and molecular weight distributions. University of Waterloo MWD I computer program was used for this purpose. The analysis of polystyrene standards indicated a very good agreement between the values of molecular weight and polydispersity supplied by the manufacturer and those computed by the program. Table VIII compares the values of polydispersity ratio  $\bar{M}_w/\bar{M}_n$  for six polystyrene samples.

TABLE VIII

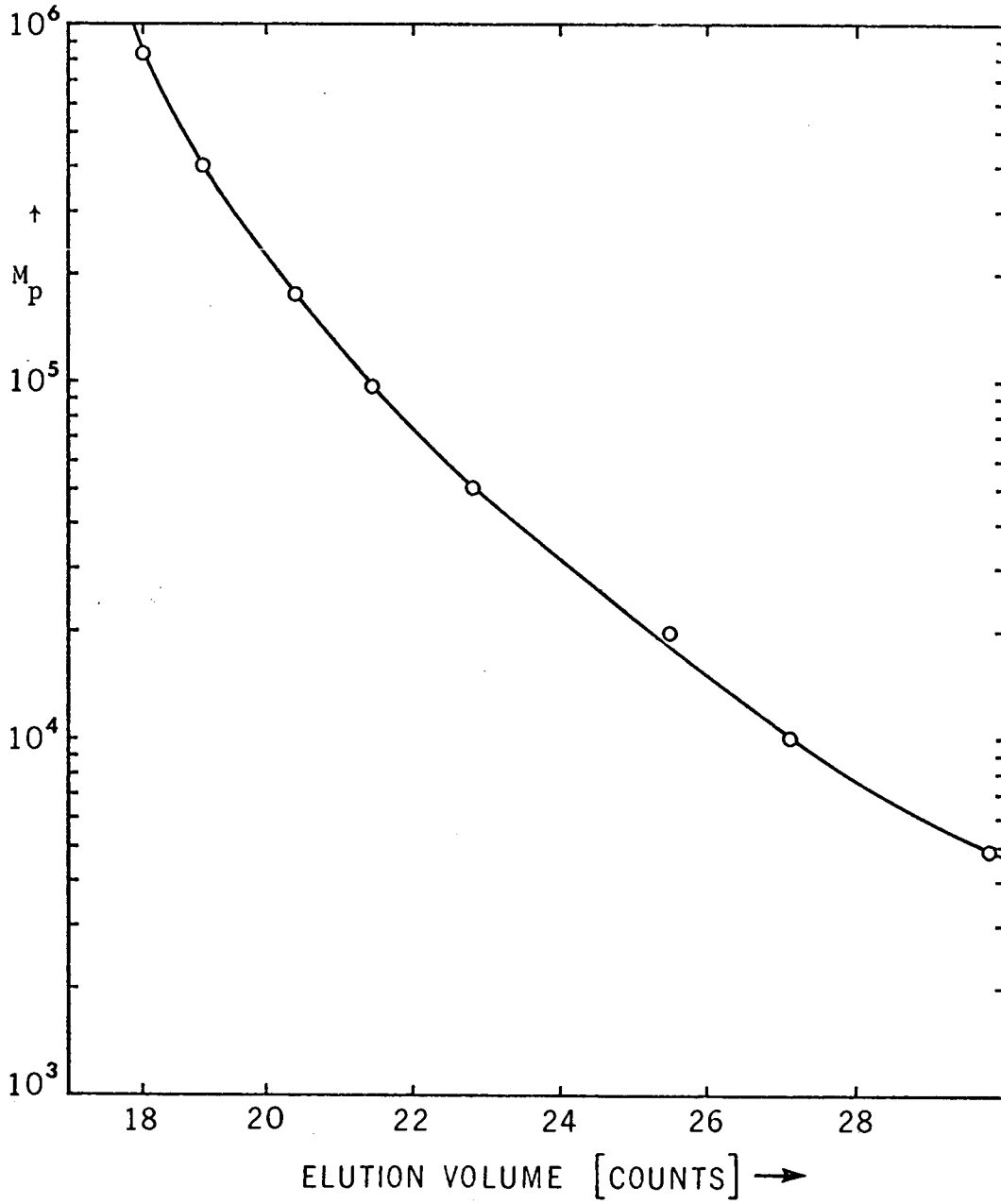
Evaluation of Polystyrene Standards by the MWD I Program.

| Sample | $\bar{M}_n$ | $\bar{M}_w/\bar{M}_n$ |          |
|--------|-------------|-----------------------|----------|
|        |             | Manufacturer          | Computed |
| 41984  | 163000      | 1.055                 | 1.070    |
| 41995  | 96200       | 1.021                 | 1.066    |
| 25170  | 49000       | 1.041                 | 1.047    |
| 25168  | 19650       | 1.010                 | 1.085    |
| 25171  | 9700        | 1.062                 | 1.085    |
| 25169  | 4600        | 1.087                 | 1.067    |

Figure 9. PRIMARY POLYSTYRENE CALIBRATION GRAPH FOR GPC

$M_p$ ..... GPC peak molecular weight

FIGURE 9



The MWD I program does not correct the chromatographic data for instrumental peak spreading. Such a correction was attempted employing the MWD II computer program of Chang and Huang (105). However, this program seemed to overcorrect the results regardless of the value of the resolution coefficient  $h$ , and the spreading correction was therefore not applied.

The considerations concerning the evaluation of polybutadiene chromatograms on the basis of the polystyrene calibration will be dealt with in a separate section.

### 2.5. Determination of the Limiting Viscosity Number

The viscosity measurements necessary for the GPC universal calibration were carried out in a Ubbelohde suspended level dilution viscometer. The flow times were measured at four concentrations and the limiting viscosity number calculated by the least squares method according to the equations given by Huggins (106)

$$\frac{\eta_{sp}}{c} = [\eta] + k' [\eta]^2 c \quad (47)$$

and Kraemer (107)

$$\frac{\ln \eta_r}{c} = [\eta] - k'' [\eta]^2 c \quad (48)$$

The values of  $[\eta]$  determined from these two equations agreed well in all cases and their arithmetic average was used for further calculations.

All measurements were carried out in tetrahydrofuran at  $20 \pm 0.05^\circ\text{C}$ . The initial concentration of polymer ranged from 0.5g/dl to 2.0 g/dl according to the molecular weight and the flow time desired.

### 2.6. Cyclic Voltammetry.

The cyclic voltammetry experiments were carried out according to the procedure described by Funt and Gray (14, 15). Tetrabutylammonium perchlorate and tetramethylammonium tetraphenylboride were used as supporting electrolytes.

### 3. RESULTS AND DISCUSSION

#### 3.1. Introduction.

A number of different approaches are possible to explore the various potentialities of electropolymerization reactions. A living polymerization technique provides, before all, an extremely powerful tool enabling the experimenter to produce polymers with pre-determined and "tailored" molecular weights and molecular weight distributions. The feasibility of performing such controlled reactions goes hand in hand with the basic simplicity of the living polymerization. As the molecular weight of a growing chain is, at constant temperature, only a function of time of polymerization and the concentration of monomer, it can be altered at will by any change in these parameters. Keeping the concentration of the monomer invariant, control of the molecular weight parameters may be effected by varying the time profile of the living end concentration in a pre-selected manner.

Electrolytic initiation of living polymers appears to be advantageous for this purpose as it permits one to create or destroy the required amount of living anions by a simple variation of electrochemical parameters. Although this type of control was qualitatively demonstrated previously in this laboratory (58), attempts to apply such methods quantitatively were thwarted as styrene was used as the monomer. The propagation rate of styrene was simply too high to permit the application of a direct electrolyte initiation with any degree of control.

Pilot experiments indicated that butadiene could be more suitable to continue these investigations. The relatively low propagation rate made possible propagation times sufficiently longer than the time of initiation, and consequently polymers of low polydispersity could be obtained.

#### 3.2. Polymerization of Butadiene.

##### 3.2.1. Kinetics of Polymerization.

The main objective was to produce polymers with pre-determined



molecular weights and molecular weight distributions. However, such work entails an accurate knowledge of the rate constants in the system under study. This investigation was undertaken because the rate constants available from the previous work (82, 86) were found not to be valid in the systems used. Furthermore, it became clear that the method of electrolytic initiation would provide a very suitable means for conducting kinetic measurements whose validity and applicability would extend beyond the immediate needs.

An electrolytic polymerization requires the presence of an electrolyte to render the solution sufficiently conductive. Provided the concentration of the electrolyte is high enough, the rates measured under such conditions correspond to the ion-pair growth (Section 1.3.2.).

In polar solvents such as tetrahydrofuran, the electron transfer initiation is known to be very fast (21, 89). Therefore, the propagation reaction is the rate-determining process. In the presence of an excess of a tetraphenylboride salt, the propagation of a living anionic polymerization was reported to proceed exclusively via ion-pairs (33, 34, 35). From these observations it follows that the propagation rate constant can be evaluated directly from the degree of conversion. The rate of polymer formation is equal to the rate of monomer disappearance and is given by:

$$-\frac{d[M]}{dt} = k_p [LE] [M] \quad (49)$$

where [LE] is the concentration of living anions, [M] is the instantaneous concentration of monomer and  $k_p$  is the second order rate constant.

The polymerization was initiated by passing a current  $i$  through the solution for time  $t_i$  secs, whereby a concentration [LE] of living ends was produced in the cathodic compartment:

$$[LE] = \frac{1000 i t_i}{FV} = \frac{1000 Q}{FV} \quad [\text{mole/litre}] \quad (50)$$

where  $F$  is the Faraday constant

$V$  is the volume of the cathodic compartment in [ml]

and  $Q$  is the charge passed in [coulombs].

The initiation is followed by a propagation period  $t_p$  during which no current is passed and the chains are allowed to grow. In the third phase the current is reversed, causing a stoichiometric destruction of living ends. If no attrition reactions were present the termination period  $t_t$  would equal  $t_i$  for a given current. The whole cycle may be repeated any number of times.

In order to solve Equation 49 for  $k_p$ , it is necessary to determine the effective average concentration of living ends  $[\overline{LE}]$  throughout the cycle:

$$\ln \frac{[M]_o}{[M]} = k_p \int_0^t [LE] dt = k_p [\overline{LE}] t \quad (51)$$

Equation 51 is valid for one initiation-propagation-termination cycle, but it is also applicable to the cumulative degree of conversion after any number of cycles:

$$\ln \frac{[M]_o}{[M]_{\text{final}}} = \bar{k}_p [\overline{LE}] t_{\text{total}} \quad (52)$$

In Equation 52,  $[\overline{LE}]$  is the average concentration of living ends over  $n$  cycles. The net effect of repeated initiation-propagation-termination cycles is to average the  $k_p$  value, which, instead of being calculated for one isolated experiment, is now obtained as an average value of  $n$   $k_p$ 's respective to the individual cycles.

The evaluation of the average effective concentration of living ends is complicated by the occurrence of side reactions. The active chain ends can isomerize to give inactive species, or their concentration may be gradually reduced by the scavenging effects of slowly reacting impurities, the solvent or the supporting electrolyte. As the exact nature of the side reactions taking place is indeterminate in this system, it is necessary to postulate the

overall reaction kinetics. In the ensuing reaction scheme, it is assumed that the overall rate of attrition is constant throughout the interval  $(t_i + t_p + t_t)$  and independent of the concentration of living ends.

$$-\frac{d[LE]}{dt} = K \quad (53)$$

Such an assumption is reasonable due to the low extent of the attrition reaction (10%). For the accuracy attainable in these systems, it is not possible to distinguish between this and a first-order attrition mechanism.

With a spontaneous decay of living ends, the time  $t_t$  of the electrolytic termination is not equal to the time  $t_i$  of the electrolytic initiation. The difference  $\Delta t = t_i - t_t$  is determined experimentally by the electrolytic titration and represents a measure of the attrition rate expressed by Equation 53. For simplicity, the charge passed,  $Q$ , is considered as the measure of the number of living ends generated in the system. The time profile of the living end concentration in the various phases of one cycle, which is illustrated in Figure 10, consists of the following stages:

I Initiation:

$$Q = it - Kt, \quad 0 < t < t_1 \quad (54)$$

II Propagation:

$$Q = it_1 - Kt, \quad t_1 < t < t_2 \quad (55)$$

III Termination:

$$Q = it_1 - i(t-t_2) - Kt, \quad t_2 < t < t_3 \quad (56)$$

The times  $t_1$ ,  $t_2$ , and  $t_3$  in Equations 54, 55 and 56 are defined as follows:

$$t_1 = t_i; \quad t_2 = t_i + t_p; \quad t_3 = t_i + t_p + t_t$$

The propagation phase II should not be confused with the "true" propagation, which takes place in all three phases.

Figure 10. MODEL PROFILE OF LIVING ANION CONCENTRATION DURING ONE ELECTROCHEMICAL CYCLE; BROKEN CURVE IDEAL WITHOUT ATTRITION; SOLID CURVE CORRECTED FOR ATTRITION

LIVING ANIONS

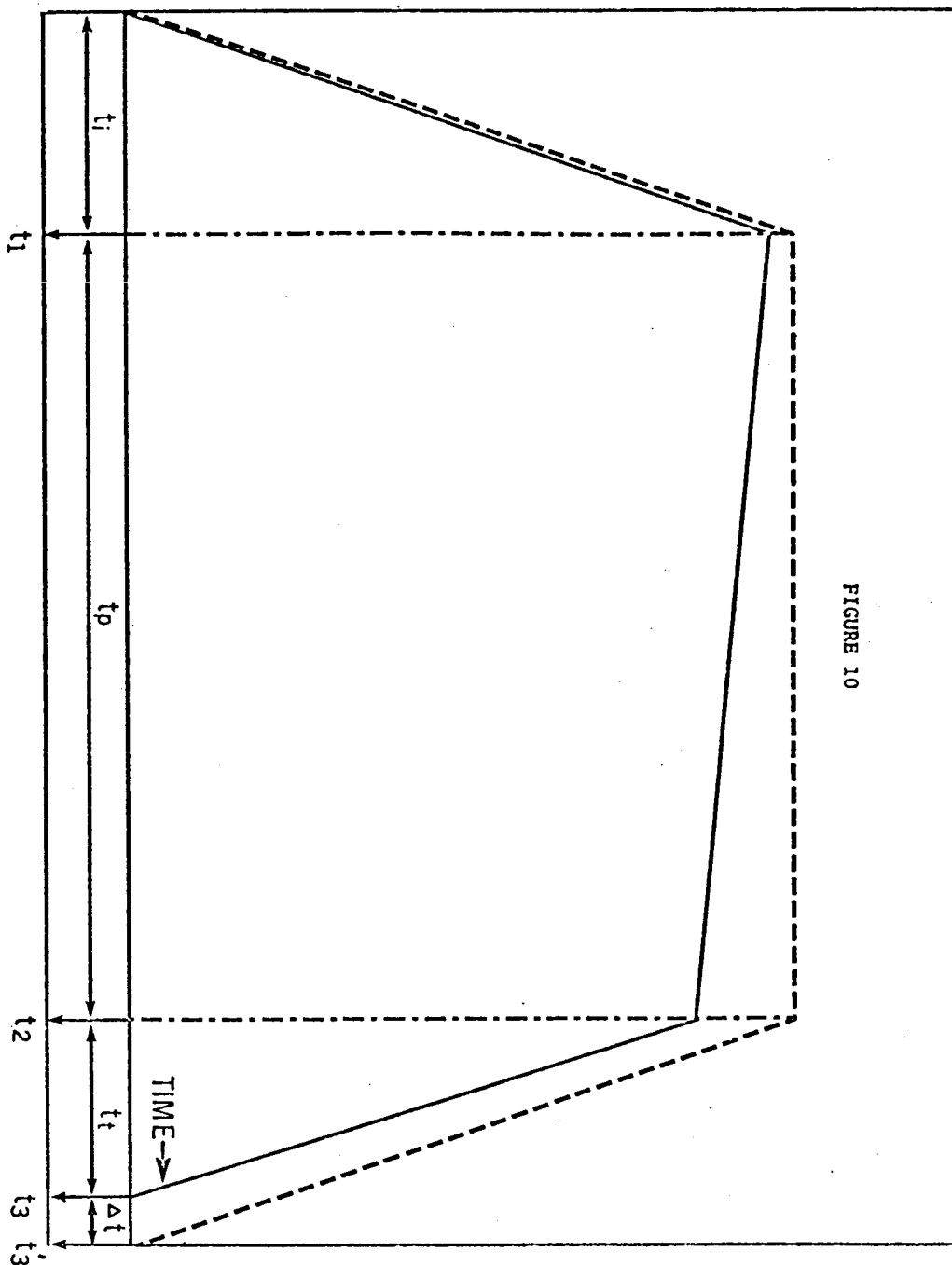


FIGURE 10

Obviously, for  $t = t_3$  the quantity  $Q = 0$ . The constant  $K$  of Equation 53 may be determined from the difference  $\Delta t$  defined earlier and is given by:

$$K = \frac{i\Delta t}{t_3} \quad (57)$$

Once  $K$  is known, the instantaneous value of  $Q$  can be calculated for any given time, such as  $t_1$  or  $t_2$ . Subsequently, the average effective values of  $Q$  for the three intervals are:

$$\bar{Q}_i = \frac{0 + Q_1}{2}, \quad \bar{Q}_p = \frac{Q_1 + Q_2}{2}, \quad \bar{Q}_t = \frac{Q_2 + 0}{2} \quad (58)$$

The average effective value of  $Q$  over the whole cycle is computed as the weighted average of  $Q$  throughout the cycle:

$$\bar{Q} = \frac{t_i \bar{Q}_i + t_p \bar{Q}_p + t_t \bar{Q}_t}{t_i + t_p + t_t} \quad (59)$$

The average molar concentration of living ends is obtained from Equation 50 and the value of  $k_p$  from Equation 52.

Table IX shows the reproducibility of the kinetic results for five experiments. The rate constants for runs B106, B107 and B108 illustrated remarkable agreement. The lower value shown by sample B109 may be due to the high viscosity of the solution, reflecting the high molecular weight polymer formed. Furthermore, with the high concentration of butadiene in this experiment the gross dielectric constant of the medium was lower than in the other experiments and thus a lower rate of polymerization would be expected. The low value of  $k_p$  in run B103 is attributed to experimental error.

The values of  $k_p$  uncorr. are listed in Table IX for comparison. They were calculated with the assumption that the attrition reactions were absent, and the difference ( $k_p$  corr. -  $k_p$  uncorr.) reflects the actual extent of such reactions.

The rate of polymerization was investigated as a function

TABLE IX

Determination of Rate Constants at -10°C

$$[\text{NaBPh}_4] = 1.8 \times 10^{-2} \text{ mole/litre}$$

| Sample | [M] <sub>o</sub><br>[mole/l] | [LE]*<br>[mole/l]x10 <sup>5</sup> | k <sub>p</sub> uncorr.<br>[l/mole sec.] | k <sub>p</sub> corr.<br>[l/mole sec.] | Conversion<br>% |
|--------|------------------------------|-----------------------------------|---|---------------------------------------|-----------------|
| B103   | 0.806                        | 7.19                              | 0.84                                    | 0.89                                  | 24.2            |
| B106   | 0.806                        | 7.23                              | 0.98                                    | 1.09                                  | 31.7            |
| B107   | 0.806                        | 7.44                              | 1.01                                    | 1.14                                  | 32.9            |
| B108   | 0.806                        | 7.20                              | 1.03                                    | 1.12                                  | 33.4            |
| B109   | 4.030                        | 7.49                              | 0.93                                    | 0.94                                  | 10.1            |

\*Represents the effective average concentration of living ends after correction.

of temperature at a constant concentration of the supporting electrolyte.

The values of k<sub>p</sub> determined in the temperature interval -10 to -72°C (with [NaBPh<sub>4</sub>] = 1.8 x 10<sup>-2</sup> mole/litre) are listed in Table X.

TABLE X

Temperature Dependence of Reaction Rate at High Concentration of Supporting Electrolyte.

$$[\text{NaBPh}_4] = 1.8 \times 10^{-2} \text{ mole/litre}$$

| t[°C] | 1/T x 10 <sup>3</sup> (°K <sup>-1</sup> ) | k <sub>p</sub><br>[l/mole sec.] | k <sub>p</sub> *<br>[l/mole sec.] |
|-------|---|---------------------------------|-----------------------------------|
| -10   | 3.80                                      | 1.12                            | 1.15                              |
| -20   | 3.95                                      | 0.91                            | 0.86                              |
| -30   | 4.11                                      | 0.59                            | 0.70                              |
| -40   | 4.29                                      | 0.40                            | 0.55                              |
| -50   | 4.48                                      | 0.44                            | 0.43                              |
| -60   | 4.69                                      | 0.39                            | 0.33                              |
| -72   | 4.97                                      | 0.23                            | 0.23                              |

k<sub>p</sub>\* calculated from Eq. 60

The variation of  $k_p$  with temperature followed a smooth linear Arrhenius plot shown in Figure 11. The Arrhenius parameters A and  $E_a$  were evaluated by the method of least squares and show the following dependence of rate on temperature:

$$k_p = 1.45 \times 10^2 \exp\left(-\frac{2600}{RT}\right) \quad (60)$$

The apparent activation energy  $E_a = 2.6$  kcal/mole is considerably lower than the value of 6.1 kcal/mole reported by Morton et al. (86) for butyllithium initiated polymerizations in tetrahydrofuran, and lies between the values of 4.4 kcal/mole and 1.4 kcal/mole determined by Medvedev et al. (83) for systems with a sodium counterion, for temperatures above and below  $-56^\circ\text{C}$  respectively. In Figure 12, the Arrhenius plots of Morton et al., Medvedev et al. and the present work are compared.

An interesting phenomenon was observed at a lower concentration of sodium tetraphenylboride and is demonstrated in Table XI. The Arrhenius plot of these data (Figure 13) shows that the rate of propagation at high temperatures ( $t > -30^\circ\text{C}$ ) is considerably higher than in the former case. The slope levels off under  $-30^\circ\text{C}$ , where the observed rates are similar to those obtained in the previous system.

TABLE XI

Temperature Dependence of Reaction Rate at Low Concentration of Supporting Electrolyte.

$$[\text{NaBPh}_4] = 3.6 \times 10^{-3} \text{ mole/litre}$$

| $t$ [ $^\circ\text{C}$ ] | $1/T \times 10^3$ [ $^\circ\text{K}^{-1}$ ] | $k_p$<br>[ $\ell$ /mole sec.] |
|--------------------------|---|-------------------------------|
| -10                      | 3.80  | 1.35                          |
| -10                      | 3.80  | 1.55                          |
| -10                      | 3.80  | 1.61                          |
| -30                      | 4.11  | 0.87                          |
| -30                      | 4.11  | 0.68                          |
| -50                      | 4.48  | 0.41                          |
| -60                      | 4.69  | 0.33                          |
| -70                      | 4.92  | 0.28                          |



Figure 11. DEPENDENCE OF PROPAGATION RATE CONSTANT ON TEMPERATURE  
AT HIGH CONCENTRATION OF SODIUM TETRAPHENYLBORIDE.  
SOLID LINE LEAST SQUARES FIT TO DATA.  
Error bars denote limit of error derived from  
propagation-of-error analysis (Appendix I)

FIGURE 11

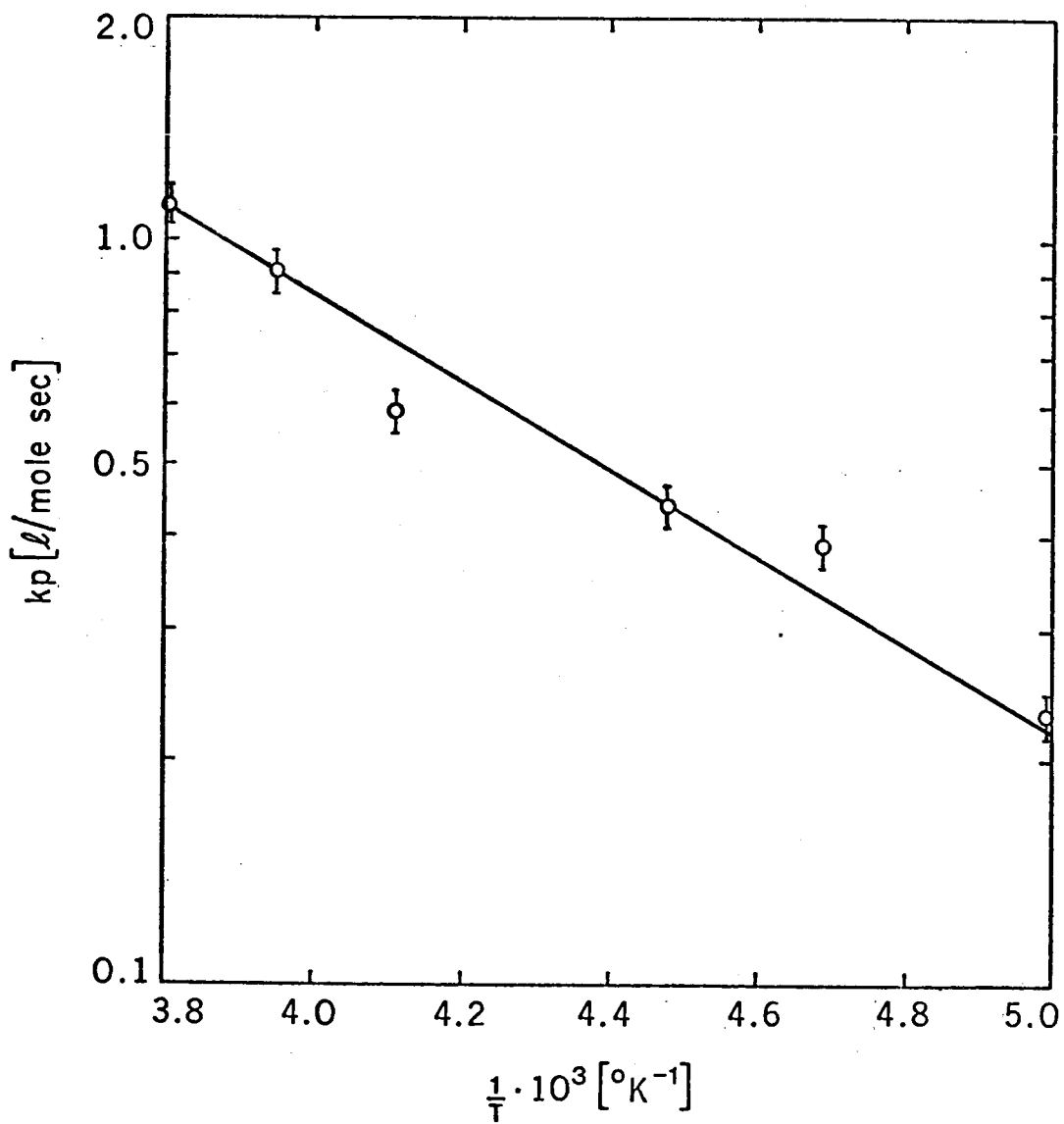


Figure 12. COMPARISON OF PRESENT KINETIC DATA WITH THOSE OF  
MORTON (86) AND MEDVEDEV (82)

FIGURE 12

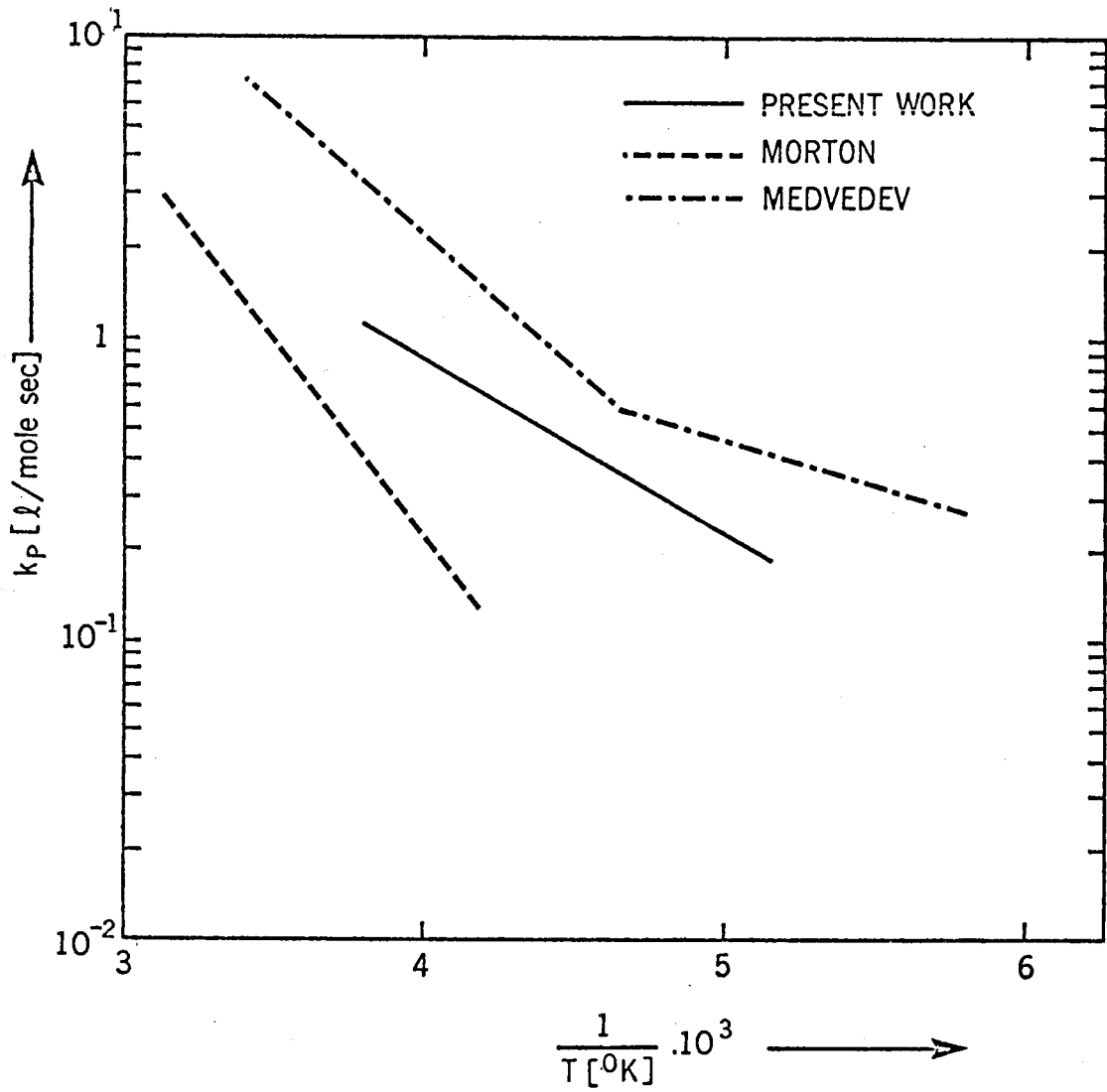
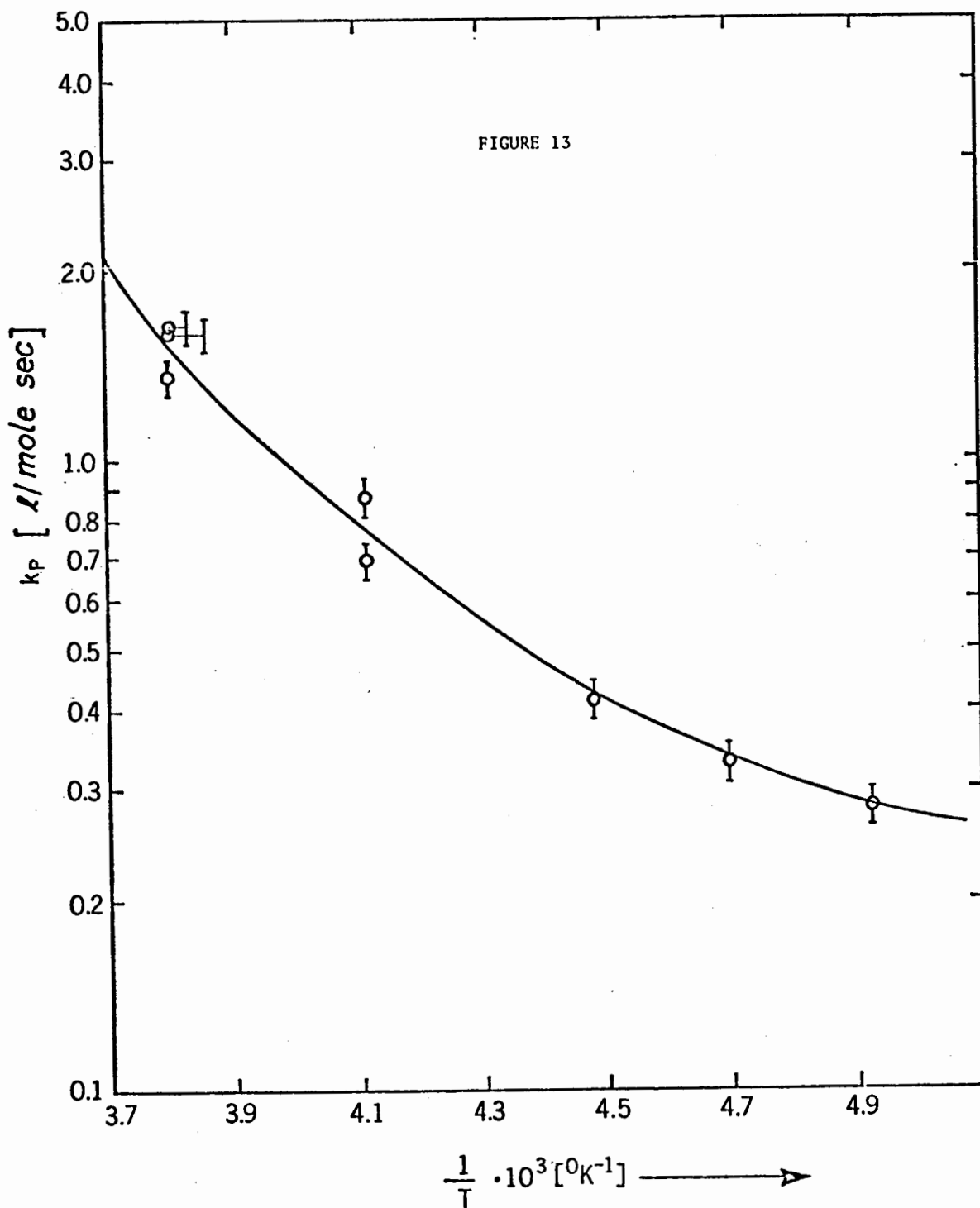


Figure 13. DEPENDENCE OF PROPAGATION RATE CONSTANT ON TEMPERATURE  
AT LOW CONCENTRATION OF SODIUM TETRAPHENYLBORIDE.  
Error bars denote limit of error derived from  
propagation-of-error analysis ( Appendix I )



There seems to be no simple explanation for this behavior. In the case of polystyrene, Shimomura et al. (32) observed a pronounced dependence of the rate on the concentration of sodium tetraphenylboride even when the latter was as high as  $10^{-3}$  mole/litre. However, the dissociation constant of polybutadienyl sodium would be expected to be substantially lower than that of polystyryl sodium. Consequently, a variation of the concentration of sodium tetraphenylboride should have a negligible influence on the polymerization rate in the present work.

The negative linear Arrhenius plot of Figure 11 indicates that only one type of ion-pair participated in the reaction. There is no evidence for a change in the rate, as would be caused by different degrees of ion-pair solvation at the various temperatures. However, it is possible, that greater complexity is obscured within the temperature interval of our experiments.

### 3.2.2. Molecular Weights.

This section deals with the molecular weights and polydispersities of polymers isolated in the kinetic experiments. Such studies are of primary importance in the preparation of polymers with pre-determined molecular weights. The difference between the theoretical molecular weight expected on the basis of simple model calculations and the value found would be indicative of the mechanism of the reaction and would reflect the occurrence of side reactions such as chain transfer by monomer, termination by solvent or by other components of the system and other possible reactions.

Table XII displays the molecular weights and polydispersities of polymers prepared with the high concentration of the supporting electrolyte.

The theoretical molecular weights were calculated considering the extent of living end attrition determined in each experiment by electrochemical titration. Apart from this, the reaction was assumed to proceed ideally. This involves the absence of chain

TABLE XII

Molecular Weights and Polydispersities of Butadiene Polymers at High Concentration of Supporting Electrolyte

$$[\text{NaBPh}_4] = 1.8 \times 10^{-2} \text{ mole/litre}$$

| Sample | t [°C] | $\bar{M}_n$<br>(calculated) | $\bar{M}_n$<br>(GPC) | $\bar{M}_w/\bar{M}_n$<br>(GPC) |
|--------|--------|-----------------------------|----------------------|--------------------------------|
| B103   | -10    | 19600                       | 19500                | 1.20                           |
| B106   | -10    | 25500                       | 32000                | 1.20                           |
| B107   | -10    | 25700                       | 31800                | 1.17                           |
| B108   | -10    | 27000                       | 28800                | 1.25                           |
| B109   | -10    | 118000                      | 85000                | -                              |
| B112   | -20    | 22100                       | 19100                | 1.10                           |
| B110   | -30    | 15700                       | 18100                | 1.23                           |
| B113   | -40    | 10300                       | 11100                | 1.15                           |
| B111   | -50    | 12000                       | 12900                | 1.35                           |
| B114   | -60    | 9700                        | 9000                 | 1.15                           |
| B115   | -72    | 5900                        | 7100                 | 1.16                           |

transfer and the thermodynamic irreversibility of the polymerization process. In such a case, the number average molecular weight  $\bar{M}_n$  of the resulting polymer is given by the expression:

$$\bar{M}_n = 2 \cdot \frac{[M]}{[LE]} \cdot MW, \quad (61)$$

where [M] is the number of moles of the monomer consumed by the reaction, [LE] is the average concentration of living ends over the time interval of polymerization and MW is the molecular weight of the monomer. The di-ended growth is well confirmed by the results in Table XII.

Comparison of theoretical molecular weights and those determined by GPC listed in Table XII show a very good agreement.



For most polymers, the two quantities are practically equal within the limits of the experimental error of GPC measurements. However, there is a noticeable tendency for the GPC values to be somewhat higher than the theoretical molecular weights. It is likely that this effect is caused by crosslinking. Polybutadiene is very susceptible to branching and crosslinking reactions due to the presence of unsaturation both in the chain backbone and in the pendant vinyl groups. Preliminary experiments indicated, that polymerization taken to high conversion and high molecular weight yielded only partly soluble, crosslinked products. Although such crosslinking reactions may occur spontaneously, especially through transfer to dead polymer chains, another mechanism seems viable in these systems. Since the electrolytic initiation is not carried out at a constant potential, it is possible to consider a scheme whereby an electron would be transferred to an isolated double bond of a terminated polymer chain, or of a growing chain adsorbed on the surface of the electrode. Such reactions, even if they represented only a very small fraction of the total number of transferred electrons, would give rise to branching and, especially at high conversions, to crosslinking and to the formation of three-dimensional structures.

The effect of temperature should also be noted. Most experiments carried out at higher temperatures ( $-10^{\circ}\text{C}$ ) gave rise to polymers having molecular weights higher than calculated. Molecular weights of polymers prepared at low temperatures generally agreed well with the calculated values. These phenomena cannot be explained by a temperature dependence of the rate of the spontaneous termination and/or attrition of living anions, for such effects have been considered and accounted for in the calculation of  $[\overline{\text{LE}}]$ .

In this context, it is interesting to compare the previously discussed results with those compiled in Table XIII. This table lists

the molecular weights of polymers produced in the presence of a lower concentration of the supporting electrolyte.

TABLE XIII

Molecular Weights and Polydispersities of Butadiene Polymers at Low Concentration of Supporting Electrolyte.

$$[\text{NaBPh}_4] = 3.6 \times 10^{-3} \text{ mole/litre}$$

| Sample | t [°C] | $\bar{M}_n$<br>(calculated) | $\bar{M}_n$<br>(GPC) | $\bar{M}_w/\bar{M}_n$<br>(GPC) |
|--------|--------|-----------------------------|----------------------|--------------------------------|
| B92    | -10    | 65200                       | 57000                | 1.56                           |
| B94    | -10    | 28600                       | 22600                | 1.33                           |
| B97    | -10    | 28400                       | 19500                | 1.49                           |
| B95    | -30    | 13900                       | 13800                | 1.18                           |
| B98    | -30    | 22700                       | 18900                | 1.43                           |
| B100   | -50    | 15600                       | 14700                | 1.31                           |
| B102   | -70    | 11100                       | 10400                | 1.29                           |

It is evident, that the situation is different in this case. At higher temperatures, the experimental molecular weights are significantly lower than the calculated values; once again a good agreement between the two values is seen at lower temperatures. This is a rather striking difference between the two sets of experiments. The effect of salt concentration is more clearly demonstrated in Table XIV, which compares four samples polymerized under similar conditions except for the varying concentration of sodium tetraphenylboride. The quantity x listed in the last column of Table XIV is defined as follows:

$$x = \frac{\bar{M}_n \text{ (calculated)} - \bar{M}_n \text{ (GPC)}}{\bar{M}_n \text{ (calculated)}} \cdot 100 \text{ [\%]} \quad (62)$$

TABLE XIV

Effect of Salt Concentration on Molecular Weight of Butadiene Polymers.  
 $t = -10^{\circ}\text{C}$

| Sample | $[\text{NaBPh}_4]$<br>[mole/litre] | $\bar{M}_n$<br>(calculated) | $\bar{M}_n$<br>(GPC) | x<br>[%] |
|--------|------------------------------------|-----------------------------|----------------------|----------|
| B103   | $1.8 \times 10^{-2}$               | 19600                       | 19500                | 0        |
| B105   | $7.2 \times 10^{-3}$               | 27900                       | 25100                | 10       |
| B97    | $3.6 \times 10^{-3}$               | 28400                       | 17600                | 38       |
| B104   | $1.8 \times 10^{-3}$               | 31700                       | 17100                | 43       |

As the concentration of the salt decreases, the molecular weight of the polymer also decreases as compared with the calculated value. This is quantitatively expressed by the factor x, which grows steadily with the decreasing concentration of sodium tetraphenylboride.

This behavior is somewhat surprising. It has been shown above, that the second order rate constants at  $-10^{\circ}\text{C}$  were higher at the lower concentration of the salt. Accordingly, higher molecular weights would be expected to result from such experiments.

Chain transfer by monomer might play a significant role in these polymerizations in combination with the electric field effect. The low conductivity of tetrahydrofuran solutions necessitates an application of high voltages across the cell, particularly at low concentrations of the supporting electrolyte. In the present experiments the applied voltage varied from 150-200 V at  $[\text{NaBPh}_4] = 1.8 \times 10^{-2}$  mole/litre up to 900-1000 V at  $[\text{NaBPh}_4] = 1.8 \times 10^{-3}$  mole/litre. This corresponds to a field strength of 20-120 V/cm. Results reported by Ise and coworkers (108, 109, 110, 111) demonstrated the accelerating effects of high electric fields (3000-5000 V/cm) on the propagation reaction in living polymerization. The electric

fields present in the experiments under discussion were substantially lower than those considered by Ise and their influence on the propagation reaction would be negligible. It is possible, however, that even a weak electric field could promote transfer reactions, whereby the molecular weight of the resulting polymer would be lowered.

The breadths of the molecular weight distributions as expressed by the polydispersity values  $\bar{M}_w/\bar{M}_n$  for the individual polymers, depend primarily on the ratio of the initiation and termination periods to the total time of the reaction. This is amply demonstrated on a series of samples listed in Table XV.

TABLE XV  
Effects of Initiation-Time/Propagation-Time Ratio on Polydispersity of Butadiene Polymers.

| Sample | $t_i$ [sec] | $t_p$ [sec] | $\bar{M}_n$ | $\bar{M}_w/\bar{M}_n$ | $i$ [mA] | $\tau$ |
|--------|-------------|-------------|-------------|-----------------------|----------|--------|
| B107   | 25          | 270         | 31800       | 1.17                  | 20       | 1.16   |
| B106   | 33          | 262         | 32000       | 1.20                  | 15       | 1.20   |
| B108   | 50          | 245         | 28800       | 1.25                  | 10       | 1.29   |

These three samples were polymerized under the same conditions except for the  $t_i/t_p$  ratio. The current intensities were so adjusted so as to produce the same total concentration of living anions in each case. The  $\bar{M}_n$  values of the three samples show a good agreement. It is obvious that the polydispersity values reflect the variations in the  $t_i/t_p$  ratio. It is thought reasonable to describe the width of a molecular weight distribution for a particular experiment by a factor  $\tau$ , defined as follows:

$$\tau = 1 + \frac{t_i + t_t}{t_i + t_p + t_t} \quad (63)$$

Assuming that the time of termination  $t_t$  is equal to the time of initiation (i.e. no attrition reactions occur), the values of  $\tau$  were calculated and listed in Table XV. They show a remarkable agreement with the corresponding polydispersity values  $\overline{M}_w/\overline{M}_n$ . However, the agreement in numerical values appears to be rather fortuitous as the underlying concept does not fully account for all the processes taking place in the reaction. Nevertheless, this highly simplified model seems to be adequate to compare the expected molecular weight distribution with those obtained, at least in the first approximation. Because of this and because very little is known about the nature of the spontaneous termination reactions, no attempt will be made to describe the expected molecular weight distributions in a more exact mathematical form.

### 3.2.3. Preparation of Polymers with Multimodal Molecular Weight Distributions.

The results discussed in the preceding two sections indicate that it is possible to attempt to synthesize polymers with predetermined molecular weights and molecular weight distributions employing the present system. However, there are some limitations, which are explicable in the light of the previous discussion in Section 1.3.3. Firstly, the very low conductivity of the reaction medium makes it virtually impossible to impose the high currents necessary to produce an instantaneous initiation. Consequently, there will always be a predictable spread in the resultant molecular weight distributions. Even if high currents could be obtained by using extremely high voltages and by placing electrodes of large area close to the fritted disc separating the compartments of the cell, diffusion and electromigration effects would cause a spread (this time unpredictable) in the molecular weight distribution.

Secondly, termination due to the spontaneous decay of living anions will once again tend to broaden the distribution and will

at the same time lower the number average molecular weight of the product. The latter effect is hardly controllable as follows from the statistical character of such termination reactions. Therefore, to achieve the best possible results it is necessary to keep the extent of the attrition reactions down, either by working at low temperatures, or by keeping the total duration of the reaction as short as possible by increasing the initial concentration of the monomer.

Two different approaches were tested to produce polymers with multimodal molecular weight distributions. In the first method, a given number of living ends  $LE_1$  were allowed to grow for a certain time  $t_1$ . Subsequently, the number of living anions was reduced to  $LE_2$ , e.g. 1/10 of the original value, and the polymerization continued for time  $t_2$ . Under ideal conditions, such a polymerization would be expected to produce a bimodal polymer with the distribution dependent on the two concentrations of living ends and the times  $t_1$  and  $t_2$ . However, this method was found impracticable with the present systems because of the preponderant effect of attrition reactions on the distribution.

For this reason the second approach was employed, whereby two or more fractions were prepared in the reaction cell taking advantage of the electrolytic titration technique. By this method, it is possible to prepare a given amount of one fraction at one time, then destroy the entire population of the living ends completely and reinitiate the system to produce another fraction. The whole procedure can be repeated any number of times. A typical time-current profile is shown in Figure 14.

If  $[M]$  moles of monomer are polymerized by  $[LE]$  moles of living anions, the number average molecular weight  $\bar{M}_n$  is given by Equation 61. It is evident that at a constant temperature and constant concentration of living ends, the resultant molecular

Figure 14. SCHEMATIC REPRESENTATION OF TIME - CURRENT PROFILE

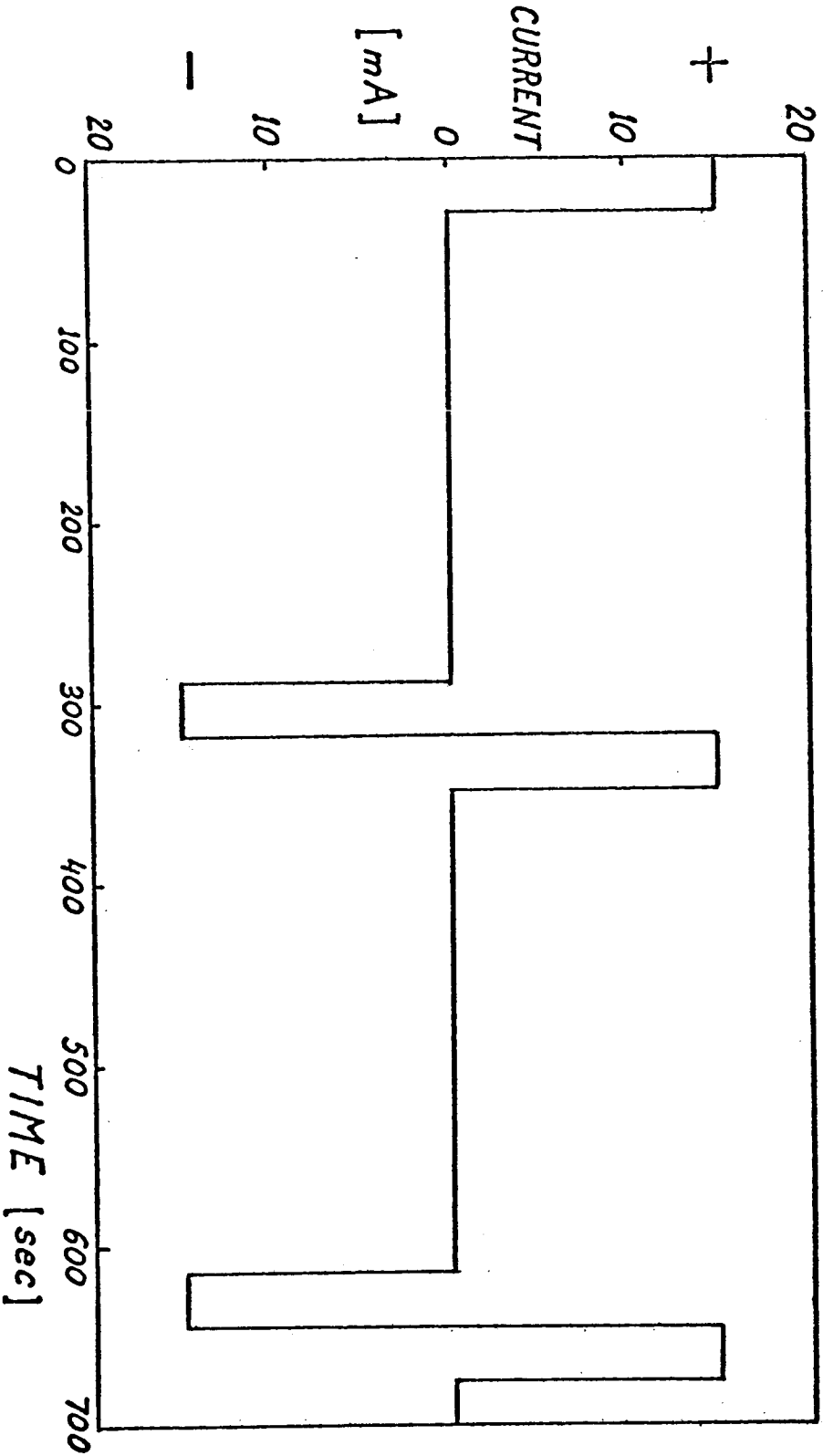


FIGURE 14



weight is determined by the original concentration of monomer and the time of polymerization. However, if several cycles are required to produce a given amount of polymer of a constant molecular weight, the duration of each subsequent polymerization period is prolonged due to the depletion of monomer.

For example, consider the conditions necessary to produce a polymer with a bimodal molecular weight distribution containing a weight ratio of two components of 1:1 and respective number average molecular weight of 50,000 (I) and 10,000 (II). The initial concentration of the monomer was chosen as 1.6120 mole/litre and an initiation period of 30 seconds at 15 mA was selected and used throughout. This corresponds to a living end concentration of  $8.18 \times 10^{-5}$  moles/litre at the end of the initiation period. A calculation of the amount of monomer necessary to produce the required molecular weight is:

$$\begin{aligned} \text{I:} \quad [M]_{\text{I}} &= \frac{(\bar{M}_n) [\text{LE}]}{2 \text{ MW}} = \frac{(50000) (8.18 \times 10^{-5})}{(2) (54.09)} = 0.03780 \text{ mole/litre} \\ \text{II:} \quad [M]_{\text{II}} &= \frac{(\bar{M}_n) [\text{LE}]}{2 \text{ MW}} = \frac{(10000) (8.18 \times 10^{-5})}{(2) (54.09)} = 0.00756 \text{ mole/litre} \end{aligned}$$

Five cycles of II are necessary to produce the same amount of polymer as one cycle of I.

If  $-10^\circ\text{C}$  is chosen for phase I, the rate constant at this temperature was determined to be 1.04 litre/mole sec. The total propagation time required for one cycle, is obtained from Equation 64:

$$t_{\text{av}} = \frac{2.303}{k_p [\text{LE}]} \log \frac{[M]_0}{[M]_1} \quad [\text{sec}] \quad (64)$$

$$\text{where } [M]_1 = [M]_0 - [M]_{\text{I}}. \quad (65)$$

This corresponds to the average time of growth of the living ends. Assuming no attrition of living ends the average is directly related to the lengths of the initiation, growth and termination periods

of the cycle. These are related as follows:

$$t_{av} = t_p + \frac{t_i + t_t}{2} \quad (66)$$

where  $t_i$  is the time of initiation during which current flows,  
 $t_p$  is the period of propagation in the absence of current,  
 $t_t$  is the termination period during which reverse current is applied.

The corresponding duration of the growth phase (no current) is calculated by subtracting the time of initiation  $t_i$  from  $t_{av}$ . In order to produce the same molecular weight in each cycle, the duration of the growth phase is prolonged for each consecutive cycle. The calculated values for four cycles are shown in Table XVI.

TABLE XVI

Compensation for Monomer Depletion at  $-10^{\circ}\text{C}$ .

| Cycle | Initial conc. of monomer [mole/litre] | $t_{av}$ [Sec] | $t_p$ [Sec] |
|-------|---------------------------------------|----------------|-------------|
| 1     | 1.612                                 | 290            | 260         |
| 2     | 1.574                                 | 297            | 267         |
| 3     | 1.536                                 | 304            | 274         |
| 4     | 1.461                                 | 313            | 283         |

A lower temperature of  $-50^{\circ}\text{C}$  was chosen for the second step of the polymerization in order to provide a longer and more convenient propagation time. The rate constant at this temperature had previously been determined to be 0.431 litre/mole sec in this system. This choice was made to keep the ratio of  $t_p:t_i$  as high as possible. 20 complete cycles were necessary to produce the required amount of polymer and the conditions employed are listed

in Table XVII.

TABLE XVII

Compensation for Monomer Depletion at  $-50^{\circ}\text{C}$ .

| Cycle | Initial conc. of monomer [M], [mole/litre] | $t_{av}$ [Sec] | $t_p$ [Sec] |
|-------|--|----------------|-------------|
| 1     | 1.461                                      | 144            | 114         |
| 2     | 1.453                                      | 145            | 115         |
| 3     | 1.446                                      | 146            | 116         |
| 4     | 1.438                                      | 147            | 117         |
| 5     | 1.431                                      | 148            | 118         |
| 6     | 1.423                                      | 149            | 119         |
| 7     | 1.415                                      | 150            | 120         |
| 8     | 1.408                                      | 151            | 121         |
| 9     | 1.400                                      | 152            | 122         |
| 10    | 1.393                                      | 153            | 123         |
| 11    | 1.385                                      | 154            | 124         |
| 12    | 1.378                                      | 155            | 125         |
| 13    | 1.370                                      | 156            | 126         |
| 14    | 1.363                                      | 157            | 127         |
| 15    | 1.355                                      | 158            | 128         |
| 16    | 1.347                                      | 159            | 129         |
| 17    | 1.340                                      | 160            | 130         |
| 18    | 1.332                                      | 161            | 131         |
| 19    | 1.325                                      | 162            | 132         |
| 20    | 1.317                                      | 163            | 133         |

By varying the number of cycles for each of the two steps, bimodal samples were prepared with a predetermined weight composition of each and the required ratio of the two molecular weights. The

experimental conditions and the data obtained are shown in Table XVIII. A good correspondence between the calculated and experimental values is evident.

TABLE XVIII

Comparison of Experimental and Calculated Distributions for Bimodal Polymers.

| SAMPLE | $\bar{M}_n$ of component |       |       |       | Weight % of component |       |       |       |
|--------|--------------------------|-------|-------|-------|-----------------------|-------|-------|-------|
|        | I                        |       | II    |       | I                     |       | II    |       |
|        | Calc.                    | Found | Calc. | Found | Calc.                 | Found | Calc. | Found |
| B116   | 50000                    | 50000 | 10000 | 7500  | 50                    | 55    | 50    | 45    |
| B117   | 50000                    | 52000 | 10000 | 8000  | 67                    | 70    | 33    | 30    |
| B118   | 50000                    | 55000 | 10000 | 8000  | 33                    | 41    | 67    | 59    |

Figures 15, 16 and 17 show the molecular weight distributions for each of the three samples, and depict the bimodal character of the resultant polymers. The three integral curves are superimposed in Figure 18.

One polymer with a trimodal distribution was prepared and the relevant data are shown in Table XIX. Again, good agreement between the calculated and the experimental values of molecular weight and composition is apparent. The trimodal character of the distribution is shown in Figure 19.

The agreement between calculated and experimental values is all the more remarkable when one considers that the calculations employed here assume ideal conditions which are only approximated in real systems. For example, the process of electrochemical titration employed here relies on the determination of an end-point by optical means. The accuracy of this method is indeed limited

Figure 15. MOLECULAR WEIGHT DISTRIBUTION FOR BIMODAL POLYMER B116  
solid line..... integral distribution  
broken line..... differential distribution

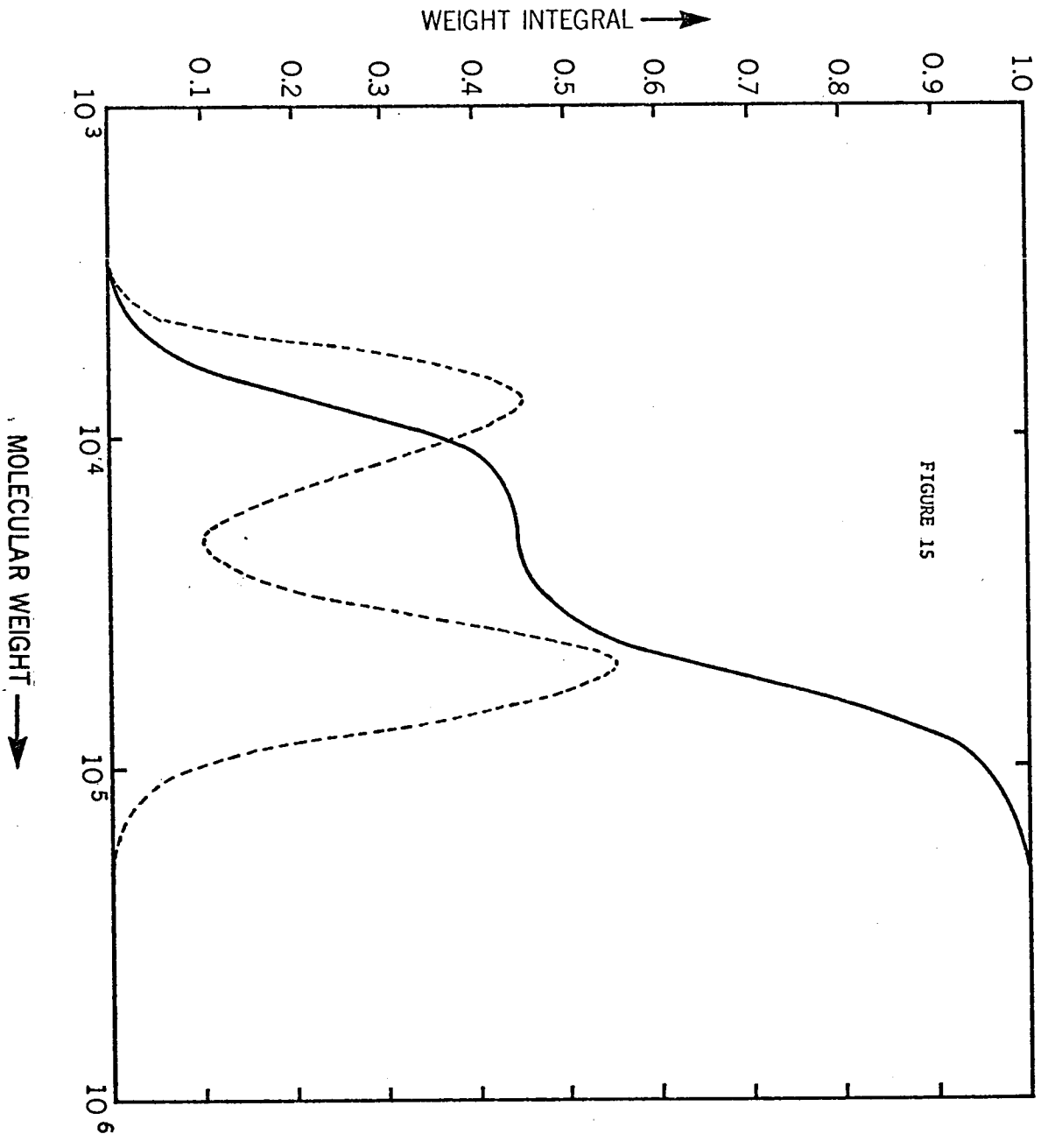


Figure 16. MOLECULAR WEIGHT DISTRIBUTION FOR BIMODAL POLYMER B117  
solid line..... integral distribution  
broken line..... differential distribution

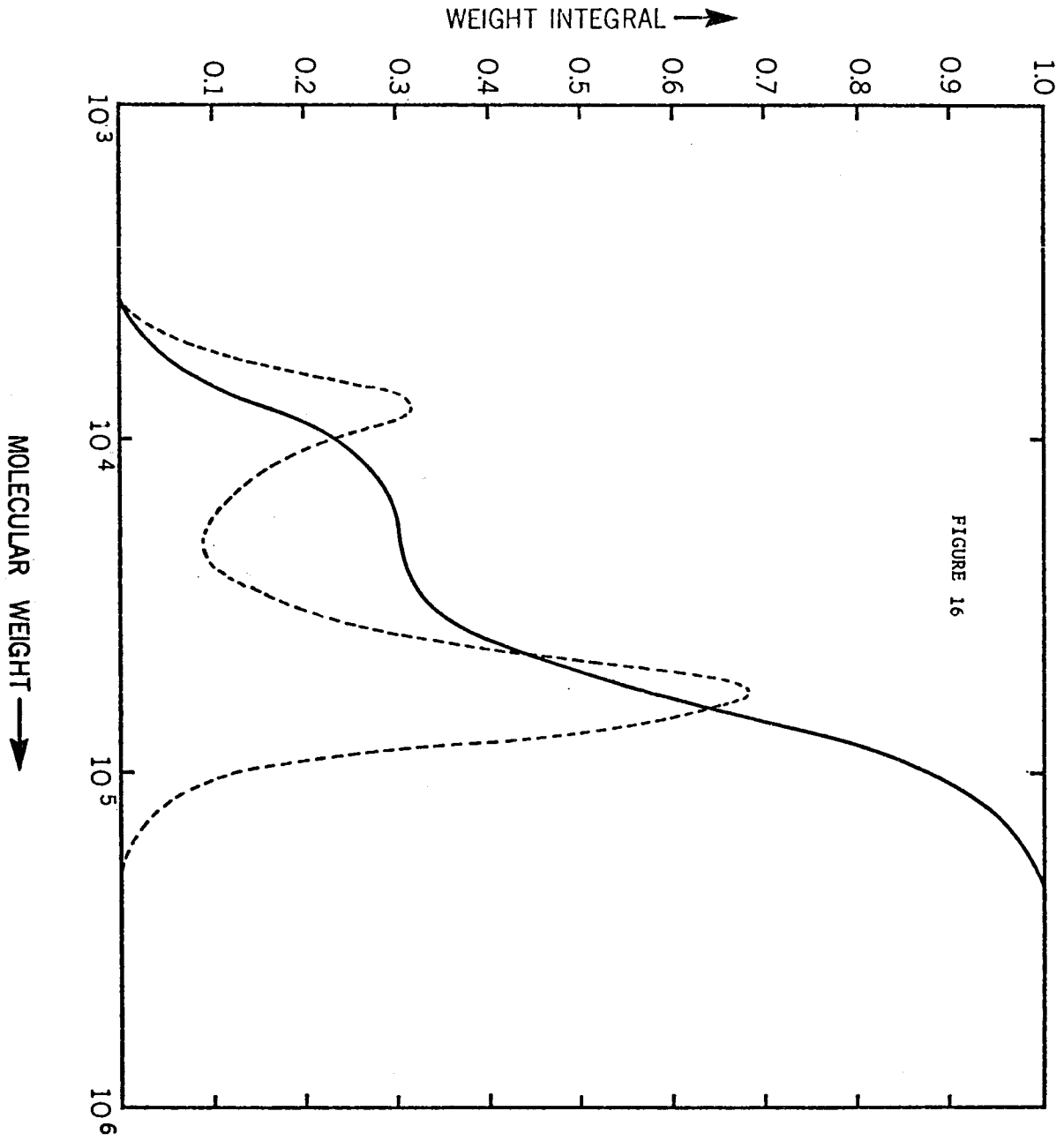




Figure 17. MOLECULAR WEIGHT DISTRIBUTION FOR BIMODAL POLYMER B118  
solid line..... integral distribution  
broken line..... differential distribution

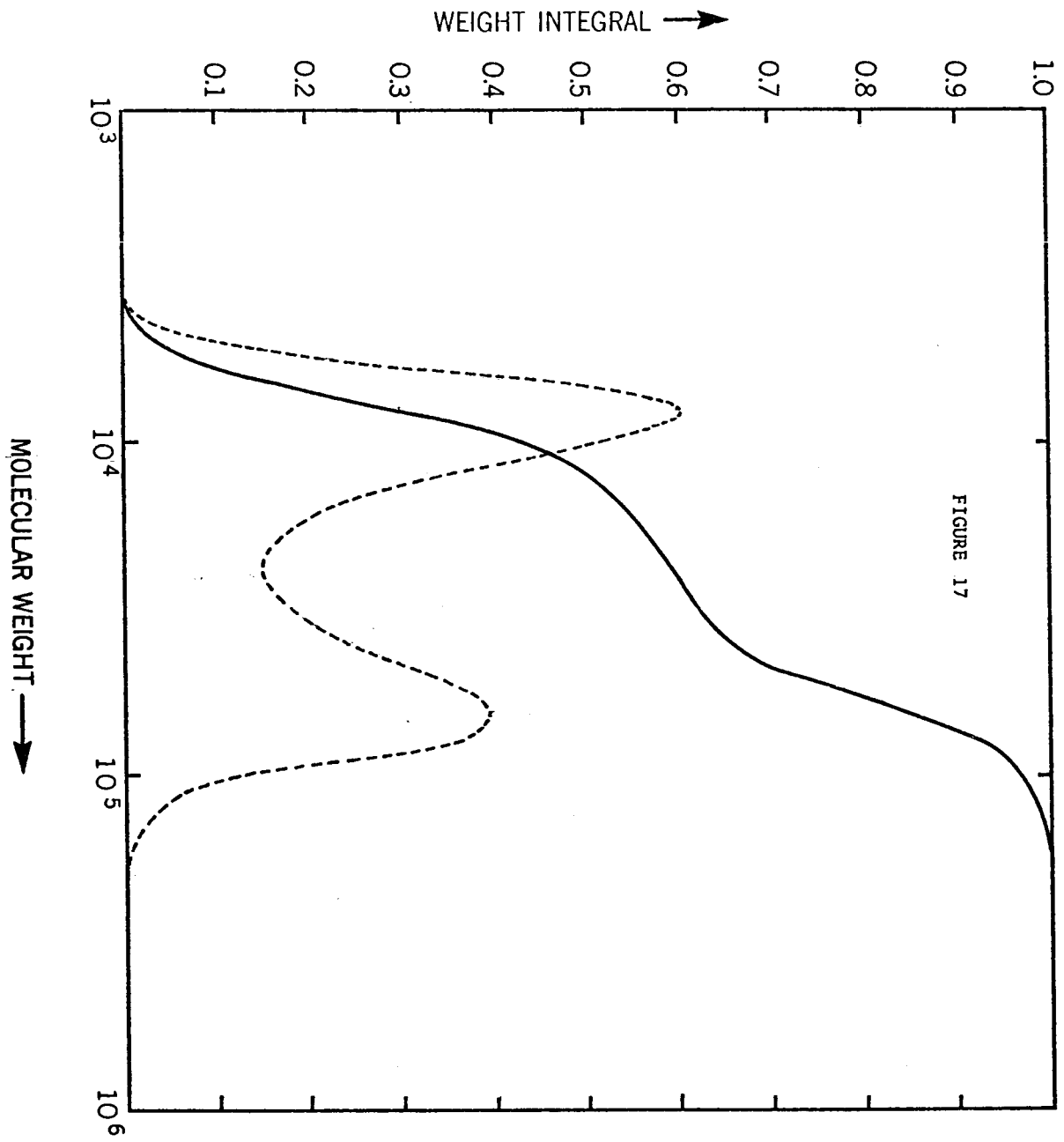


Figure 18. SUPERIMPOSED INTEGRAL DISTRIBUTION CURVES FOR  
BIMODAL POLYMERS B116, B117 and B118

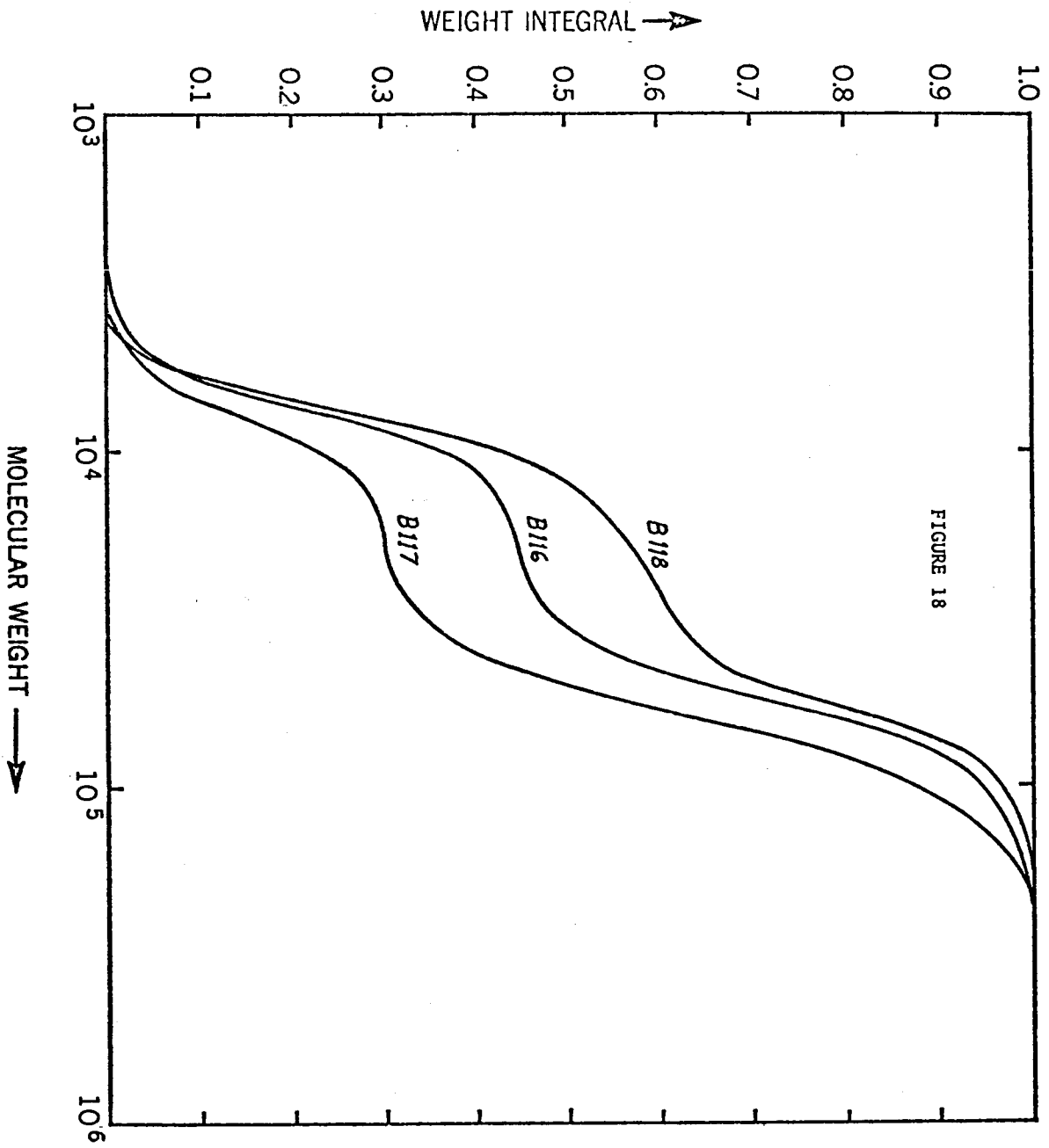


Figure 19. MOLECULAR WEIGHT DISTRIBUTION FOR TRIMODAL POLYMER B119  
solid line..... integral distribution  
broken line..... differential distribution

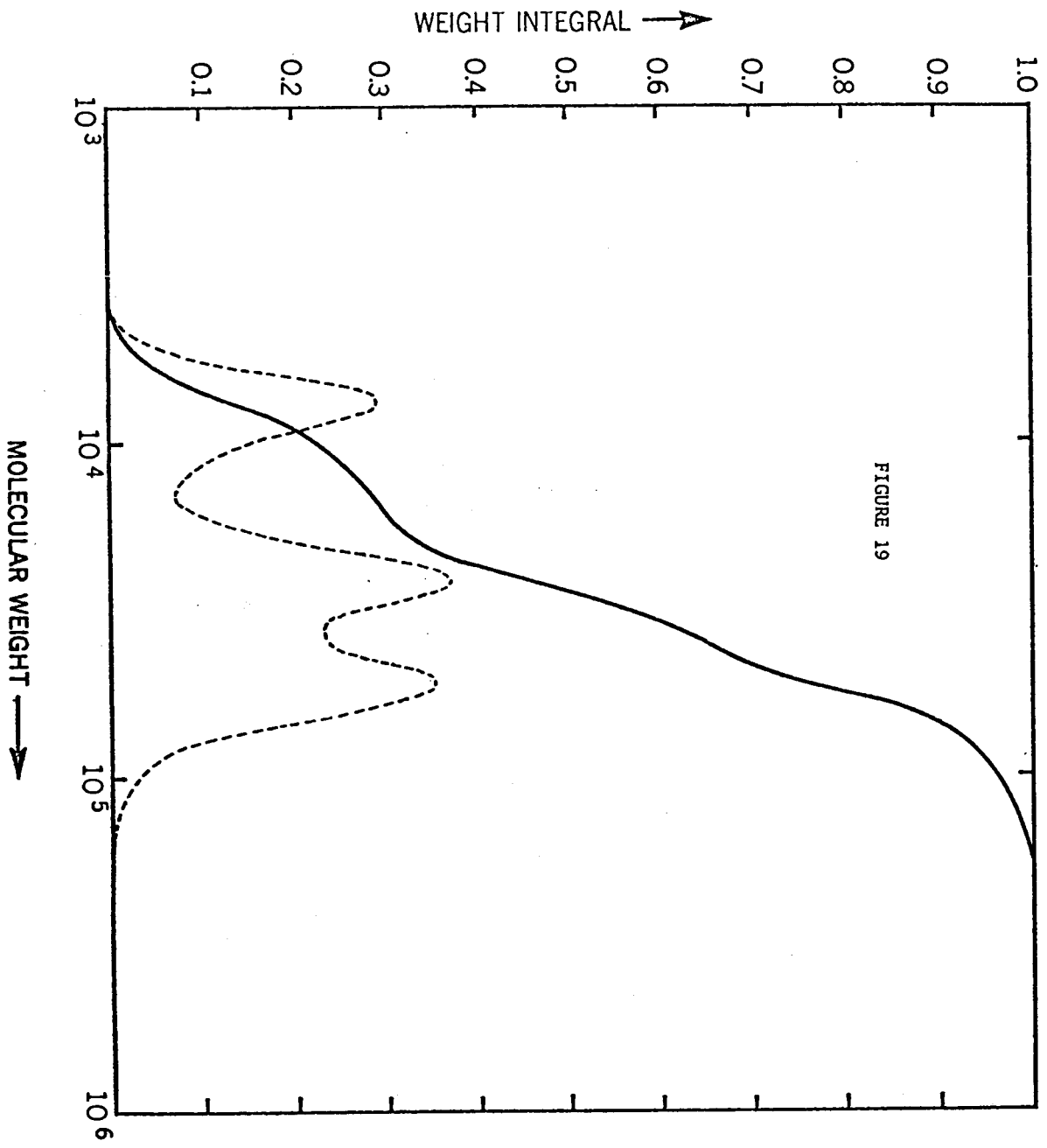


TABLE XIX  
 Comparison of Experimental and Calculated Distributions for Trimodal Polymer.

| SAMPLE | $\bar{M}_n$ of component |             |             | Weight % of component |             |             |
|--------|--------------------------|-------------|-------------|-----------------------|-------------|-------------|
|        | I                        | II          | III         | I                     | II          | III         |
|        | Calc. Found              | Calc. Found | Calc. Found | Calc. Found           | Calc. Found | Calc. Found |
| B119   | 50000 55000              | 30000 27000 | 10000 8000  | 33.3 35               | 33.3 37     | 33.3 28     |

and consequently a small fraction of living ends may persist from one cycle into the next. On the other hand, if the titration is carried past the end-point, some of the living ends generated in the following cycle will be destroyed, and will not take part in the propagation reaction. These factors all tend to broaden the molecular weight distributions of the resulting polymers. However, the dominant factor determining the breadth of the distribution is the  $t_i/t_p$  ratio itself, as discussed above. The results show, that the polydispersity values are in the range  $1.1 < \bar{M}_w/\bar{M}_n < 1.25$  (computed for each particular fraction of each sample).

The results in Tables XVIII and XIX indicate that although the agreement between calculated and observed values in molecular weight is fairly good some discrepancies exist, particularly at lower molecular weights. These are due in part to uncertainty in the molecular weight determination, which is approximately  $\pm 5\%$  in this region. However, the most important factor is believed to be the relative instability of the polybutadienyl anions in tetrahydrofuran. This view is supported by the results of Fetters (112) on the anionic synthesis of block copolymers, where deviations between calculated and measured total molecular weights may be attributed to the polydiene segments.

#### 3.2.4. Effect of Solvent and Counterion on Microstructure.

It was shown earlier in Section 1.4.2., that the effects of counterion on the microstructure of the resulting polymer are most apparent in non-polar hydrocarbon solvents. Thus electrolytic methods requiring polar media to provide the required conductivity would not be ideal for such studies. Table IV, however, indicates that other, less important, effects may occur in polar media as well. The studies described below were carried out with the aim of determining the predominant microstructure of polymers arising from our syntheses and to find means to vary the relative amounts



of the individual stereoisomers.

The results of the first set of experiments are shown in Table XX. All these experiments were carried out in tetrahydrofuran with sodium tetraphenylboride as the supporting electrolyte. The variable parameter was the total charge passed through the solution, which corresponds to the concentration of living anions at the end of the initiation period. In each instance the yellow living anion color was produced at the cathode, but faded gradually in the course of the reaction due to attrition reactions. The polymers isolated from these experiments showed practically no variation of the microstructure and were composed predominantly of 1,2 stereoisomer with some 1,4-trans and very little 1,4-cis structure.

In the next set of experiments an attempt was made to vary the dielectric constant of the solvent by using tetrahydrofuran-cyclohexane mixtures in various ratios. Data compiled in Table XXI show that, once again, the steric configuration was predominantly of the 1,2 type and no systematic variation was effected by the presence of different concentrations of cyclohexane. Also, this line of experiments appeared to be rather impractical from the electrochemical standpoint, as the presence of larger quantities of cyclohexane sharply decreased the conductivity of the solution.

A small yet marked change was observed when hexamethylphosphoramide (HMPA) was used as solvent. As evidenced in Table XXII, the 1,4-cis structure completely disappeared and instead a greater proportion of the 1,4-trans configuration was found in the polymer. This effect is probably linked with another observation, namely that the polymerization rate was much faster in HMPA than in the tetrahydrofuran solvent. It has been shown recently (113) that sodium salts of radical-ions are virtually completely dissociated in HMPA. This solvent forms stable blue solutions of solvated

TABLE XX  
 Effect of Charge Passed on Polybutadiene Microstructure  
 $[\text{NaBPh}_4] = 7.32 \times 10^{-3}$  mole/litre;  $t = 0^\circ\text{C}$ , solvent  $\equiv$  THF

| Sample | Charge Passed <sup>5</sup><br>[F x 10 <sup>5</sup> ] | Time of Polymerization<br>[hours] | Conversion [%] | Configuration (%) |         |
|--------|--|-----------------------------------|----------------|-------------------|---------|
|        |  |                                   |                | 1,4 trans         | 1,2 cis |
| B2     | 2.24   | 48                                | 95             | 9                 | 2       |
| B7     | 1.68   | 48                                | 85             | 8                 | 2       |
| B3     | 1.12   | 48                                | 61             | 10                | 1       |
| B4     | 0.56   | 20                                | 24             | 9                 | 2       |
| B5     | 1.12   | 72                                | 86             | 8                 | 2       |
| B9     | 1.12   | 36                                | 81             | 8                 | 3       |

TABLE XXI

Polymerization of Butadiene in THF - Cyclohexane Mixture

$[\text{NaBPh}_4] = 7.32 \times 10^{-3}$  mole/litre;  $t = 0^\circ\text{C}$

| Sample | Solvent<br>[Vol. %<br>CH in<br>THF] | Charge<br>Passed<br>[F] x<br>$10^5$ | Time of<br>Polymeri-<br>zation<br>(hrs.) | Conver-<br>sion<br>[%] | Configuration |                   |
|--------|-------------------------------------|-------------------------------------|--|------------------------|---------------|-------------------|
|        |                                     |                                     |  |                        | 1,4<br>trans  | 1,2<br>1,4<br>cis |
| B6     | 0                                   | 1.12                                | 24                                       | 87                     | 8             | 89 3              |
| B24    | 12.5                                | 0.75                                | 24                                       | 74                     | 6             | 93 1              |
| B21    | 25.0                                | 0.25                                | 24                                       | 39                     | 7             | 92 1              |
| B22    | 37.5                                | 0.12                                | 24                                       | 55                     | 4             | 93 3              |
| B20    | 50.0                                | 0.25                                | 24                                       | 51                     | 7             | 89 4              |
| B23    | 62.5                                | 1.12                                | 24                                       | 61                     | 6             | 92 2              |

TABLE XXII  
 Polymerization of Butadiene in HMPA with Different Cations  
 $[\text{MBPh}_4] = 3.66 \times 10^{-3}$  mole/litre;  $t = 0^\circ\text{C}$

| Sample | Cation            | Charge Passed<br>[F] x 10 <sup>5</sup> | Time of Polymerization<br>(hrs.) | Conversion | Configuration (%) |         |
|--------|-------------------|--|----------------------------------|------------|-------------------|---------|
|        |                   |  |                                  |            | 1,4 trans         | 1,2 cis |
| B61    | Li                | 3.1                                    | 24                               | 58.5       | 11                | 89      |
| B62    | Na                | 3.1                                    | 24                               | 91.0       | 9                 | 91      |
| B63    | K                 | 6.2                                    | 24                               | 58.0       | 11                | 89      |
| B64    | Rb                | 6.8                                    | 24                               | 96.0       | 14                | 86      |
| B65    | Bu <sub>4</sub> N | 37.3                                   | 24                               | traces     | -                 | -       |

TABLE XXIII

Polymerization of Butadiene in THF - HMPA Mixture with Different Cations

[MBPh<sub>4</sub>] = 3.66 x 10<sup>-3</sup> mole/litre; t = 0°C

| Sample | Cation            | Charge Passed [F] x 10 <sup>5</sup> | Time of Polymerization (hrs.) | Conversion (%) | Configuration (%) |     |         |
|--------|-------------------|-------------------------------------|-------------------------------|----------------|-------------------|-----|---------|
|        |                   |                                     |                               |                | 1,4 trans         | 1,2 | 1,4 cis |
| B72    | Li                | 56.0                                | 24                            | 7              | 9                 | 91  | 0       |
| B71    | Na                | 9.3                                 | 24                            | 91             | 14                | 86  | 0       |
| B73    | K                 | 9.3                                 | 24                            | 93             | 12                | 88  | 0       |
| B74    | Rb                | 9.3                                 | 24                            | 81             | 13                | 87  | 0       |
| B75    | Bu <sub>4</sub> N | 56.0                                | 24                            | traces         | -                 | -   | -       |

electrons by the reaction with alkali metals. In the present experiments, the electrolysis was accompanied by the formation of a dark blue color at the cathode, which turned amber in the bulk of the solution with sodium as counterion. The situation was similar with lithium as counterion. With potassium tetraphenylboride as supporting electrolyte, however, the originally formed blue and amber colors turned into the final reddish brown. In the case of  $\text{Rb}^+$  as counterion, once again reddish brown was the final color with violet as an intermediate. Evidently, the ionic equilibria giving rise to such a display of colors are rather complex and preclude any conclusions without a more thorough investigation of other aspects of such systems. Nevertheless, it is conceivable that the high solvating strength of the HMPA solvent gives rise to a predominantly free-ion or strongly solvent-separated ion-pair propagation, as compared with the governing contact ion-pair propagation in the case of tetrahydrofuran. The changed character of the activated complex would be reflected in the microstructure.

It is also evident from Table XXII, that the effect of the nature of the counterion was negligible. The same observation is once again noted in Table XXIII, which lists the results of experiments carried out using a 1:1 (by volume) mixture of tetrahydrofuran and HMPA as the solvent. Table XXIV compares the present results with the data published by Tobolsky et al. (80) for conventionally initiated polymerizations. It is seen, that in the present

TABLE XXIV  
Effect of Counterion on Microstructure

| Structure | Metal        | Li | Na | K    | Rb   |
|-----------|--------------|----|----|------|------|
| 1,2       | Present work | 91 | 86 | 88   | 87   |
|           | Ref. (80)    | 96 | 91 | 82.5 | 75.3 |
| 1,4       | Present work | 9  | 14 | 12   | 13   |
|           | Ref. (80)    | 4  | 9  | 17.5 | 24.7 |

work employing electrolytic initiation the variation of microstructure was much smaller than that observed by the previous workers, and that it did not reveal any specific trend.

This apparent discrepancy between the results obtained here and by Tobolsky et al. (80) might be explained in terms of two types of propagation. Radical-anions produced by an electron-transfer reaction can grow by both ionic and radical mechanisms (114, 115). Of the two, the radical growth produces more 1,4 structure. The role of the radical reaction depends on the ratio of the rate of polymerization to the rate of radical dimerization (or disproportionation). When the dimerization reaction of radical-anions is very fast, one can expect a product formed exclusively by the anionic reaction. This can be the case in the present systems, where the radical-anions are generated on the surface of an electrode and probably dimerize before entering the bulk of the solution. Such fast dimerization caused by the localized occurrence of radical-anions would overwhelm the possible effects of counterions. On the contrary, in the systems used by Tobolsky et al. (80) initiation takes place randomly throughout the whole volume of the reaction mixture and no such effects are expected.

It is difficult to estimate the rate of dimerization of butadiene radical-anions as no relevant data has been published. However, the recombination rate of ion-radicals is known to be relatively slow when compared with that of ordinary radicals (21, p. 372). Szwarc (21, p. 368) notes that the contribution of the radical reaction is usually insignificant whenever the anionic growth is fast compared with the radical propagation. This is true in the case of styrene. The radical propagation rate constant of this monomer at 0°C is 6.91 litre/mole sec (116), whilst the ion-pair anionic rate constant has the value of 90 litre/mole sec (32).

On the contrary, with butadiene the rate of radical propagation at 10°C is 8.4 litre/mole sec (117), whereas the ion-pair propagation constant extrapolated from present measurements has a substantially lower value of 1.45 litre/mole sec. Therefore, much greater participation of the radical polymerization can be expected for this monomer.

The same concept can also be employed to explain the effects of temperature on microstructure observed by Arest-Yakubovich and Medvedev (82) (Table V). Axford (118) determined the activation energy of the radical propagation of butadiene to be 9.3 kcal/mole. This is much higher than the value of 2.6 kcal/mole determined by present studies for an ion-pair propagation. As the temperature is decreased, the rate of radical propagation drops substantially faster than the ionic rate. At low temperatures, therefore, the role of the radical process can be expected to become negligible and the microstructure of the resultant polymer will be defined exclusively by the anionic polymerization mechanism.

It is possible to calculate the extent of radical reaction in systems used by Tobolsky and coworkers (80). For example, polymerization initiated by rubidium naphthalenide at 0°C yielded a polymer (I) with 75.3% 1,2 and 24.7% 1,4 structures. A radical polymerization of butadiene at the same temperature gives rise to approximately 80% of the 1,4 structure. An anionic polymerization (such as in present experiments) produces about 90% of the 1,2 isomer. Using these data, it is found that 79% of polymer (I) was formed by an anionic mechanism, whilst radical growth accounted for 21% of the product. This result seems reasonable in the light of the foregoing discussion.

The presence of a radical growth competing with the dominant living anionic mechanism would no doubt have an effect on the molecular weight distribution of the polymer. However, at a low extent of this reaction such effects would probably be masked by the spreading



influence of living end attrition and chain transfer and would not be readily detected.

Practically no polymer was obtained when tetrabutylammonium tetraphenylboride was employed as a supporting electrolyte. This is illustrated on samples B65 and B75 listed in Tables XXII and XXIII respectively. During an electrolysis in an unstirred solution, formation of pale yellow color was observed at the cathode, which disappeared immediately in the solution. This is in keeping with the interaction of the tetrabutylammonium cations in living systems and is a reflection of the ease of proton abstraction. These results are in agreement with the results of Yamazaki et al. (12).

Compositions shown in Tables XX-XXIV are those determined by the IR analysis. Because of the limited solubility of the polymer samples, the NMR method could not be applied to most polymers and was only used to verify the results of the IR assay in several instances. A good agreement between the results of the two methods was obtained and is demonstrated in Table XXV.

TABLE XXV  
Comparison of IR and NMR Analysis of Anionic Polybutadienes

| Sample | 1,2 [%] |     | 1,4 [%] |     |
|--------|---------|-----|---------|-----|
|        | IR      | NMR | IR      | NMR |
| B63    | 89      | 89  | 11      | 11  |
| B64    | 86      | 85  | 14      | 15  |
| B115   | 91      | 93  | 9       | 7   |

### 3.2.5. Butadiene-Styrene Copolymerization.

The primary objective of these several experiments was to investigate the electrolytic behavior of butadiene-styrene systems, capable of living polymerization. Anionic copolymerizations are intrinsically more complex than the homopolymerization reactions because of the presence of two structurally different carbanions.

In all experiments, polymerization was initiated at the cathode by passing a 5 mA current for 300 sec. After this time, the current was discontinued and the mixture was allowed to react for another 60 sec. All experiments were carried out at -20°C.

Table XXVI shows the total yield and molecular weight of copolymers prepared with four different monomer feed ratios.

TABLE XXVI

Butadiene-Styrene Copolymerization.

$$[\text{NaBPh}_4] = 1.8 \times 10^{-2} \text{ mole/litre;} \\ t = -20^\circ\text{C}$$

| Sample | B:S (Feed)<br>[mole/mole] | Monomer [g] |      | Yield<br>[g] | Molecular<br>Weight |
|--------|---------------------------|-------------|------|--------------|---------------------|
|        |                           | B           | S    |              |                     |
| BS1    | 1:9                       | 0.22        | 3.75 | 3.20         | $2.0 \times 10^6$   |
| BS2    | 3:7                       | 0.65        | 2.91 | 3.21         | $1.2 \times 10^6$   |
| BS3    | 1:1                       | 1.08        | 2.08 | 2.10         | $5.0 \times 10^5$   |
| BS4    | 7:3                       | 1.51        | 1.25 | 0.61         | $2.5 \times 10^5$   |

The values of molecular weights listed in Table XXVI are the peak molecular weights, estimated directly from the corresponding GPC chromatograms using the polystyrene calibration curve. It is evident that both the molecular weight and yield decrease sharply with the increasing proportion of butadiene in the feed.

The composition of the copolymers was determined by NMR. The results are shown in Table XXVII. It is seen, that the styrene moiety is predominant in all four cases, although the proportion of the butadiene component grows steadily with the increasing amount of this monomer in the feed.

TABLE XXVII

Composition of Butadiene-Styrene Copolymers

| Sample | Feed B:S<br>[mole/mole] | Composition [mole%] |      | Consumption [mole%] |       |
|--------|-------------------------|---------------------|------|---------------------|-------|
|        |                         | B                   | S    | B                   | S     |
| BS1    | 1:9                     | 1.0                 | 99.0 | 9.3                 | 84.8  |
| BS2    | 3:7                     | 3.8                 | 96.2 | 9.3                 | 100.0 |
| BS3    | 1:1                     | 16.7                | 83.3 | 18.5                | 100.0 |
| BS4    | 7:3                     | 18.0                | 82.0 | 2.6                 | 44.0  |

The preferential incorporation of styrene into the copolymer, observed in this work is in accordance with data published by other authors for conventional systems. Spirin and coworkers (85, 119) found 85% of the styrene moiety in a copolymer prepared with a 1:1 (by mole) feed ratio in tetrahydrofuran at  $-35^{\circ}\text{C}$ . Similar results were reported by Tobolsky and coworkers (80).

From the data on yield and composition given in Tables XXVI and XXVII, it is possible to calculate the individual consumption of each monomer during the reaction. The results are listed in the last two columns of Table XXVII. It is evident, that in the first three experiments the conversion of styrene into polymer is virtually complete. The yields and molecular weights of the individual polymers indicate, that the overall rate of polymerization drops with the increasing amount of butadiene in the feed. The relative consumption of butadiene reaches its maximum value for the feed ratio (1:1) and then drops again.

These observations are in a good interrelation with the electrolytic behavior of the systems. In experiment BS1, the orange color of styrene anions was formed at the cathode. Rapid (almost explosive) polymerization ensued and after about 2 minutes the color

of the reaction mixture turned yellow, reflecting the presence of butadienyl anions. The last phenomenon is similar to that observed by Tobolsky et al. (80).

With higher proportion of butadiene in the feed (BS2, BS3), the color originally produced at the cathode was yellowish-orange, reflecting the presence of both types of anions in equilibrium. Once again, the color became yellow after 3-4 minutes. In experiment BS7 only yellow color was formed, which persisted throughout the reaction.

Because of the high concentration of sodium tetraphenylboride as supporting electrolyte, the propagation of styrene (monomer 1) and butadiene (monomer 2) can be assumed to proceed through ion-pairs only. From data published by Shimomura et al. (32) the rate of addition of styrene monomer to polystyryl sodium ion-pairs is  $k_{11} = 120$  litre/mole sec (at  $-20^{\circ}\text{C}$ ). Spirin et al. (85) determined the copolymerization parameters for the system to be  $r_1 = 8$  and  $r_2 = 0.2$ . The butadiene homopolymerization rate constant determined in this work is  $k_{22} = 0.8$  litre/mole sec at  $-20^{\circ}\text{C}$ . Combining these data, the crossover rate constants can be evaluated and are  $k_{12} = 15$  litre/mole sec and  $k_{21} = 4$  litre/mole sec.

These values are in agreement with the actual behavior observed in the present experiments. Consider one isolated chain with a polystyryl active end. Surrounded by an equimolar mixture of the two monomers, the active end is 10 times more likely to add a molecule of styrene, than a molecule of butadiene. However, once it reacts with butadiene, the resulting butadienyl end commands a much slower rate of addition for both monomers, than does the corresponding polystyryl end. Therefore, the average lifetime of butadienyl anions is expected to be longer, and the solution will have a yellow color. By the same token, an increase of the concentration of butadiene in the reaction mixture will significantly lower the overall rate of polymerization.

The results under discussion are not suitable for an evaluation of the copolymerization parameters because of the high conversions. However, an estimate can be made on the basis of experiment BS4. In the first approximation, the parameter  $r_2 = \frac{k_{22}}{k_{21}}$  may be assumed to be equal to zero. In such a case, the equation proposed by Wall (120) can be applied, giving  $r_1 = 6$ . Considering the uncertainty involved in this estimation and the insensitivity of the method, the agreement with the value  $r_1 = 8 \pm 2$  published by Spirin and coworkers is remarkable.

### 3.2.6. Controlled Potential Electrolysis of 1,3-Butadiene.

All experiments described and discussed so far in this thesis were performed under the constant current conditions. This in fact means that the applied voltage initially required to impose a given current was automatically changed during the electrolysis in order to maintain a constant current. In such systems, the electrode potential was not controlled.

For reasons mentioned in Section 1.3.4., it is not possible to carry out a selective reduction of butadiene in the presence of alkali metal salts of tetraphenylboride. It seemed reasonable, however, to attempt to use the tetramethylammonium salt as suggested by Anderson (53). The tetramethylammonium cation should have a more negative reduction potential than butadiene and in such a case a selective reduction of the monomer would be possible by keeping the cathode potential sufficiently less negative.

A study of the redox behavior of butadiene was attempted using cyclic voltammetry. The measurements were carried out in tetrahydrofuran using tetramethylammonium tetraphenylboride and tetrabutylammonium perchlorate as supporting electrolytes at temperatures -10 and 25°C. No peak for the butadiene monomer was observed within the limits given by the discharge potential of both salts. Variations of the concentration of monomer and of

the supporting electrolyte showed no significant effect. It was concluded that the reduction peak of butadiene in the employed system coincided with the discharge of the tetraalkylammonium cation. For this reason, a controlled potential electrolytic polymerization of this monomer was found not to be feasible.

The general suitability of tetramethylammonium tetraphenylboride for a living polymerization of butadiene was also investigated. The results obtained were very much the same as in the case of a tetrabutylammonium salt as supporting electrolyte. During electrolysis, a yellow color was formed at the cathode which quickly disappeared on mixing with the solution. Only a very small amount of low molecular weight polymer was isolated.

This last finding is in disagreement with the results of Anderson (53), who found that tetramethylammonium tetraphenylboride did not terminate living polymers of styrene. It is believed that this apparent discrepancy can be explained by the lesser general stability of polybutadienyl anions and possible abstraction of methyl groups from the tetramethylammonium cation.

### 3.3. Criteria for a Simplified Universal Calibration in Gel Permeation Chromatography.

#### 3.3.1. General Considerations.

The interpretation of data in gel permeation chromatography requires the evaluation of the molecular weight distribution of a particular polymer on the basis of known molecular weight distributions of a series of standard samples. As standards of most polymers are not readily available, a considerable experimental and theoretical effort has been expended to obtain universal calibration techniques based on polystyrene standards. This in fact means to transform the primary calibration curve in such a way that it can be used for polymers structurally different from the standard.

The use of the extended length of polymer chains was originally suggested (121, 122). A calibration curve was constructed by plotting the logarithm of extended chain length against the elution volume. The molecular weight of a particular polymer could be calculated by applying the Q factor, representing the molecular weight corresponding to 1 Å projected chain length. Such factors can be determined from the chain geometry and the particular bond lengths.

Because of the great simplification involved, the extended length concept was found to be unreliable with many polymers. Its validity is most likely limited to structurally very similar polymers. Heller and Moacanin (123) recently reported a good agreement for poly-1-vinylnaphthalene, poly-2-vinylnaphthalene and poly-4-vinylbiphenyl.

Obviously a more general scheme would be that based on the effective volume of the chains in solution. The feasibility of utilizing the hydrodynamic volume ( $M[\eta]$ ) as a universal parameter was demonstrated by Benoit and coworkers (124) and confirmed by other workers (125). The product ( $M[\eta]$ ) is proportional

to the cube of the hydrodynamic radius  $R_H$ , which can be considered as the actual separation parameter in GPC:

$$M[\eta] = 10\pi N_A \frac{R_H^3}{3} \quad (67)$$

A plot of either  $R_H$  or  $(M[\eta])$  against the elution volume of standard samples then provides a universal calibration curve applicable to other polymers.

When two monodisperse polymers possess the same hydrodynamic radius in solution, their molecular weights are related through their limiting viscosity numbers:

$$\frac{M_1}{M_2} = \frac{[\eta]_2}{[\eta]_1} \quad (68)$$

It should be noted that this relationship cannot be directly used to evaluate the molecular weight distribution of a polydisperse sample. Such work entails additional information relating the limiting viscosity number of each polymer to its molecular weight. This relationship is quantitatively expressed by the Mark - Houwink equation:

$$[\eta] = KM^a \quad (69)$$

Combination of Equations 68 and 69 yields:

$$\log M_2 = \frac{1}{1+a_2} \log \frac{K_1}{K_2} + \frac{1+a_1}{1+a_2} \log M_1 \quad (70)$$

Equation 70 enables one to use a primary polystyrene calibration curve directly for other polymers.

The calibration proposed by Coll and Gilding (126) employs the expression  $(M[\eta])/f(\epsilon)$  as the universal parameter, where  $f(\epsilon)$  is solely dependent on the Mark - Houwink exponent  $a$ . This leads to an expression similar to Equation 70:



$$\log M_2 = \frac{1}{1 + a_2} \log \frac{K_1 f(\epsilon_2)}{K_2 f(\epsilon_1)} + \frac{1 + a_1}{1 + a_2} \log M_1 \quad (71)$$

Equations 70 and 71 require the knowledge of Mark-Houwink constants of both polymers. However, such constants are frequently not available in the literature for the solvents and temperatures usually employed in GPC. Furthermore, values listed in the literature are often insufficiently reliable and their applicability to the present problem is difficult to assess. Direct determination of  $K$  and  $a$  based on the measurements of  $\bar{M}_w$  or other molecular weight averages is also subject to substantial errors.

Consider two polymers which are structurally different but not radically dissimilar. Their thermodynamic behavior is characterized by the exponents  $a_1$  and  $a_2$ . At the same temperature and in the same solvent, one can assume that  $a_1 \approx a_2$ . Then Equations 70 and 71 reduce to the simple expression

$$\log M_2 = \log C + \log M_1 \quad (72)$$

or 
$$M_2 = C \cdot M_1 \quad (73)$$

where  $C$  is a constant.

The exponential relationship is thus replaced by a simple linear equation. In order to prove the feasibility of such a simplification for a particular pair of polymers, it is necessary to estimate the validity of the underlying assumptions and to assess the errors introduced in the case that  $a_1$  and  $a_2$  are not identical.

The necessity to characterize polymers formed by electrochemical techniques, and to compare these to conventionally polymerized macromolecules provided an incentive to establish the validity of the foregoing simplified calibration scheme for polystyrene and 1,2-polybutadiene.

### 3.3.2. Results and Discussion.

The hydrodynamic volume concept (124) implies that if a polymer other than polystyrene is evaluated by the polystyrene calibration curve, the resulting average molecular weight can be considered equivalent to that of a hypothetical sample of polystyrene possessing the same hydrodynamic volume as the polymer analyzed. From the values of  $[\eta]$  and  $\bar{M}_n$  of standard polystyrene fractions, the products  $\bar{M}_n(\text{PS})[\eta(\text{PS})]$  have been calculated. Their logarithms were plotted against  $\log \bar{M}_n(\text{PS})$ . The relationship was linear and is shown in Figure 20.

The polybutadiene samples were characterized by their limiting viscosity numbers and their GPC chromatograms were recorded. From the computer program (Section 2.4.), one obtains values of  $\bar{M}_n(\text{PS})$  and the corresponding average values of hydrodynamic volume  $\bar{M}_n(\text{PS})[\eta(\text{PS})] = \bar{M}_n(\text{PB})[\eta(\text{PB})]$  can be extrapolated from Figure 20. Finally, the value of  $\bar{M}_n(\text{PB})$  is obtained by dividing the extrapolated hydrodynamic volume by the limiting viscosity number of the polybutadiene sample. If the assumption described in the previous text is correct, the coefficient

$$C_n = \frac{\bar{M}_n(\text{PB})}{\bar{M}_n(\text{PS})} \quad (74)$$

should be a constant.

Data compiled in Table XXVIII demonstrate that coefficient  $C_n$  remains practically constant for polybutadiene samples of various molecular weights and polydispersities. The uncertainty involved in the determination of  $C_n$  is remarkably small as reflected by the standard deviation  $\sigma = 0.013$ . It should be noted, that the 1% confidence limit gives  $\lambda = 0.035$ .

For comparison, the last column of Table XXVIII lists the values of coefficients  $C_w$  obtained with a modified procedure

Figure 20. DEPENDENCE OF HYDRODYNAMIC VOLUME ON MOLECULAR  
WEIGHT FOR POLYSTYRENE STANDARDS

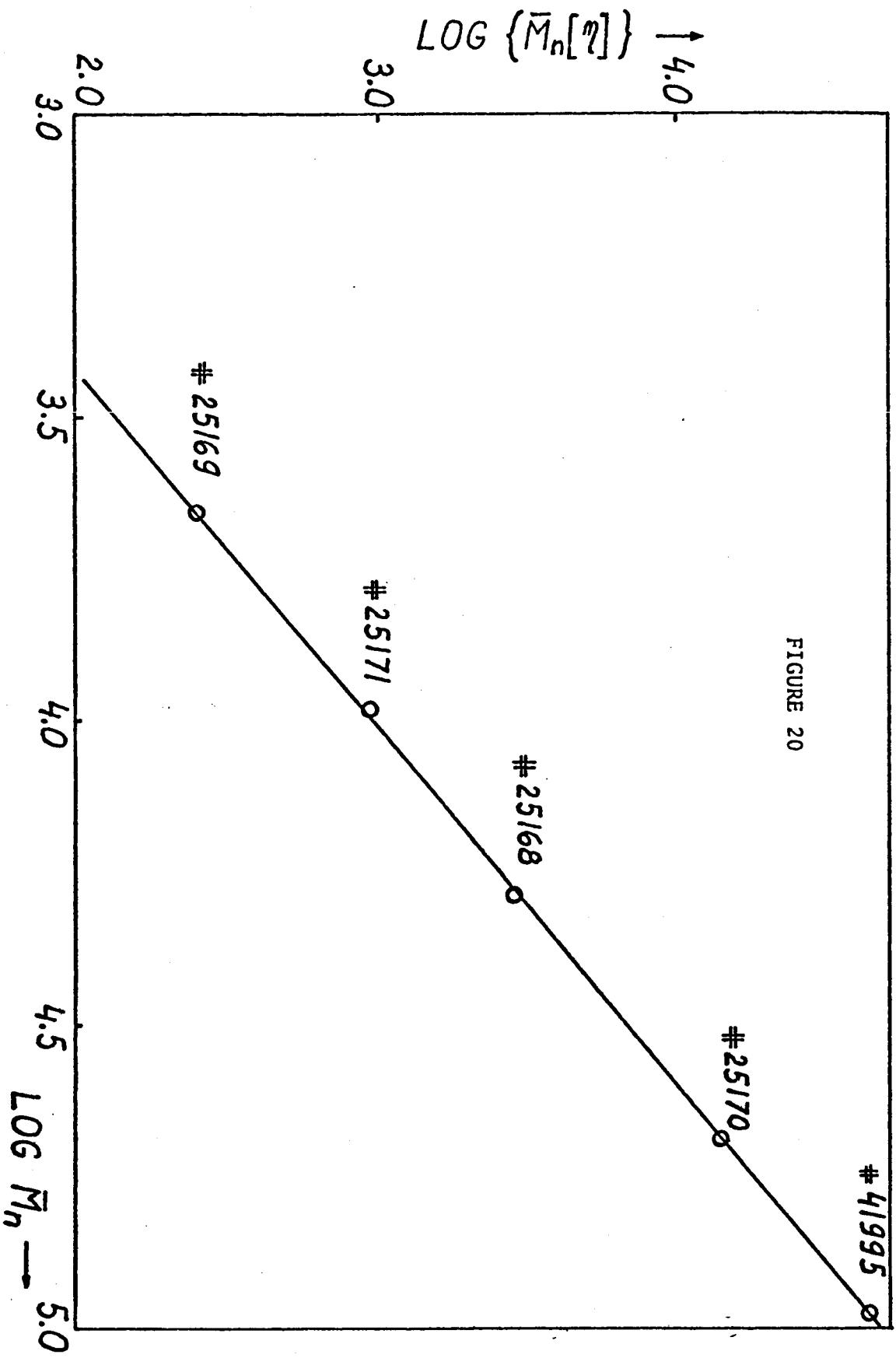


FIGURE 20

utilizing  $\bar{M}_w$  averages instead of  $\bar{M}_n$  averages. It is evident that the values of  $C_w$  vary from sample to sample and are dependent on the molecular weight distribution.

The average value of the coefficient  $C_n$  can be used to calculate number average molecular weights of unknown samples of the same polymer:

$$\bar{M}_n(\text{PB}) = 0.617 \bar{M}_n(\text{PS}) \quad (75)$$

Although it is not valid to draw conclusions about the applicability of Equation 75 beyond the region of measurements made, an estimate of errors involved may be inferred from data published by other workers.

For example, Coll and Gilding (126) found the exponential calibration curve for poly- $\alpha$ -methylstyrene:

$$\log M_{\text{PAMS}} = -0.058 + 1.021 \log M_{\text{PS}} \quad (76)$$

where PAMS and PS denote poly- $\alpha$ -methylstyrene and polystyrene respectively. The value of the coefficient C obtained when Equation 76 is replaced by a linear relationship (Equation 73) is shown in Table XXIX.

It is evident that the coefficient C varies with molecular weight. However, if an average value of C is used for a polymer whose molecular weight is from  $10^4$  to  $10^6$ , the calculated value deviates from the "true" value by approximately +5% for the lowest molecular weight and -5% for the highest molecular weight. It can be seen therefore, that unless the Mark - Houwink constants for two polymers differ significantly, there is little variation in the results obtained by using an exponential expression over that obtained by using a simplified linear relationship in Equation 73. The simple proportionality between the molecular weights of the two polymers may therefore be employed over a molecular weight range considerably greater than that investigated in these

TABLE XXVIII

Simplified Universal Calibration in GPC.

| $\bar{M}_n$ (PS) | $\bar{M}_n$ (PB) | $[\eta]$ | $\bar{M}_w/\bar{M}_n$ | $C_n$  | $C_w$  |
|------------------|------------------|----------|-----------------------|--------|--------|
| 15480            | 9420             | 0.2165   | 1.29                  | 0.6077 | 0.6155 |
| 20600            | 12400            | 0.2651   | 1.18                  | 0.6155 | 0.7436 |
| 21960            | 13340            | 0.2753   | 1.31                  | 0.6075 | 0.6855 |
| 28000            | 17100            | 0.3209   | 1.23                  | 0.6119 | 0.6471 |
| 29000            | 17800            | 0.3240   | 1.28                  | 0.6138 | 0.6684 |
| 29200            | 17600            | 0.3385   | 1.49                  | 0.6037 | 0.7208 |
| 30500            | 19480            | 0.3314   | 1.20                  | 0.6394 | 0.6579 |
| 39500            | 25130            | 0.3976   | 1.28                  | 0.6358 | 0.7010 |

TABLE XXIX

Replacement of Equation 76 by a Linear Relationship.

| $M_{PS}$ | $M_{PAMS}$ | $C$  |
|----------|------------|------|
| 10000    | 10620      | 0.94 |
| 50000    | 54900      | 0.91 |
| 100000   | 111500     | 0.90 |
| 500000   | 576000     | 0.87 |
| 1000000  | 1170000    | 0.86 |

experiments.

Dawkins (127, 128) suggests the use of unperturbed dimensions of a chain for universal calibration. The molecular weights of two polymers are related by the expression:

$$\log M_2 = \log M_1 + \log \frac{A_1}{A_2} \quad (77)$$

where  $A = (L_0^2)$  is a constant characteristic for each polymer. Insofar as Equation 77 is formally identical with Equation 72, it will be of interest to compare the coefficient  $C_n$  determined in present experiments with the factor  $A(\text{PS})/A(\text{PB})$  based on tabulated values of  $A^{1/2}$  (129). This quantity has the value of 0.67 Å for polystyrene. The value for 1,2-polybutadiene is not available in the literature, but it can be estimated with a good accuracy from the unperturbed dimensions of similar vinyl polymers such as atactic poly-1-butene and atactic polypropylene. The effective value is calculated as the sum of the relative contributions of 1,2 and 1,4 components (90% and 10% respectively), which gives  $A^{1/2} = 0.80$  Å. This results in  $A(\text{PS})/A(\text{PB}) = 0.70$  which is very close to the value of  $C_n$  determined in this work. This result indicates the validity of Dawkins' concept for this particular pair of polymers.

On the other hand, an application of the extended length calibration yields a transformation coefficient  $Q(\text{PB})/Q(\text{PS}) = 0.43$  which is substantially smaller than  $C_n$ . According to Dawkins, two polymers are comparable via their extended lengths if their  $A \cdot Q$  products are equal. In the present case,  $A(\text{PS}) \cdot Q(\text{PS}) = 21.2$ ,  $A(\text{PB}) \cdot Q(\text{PB}) = 13.0$  and the extended length concept is therefore not applicable. Thus calibration is required and the technique described here represents a simple approach.

#### 4. CONCLUSIONS

The work included in this thesis deals with only one particular type of electrochemical initiation. It is reasonable to compare the various advantages and disadvantages of this "living polymer" approach with other electroinitiation methods.

In general, the merits of the individual electroinitiation techniques may be judged from a variety of different standpoints. These can best be illustrated by some examples:

- i) Flexibility in controlling the overall rate of polymerization;
- ii) Control of molecular weight distribution through variation of the impressed current;
- iii) Possibility of preparing block copolymers;
- iv) Control of molecular architecture and the possibility of preparing stereoregular polymers;
- v) Possibility of using a wide variety of systems as regards solvents, supporting electrolytes etc.;
- vi) Control of electron transfer at the electrode.

With respect to the first two points, the living method shows a great potential. Both the rate of initiation and the rate of termination are easily controlled by the applied current. The overall rate of polymerization can also be varied by changing reaction conditions such as temperature, type of solvent etc., although not in such a wide range as one might desire. The possibility to exercise a great deal of control over the molecular weights and molecular weight distributions has been amply demonstrated in the foregoing text. This is not paralleled by any other electroinitiation technique.

The present method can be used for the preparation of block copolymers in the same manner as in a conventional living polymerization. For example, butadiene could be initiated by the passage of current and polymerized until the complete depletion



of monomer. Subsequently a second monomer ( e.g. styrene) can be added and growth continues. The resultant polymer would consist of one block of butadiene and one block of styrene, whose relative size would depend on the molar ratio of the two monomers.

The variation of reaction parameters did not have any significant effect on the microstructure of the resultant polybutadienes, nor did these polymers possess any degree of stereoregularity. Clearly the impossibility to employ hydrocarbon and other non-polar solvents is critical, as most such effects occur only in non-polar media. From this point of view, electrolytically initiated charge-transfer polymerizations might be of more interest, as stereoregularity can possibly result from adsorption on the surface of the electrode or from complexing of the monomer with the salts present in the electrolytic environment.

The severe limitations of the present method stemming from the strict requirements on the chemical and physical properties of the reaction systems have already been discussed and no further elaboration seems necessary. This problem is closely related to that of controlling the electron transfer reaction at the cathode. Tetraalkylammonium cations, suitable for a selective electrolysis of most monomers, cannot be employed as they terminate the living polymerization. On the contrary, alkali metal cations support living polymerization, but their reduction potential is less negative than that of most monomers. This dilemma has yet to be solved, if the tempting synthetic possibilities of controlled potential living polymerizations are to be realized.

The past several decades have witnessed a fast growth of both analytic and synthetic electrochemistry. Theories have been put forward to explain the processes taking place at the electrodes and to describe the kinetics and thermodynamics of electrolytic

reactions. At this stage, however, only the very basic electrode processes can be described quantitatively with some adequacy. An experimental chemist wishing to carry out a new electrochemical synthesis still has to rely a great deal on experience and intuition. Hopefully, the continuing rapid development in the field will lead to some coalescence between theory and practice.

APPENDIX I

Analysis of Errors

1. Kinetic Measurements

Rate constants were determined from a small number of experiments and, therefore, the experimental scatter could not be characterized by the standard deviation. The limits of error were estimated by the propagation-of-error treatment (130, 131).

The rate constants were evaluated from Equation 52, giving the following expression for the relative error in  $k_p$ :

$$\frac{\lambda(k_p)}{k_p} = \frac{\lambda(A)}{A} + \frac{\lambda([LE])}{[LE]} + \frac{\lambda(t)}{t} \quad (78)$$

where  $A = \ln ([M_0]/[M])$ . Therefore, relative limits of error in A, [LE] and t must be found.

(a) Limit of error in A

The volume of the monomer was measured with the uncertainty of  $\pm 0.02$  ml for the total of 5 ml. The concentration of the residual monomer was measured within  $\pm 1\%$ . The absolute

limit of error in A is given by:

$$\lambda(A) = \left| \frac{\partial A}{\partial [M_0]} \right| \lambda([M_0]) + \left| \frac{\partial A}{\partial [M]} \right| \lambda([M]) \quad (79)$$

$$\lambda(A) = \frac{\lambda([M_0])}{[M_0]} + \frac{\lambda([M])}{[M]} \quad (80)$$

$$\lambda(A) = \frac{0.02}{5.0} + 0.01 = 0.014$$

For conversion of 20 - 30%, used in these experiments,  $A \approx 0.25$

and the relative limit of error is given by:

$$\frac{\lambda(A)}{A} = \frac{0.014}{0.25} = 0.06$$

(b) Limit of error in [LE]

This is derived from Equation 50:

$$\frac{\lambda([LE])}{[LE]} = \frac{\lambda(i)}{i} + \frac{\lambda(t_i)}{t_i} + \frac{\lambda(V)}{V} \quad (81)$$

The uncertainty in current  $i$  was  $\pm 3\%$ . Time of initiation was measured with  $\pm 0.5\%$  accuracy and volume was determined within  $\pm 1.5\%$ . Equation 81 does not consider a possible imperfect correction for living end attrition. This is included as a fourth term (5%).

$$\frac{\lambda([LE])}{[LE]} = 0.03 + 0.005 + 0.015 + 0.05 = 0.10$$

(c) Limit of error in t

The absolute limit of error is the sum of uncertainties in  $t_i$ ,  $t_p$  and  $t_t$ :

$$\lambda(t) = \lambda(t_i) + \lambda(t_p) + \lambda(t_t) = 0.5 + 0.5 + 1.0 = 2 \text{ sec} \quad (82)$$

The relative limit is  $\lambda(t)/t = \frac{2}{300} = 0.007$  for the total time 300 sec.

Applying Equation 78:

$$\frac{\lambda(t_p)}{t_p} = 0.06 + 0.10 + 0.007 = 0.17 (\cong \pm 17\%), \text{ the overall relative}$$

error in  $t_p$  is calculated.

The foregoing does not consider the random cancellation of errors. A more probable limit of error  $\frac{\lambda'(k_p)}{k_p}$  is obtained when  $\frac{\lambda(k_p)}{k_p}$  is divided by  $\sqrt{n}$ , where n is the number of variables considered in the treatment. In this case,  $n = 8$  and  $\frac{\lambda'(k_p)}{k_p} = 0.17 / \sqrt{8} = 0.06 (\cong \pm 6\%)$ . This error limit is shown in Figures 11 and 13 as vertical error bars.

## 2. Arrhenius Plot

The standard deviation of the linear Arrhenius Plot (Figure 11; Table X) was evaluated by the method of least squares. Equa-

tion 60 may be re-written to include the 1% confidence limit in intercept and slope:

$$\log k_p = (2.16 \pm 0.04) - \frac{(2600 \pm 380)}{2.303 RT} \quad (83)$$

### 3. Determination of Molecular Weights

(a) Calculated values (Tables XII and XIII)

These were calculated from Equation 61 with a limit of error:

$$\frac{\lambda(\bar{M}_n \text{ calc.})}{\bar{M}_n \text{ calc.}} = \frac{\lambda([M])}{[M]} + \frac{\lambda([LE])}{[LE]} = 0.01 + 0.10 = 0.11 (\pm 11\%) \quad (84)$$

(b) GPC measurements

The GPC measurements were reproducible within  $\pm 5\%$ .

(c) Agreement between predicted and measured values of  $\bar{M}_n$  for polymers with bimodal and trimodal distributions (Tables XVIII and XIX).

The experiments used rate constants determined previously. Each experiment involves the same steps as that used for the determination of  $k_p$ , therefore,

$$\frac{\lambda(\bar{M}_n \text{ found})}{\bar{M}_n \text{ found}} = 2 \frac{\lambda(k_p)}{k_p} + \lambda_{\text{rel}}(\text{GPC}) = 2 \times 0.17 + 0.05 = 0.39 \quad (86)$$

The total number of variables is 17 in this case, therefore,

$$\frac{\lambda'(\bar{M}_n \text{ found})}{M_n \text{ found}} = \frac{0.39}{\sqrt{17}} = 0.10 (\cong \pm 10\%)$$

The difference between predicted and found molecular weights in Tables XVIII and XIX lies within this lower limit of error. The low molecular weight fractions, however, seem to exhibit a systematic deviation.

#### 4. Determination of Microstructure

The results obtained by the IR method were reproducible within  $\pm 3\%$ . This involves the instrumental precision and the uncertainty due to reading from the spectra. The absolute error of this analysis cannot be determined because no standards are available. Most authors report overall errors of  $\pm 5\%$  for this type of analysis.

5. LIST OF REFERENCES

1. M. Fleischmann, D. Pletcher: R.I.C. Reviews 1969, 87
2. E.C. Szarvasy: J. Chem. Soc. 77, 207 (1900)
3. E.A. Rembold: Ph.D. Thesis, Ohio State University (1947)
4. L.C. Wilson, E. Dineen, T.C. Schwann: Trans. Electrochem. Soc. 96, 226 (1949)
5. G. Parravano: J. Am. Chem. Soc. 73, 628 (1951)
6. J.W. Breitenbach, C.H. Srna: Pure Appl. Chem. 4, 245 (1962)
7. H.Z. Friedlander: in "Encyclopedia of Polymer Science and Technology", Vol. 5, p. 629, Interscience 1966
8. B.L. Funt: Macromol. Rev. 1, 35 (1966)
9. N. Yamazaki: Adv. Polymer Sci. 6, 377 (1969)
10. B. L. Funt, J. Tanner: in "Techniques in Electroorganic Chemistry", Chapter IX, Ed. by N.L. Weinberg, Wiley & Sons, New York, to be published
11. D.J.G. Ives, G.J. Janz: "Reference Electrodes", Academic Press, New York 1961
12. N. Yamazaki, I. Tanaka, S. Nakahama: J. Macromol. Sci. - Chem., A2, 1121 (1968)
13. S.N. Bhadani, G. Parravano: J. Polymer Sci. A-1, 8, 225 (1970)
14. B.L. Funt, D.G. Gray: J. Electrochem. Soc. 117, 1020 (1970)
15. B.L. Funt, D.G. Gray: Can. J. Chem. 46, 1337 (1968)
16. M. Szwarc: Nature 178, 1168 (1956)
17. M. Brody, M. Ladacki, R. Milkovich, M. Szwarc: J. Polymer Sci. 25, 221 (1957)
18. M. Szwarc, M. Levy, R. Milkovich: J. Am. Chem. Soc. 78, 2656 (1956)
19. M. Szwarc: Makromol. Chem. 35, 132 (1960)
20. M. Levy, M. Szwarc: J. Am. Chem. Soc. 82, 521 (1960)
21. M. Szwarc: "Carbanions, Living Polymers and Electron Transfer Processes", Interscience 1968
22. G. Allen, G. Gee, C. Stretch: J. Polymer Sci. 48, 189 (1960)
23. D.J. Worsfold, S. Bywater: Can. J. Chem. 36, 1141 (1958)



24. C. Geacintov, J. Smid, M. Szwarc: J. Am. Chem. Soc. 84, 2508 (1962)
25. D.N. Bhattacharyya, C.L. Lee, J. Smid, M. Szwarc: Polymer 5, 54 (1964)
26. D.N. Bhattacharyya, C.L. Lee, J. Smid, M. Szwarc: J. Phys. Chem. 69, 612 (1965)
27. H. Hostalka, R.V. Figini, G.V. Schulz: Makromol. Chem. 71, 198 (1964)
28. H. Hostalka, G.V. Schulz: Z. Physik. Chem. (Frankfurt) 45, 286 (1965)
29. M. Szwarc: Makromol. Chem. 89, 44 (1965)
30. M. Szwarc: Suomen Kemistilehti 43, 173 (1970)
31. D.N. Bhattacharyya, C.L. Lee, J. Smid, M. Szwarc: J. Phys. Chem. 69, 608 (1965)
32. T. Shimomura, K.J. Tölle, J. Smid, M. Szwarc: J. Am. Chem. Soc. 89, 796 (1967)
33. F.S. Dainton, K.J. Ivin, R.T. LaFlair: Eur. Polymer J. 5, 379 (1969)
34. S. Bywater, D.J. Worsfold: Can. J. Chem. 45, 1821 (1967)
35. A. Parry, J.E.L. Roovers, S. Bywater: Macromolecules 3, 355 (1970)
36. L.L. Böhlm, W.K.R. Barnikol, G.V. Schulz: Makromol. Chem. 110, 222 (1967)
37. L.L. Böhlm, G.V. Schulz: Ber. Bunsenges. 73, 260 (1969)
38. A.A. Korotkov, A.F. Podolsky: J. Polymer Sci. B, 3, 901 (1965)
39. A.A. Korotkov, A.F. Podolsky: J. Polymer Sci. B, 7, 85 (1969)
40. P.J. Flory: J. Am. Chem. Soc. 62, 1561 (1940)
41. P.J. Flory: "Principles of Polymer Chemistry", Cornell University Press 1953
42. J.F. Henderson, M. Szwarc: Macromol. Rev. 3, 317 (1968)
43. T.A. Orofino, F. Wenger: J. Chem. Phys. 35, 532 (1961)

44. R.V. Figini: Makromol. Chem. 44-46, 497 (1961)
45. M. Szwarc, M. Litt: J. Phys. Chem. 62, 568 (1958)
46. L.H. Peebles, Jr.: J. Polymer Sci. B, 7, 75 (1969)
47. V.S. Nanda, R.K. Jain: J. Polymer Sci. A-1, 5, 2269 (1967)
48. N. Yamazaki, S. Nakahama, S. Kambara: Polym. Letters 3, 57 (1965)
49. B.L. Funt, D. Richardson, S.N. Bhadani: Can. J. Chem. 44, 711 (1966)
50. B.L. Funt, S.N. Bhadani, D. Richardson: J. Polymer Sci. A-1, 4, 2871 (1966)
51. S.N. Bhadani: Ph.D. Thesis, University of Manitoba (1966)
52. D.N. Geske: J. Phys. Chem. 63, 1062 (1959)
53. J.D. Anderson: J. Polymer Sci. A-1, 6, 3185 (1968)
54. D. Laurin, G. Parravano: Polym. Letters 4, 797 (1966)
55. D. Laurin, G. Parravano: J. Polymer Sci. C, 22, 103 (1968)
56. B.L. Funt, S.N. Bhadani: J. Polymer Sci. C, 23, 1 (1968)
57. D.J. Worsfold, S. Bywater: Can. J. Chem. 42, 2884 (1964)
58. B.L. Funt, D. Richardson: J. Polymer Sci. A-1, 8, 1055 (1970)
59. D. Laurin, G. Parravano: Paper presented at the Symposium on Kinetics of Polymerization, Cleveland, May 1969
60. S.V. Lebedev: J. Russ. Phys. Chem. Soc. 42, 949 (1910)
61. K. Ziegler, K. Bahr: Chem. Ber. 61, 253 (1928)
62. K. Ziegler, H. Colonius, O. Schafer: Ann. Chem. 473, 36 (1929)
63. K. Ziegler, O. Schafer: Ann. Chem. 479, 150 (1930)
64. K. Ziegler, L. Jakob: Ann. Chem. Liebigs 511, 45 (1934)
65. Firestone Tire and Rubber Co., Australian Pat. Appln. No. 22560 (Oct. 22, 1956)
66. A.A. Korotkov: Angew. Chem. 70, 85 (1958)
67. V.A. Kropachev, B.A. Dolgoplosk, N.I. Nikolaev: Dokl. Akad. Nauk SSSR 115, 516 (1957)
68. I. Kuntz, A. Gerber: J. Polymer Sci. 42, 299 (1960)

69. H. Morita, A.V. Tobolsky: J. Am. Chem. Soc. 79, 5853 (1957)
70. H.L. Hsieh: J. Polymer Sci. A, 3, 181 (1965)
71. H.S. Makowski, M. Lynn, A.N. Bogard: J. Macromol. Sci. - Chem., A2, 665 (1968)
72. H.S. Makowski, M. Lynn: J. Macromol. Sci. - Chem., A2, 683 (1968)
73. M. Szwarc: J. Polymer Sci. 40, 583 (1959)
74. K.F. O'Driscoll: J. Polymer Sci. A, 3, 2223 (1965)
75. F.E. Naylor, H.L. Hsieh, J.C. Randall: Macromolecules 3, 486 (1970)
76. J.C. Randall, F.E. Naylor, H.L. Hsieh: Macromolecules 3, 497 (1970)
77. J.C. Randall, R.S. Silas: Macromolecules 3, 491 (1970)
78. F.P. Price: J. Chem. Phys. 36, 209 (1962)
79. A.W. Meyer, R.R. Hampton, J.A. Davison: J. Am. Chem. Soc. 74, 2294 (1952)
80. A. Rembaum, F.R. Ells, R.C. Morrow, A.V. Tobolsky: J. Polymer Sci. 61, 155 (1962)
81. R.V. Basova, A.A. Arest-Yakubovich, D.A. Solovykh, N.V. Desjatova, A.R. Gantmakher, S.S. Medvedev: Dokl. Akad. Nauk SSSR 149, 1067 (1963)
82. A.A. Arest-Yakubovich, S.S. Medvedev: Polymer Sci. U.S.S.R. 8, 748 (1966)
83. A.A. Arest-Yakubovich, S.S. Medvedev: Dokl. Akad. Nauk SSSR 159, 1065 (1964)
84. M. Morton, L.J. Fetters, R.A. Pett, J.F. Meier: Macromolecules 3, 327 (1970)
85. Yu. L. Spirin, D.K. Polyakov, A.R. Gantmakher, S.S. Medvedev: Dokl. Akad. Nauk SSSR 139, 899 (1961)
86. M. Morton, E.E. Bostick, R.A. Livigni, L.J. Fetters: J. Polymer Sci. A, 1, 1735 (1963)

87. H.L. Hsieh: J. Polymer Sci. A, 3, 153 (1965)
88. H.L. Hsieh: J. Polymer Sci. A, 3, 163 (1965)
89. J. Smid: in "Structure and Mechanism in Vinyl Polymerization",  
Ed. by T. Tsuruta and K.F. O'Driscoll, Marcel Dekker, Inc.,  
New York 1969
90. S. Bywater, A.F. Johnson, D.J. Worsfold: Can. J. Chem.  
42, 1255 (1964)
91. D.K. Polyakov, Yu.L. Spirin, A.R. Gantmakher: Dokl. Akad.  
Nauk SSSR 150, 1051 (1963)
92. A. Gourdenne, P. Sigwalt: Bull. Soc. Chim., France, 1967, 2249
93. A. Gourdenne, P. Sigwalt: Eur. Polymer. J. 3, 481 (1967)
94. N. Yamazaki: Kogyo Kagaku Zasshi 70, 1978 (1967)
95. W.B. Smith, H. Gilde: J. Am. Chem. Soc. 83, 1355 (1961)
96. W.B. Smith, H. Gilde: J. Am. Chem. Soc. 81, 5325 (1959)
97. R.V. Lindsey, Jr., M.L. Peterson: J. Am. Chem. Soc. 81,  
2073 (1959)
98. N. Yamazaki, S. Murai: Chem. Comm. 1968, 147
99. H. Schafer, E. Steckhan: Tetrahedron letters 44, 3835 (1970)
100. D.H. Levy, R.J. Myers: J. Chem. Phys. 41, 1062 (1964)
101. L.J. Fetters: J. Res. Natl. Bur. Stand. 70A, 421 (1966)
102. D. Morero, A. Santambrogio, L. Porri, F. Ciampelli: Chim.  
Ind. 41, 758 (1959)
103. W.L. Senn, Jr.: Anal. Chim. Acta 29, 505 (1963)
104. V.D. Mochel: Paper presented at a meeting of the Division  
of Rubber Chemistry, ACS, Montreal 1967
105. K.S. Chang, R.Y.M. Huang: J. Appl. Poly. Sci. 13, 1459 (1969)
106. M.L. Huggins: J. Am. Chem. Soc. 64, 2716 (1942)
107. E.O. Kraemer: Ind. Eng. Chem. 30, 1200 (1938)
108. I. Sakurada, N. Ise, H. Hirohara, T. Makina: J. Phys. Chem.  
71, 3711 (1967)
109. N. Ise: Adv. Polymer Sci. 6, 347 (1969)
110. K. Takaya, H. Hirohara, N. Ise: Makromol. Chem. 139, 277 (1970)

111. H. Hirohara, K. Takaya, M. Nakayama, N. Ise: *Trans. Faraday Soc.* 66, 3163 (1970)
112. L.J. Fetters: *J. Polymer Sci. C*, 26, 1 (1969)
113. E. Franta, J. Chandhuri, A. Cserhegyi, J. Jagur-Grodzinski, M. Szwarc: *J. Am. Chem. Soc.* 89, 7129 (1967)
114. K.F. O'Driscoll, R.J. Boudreau, A.V. Tobolsky: *J. Polymer Sci.* 31, 115 (1958)
115. C.G. Overberger, N. Yamamoto: *J. Polymer Sci. A-1*, 4, 3101 (1966)
116. C.H. Bamford, A.D. Jenkins, R. Johnston: *Proc. Roy. Soc. (London)* A239, 214 (1957)
117. J.C. Bevington, G.M. Guzman, H.W. Melville: *Proc. Roy. Soc. (London)* A221, 437 (1954)
118. D.W.E. Axford: *Proc. Roy. Soc. (London)* A197, 374 (1949)
119. Yu.L. Spirin, A.A. Arest-Yakubovich, D.K. Polyakov, A.R. Gantmakher, S.S. Medvedev: *J. Polymer Sci.* 58, 1181 (1962)
120. F.T. Wall: *J. Am. Chem. Soc.* 63, 1862 (1941)
121. J.C. Moore, J.G. Hendrickson: *J. Polymer Sci. C*, 8, 233 (1965)
122. L.E. Maley: *J. Polymer Sci. C*, 8, 253 (1965)
123. J. Heller, J. Moacanin: *Pol. Letters* 6, 595 (1968)
124. H. Benoit, Z. Grubisic, P. Rempp, D. Decker, J.G. Zilliox: *J. Chim. Phys.* 63, 1507 (1966)
125. K.A. Boni, F.A. Sliemers, P.B. Stickney: *J. Polymer Sci. A-2*, 6, 1567 (1968)
126. H. Coll, D.K. Gilding: *J. Polymer Sci. A-2*, 8, 89 (1970)
127. J.V. Dawkins: *J. Macromol. Sci. - Phys.*, B2, 623 (1968)
128. J.V. Dawkins: *Eur. Polymer. J.* 6, 831 (1970)
129. *Polymer Handbook*, Ed. by J. Brandrup and E.H. Immergut, Interscience 1967, p. IV-47
130. D.P. Shoemaker, C.W. Garland: in "*Experiments in Physical Chemistry*", McGraw-Hill 1962
131. P.R. Bevington: in "*Data Reduction and Error Analysis in Physical Sciences*", McGraw-Hill 1969